7

Physical Climate Processes and Feedbacks

Co-ordinating Lead Author
T.F. Stocker

Lead Authors
G.K.C. Clarke, H. Le Treut, R.S. Lindzen, V.P. Meleshko, R.K. Mugara, T.N. Palmer,
R.T. Pierrehumbert, P.J. Sellers, K.E. Trenberth, J. Willebrand

Contributing Authors
R.B. Alley, O.E. Anisimov, C. Appenzeller, R.G. Barry, J.J. Bates, R. Bindschadler, G.B. Bonan,
C.W. Böning, S. Bony, H. Bryden, M.A. Cane, J.A. Curry, T. Delworth, A.S. Denning, R.E. Dickinson,
K. Echelmeyer, K. Emanuel, G. Flato, I. Fung, M. Geller, P.R. Gent, S.M. Griffies, I. Held,
A. Henderson-Sellers, A.A.M. Holtslag, F. Hourdin, J.W. Hurrell, V.M. Kattsov, P.D. Killworth,
Y. Kushnir, W.G. Large, M. Latif, P. Lemke, M.E. Mann, G. Meehl, U. Mikolajewicz, W. O'Hirok,
C.L. Parkinson, A. Payne, A. Pitman, J. Polcher, I. Polyakov, V. Ramaswamy, P.J. Rasch, E.P. Salathe,
C. Schär, R.W. Schmitt, T.G. Shepherd, B.J. Soden, R.W. Spencer, P. Taylor, A. Timmermann,
K.Y. Vinnikov, M. Visbeck, S.E. Wijffels, M. Wild

Review Editors
S. Manabe, P. Mason

Contents

Executive Summary

Considerable advances have been made in the understanding of processes and feedbacks in the climate system. This has led to a better representation of processes and feedbacks in numerical climate models, which have become much more comprehensive. Because of the presence of non-linear processes in the climate system, deterministic projections of changes are potentially subject to uncertainties arising from sensitivity to initial conditions or to parameter settings. Such uncertainties can be partially quantified from ensembles of climate change integrations, made using different models starting from different initial conditions. They necessarily give rise to probabilistic estimates of climate change. This results in more quantitative estimates of uncertainties and more reliable projections of anthropogenic climate change. While improved parametrizations have built confidence in some areas, recognition of the complexity in other areas has not indicated an overall reduction or shift in the current range of uncertainty of model response to changes in atmospheric composition.

Atmospheric feedbacks largely control climate sensitivity. Important progress has been made in the understanding of those processes, partly by utilising new data against which models can be compared. Since the Second Assessment Report (IPCC, 1996) (hereafter SAR), there has been a better appreciation of the complexity of the mechanisms controlling water vapour distribution. Within the boundary layer, water vapour increases with increasing temperatures. In the free troposphere above the boundary layer, where the greenhouse effect of water vapour is most important, the situation is less amenable to straightforward thermodynamic arguments. In models, increases in water vapour in this region are the most important reason for large responses to increased greenhouse gases.

Water vapour feedback, as derived from current models, approximately doubles the warming from what it would be for fixed water vapour. Since the SAR, major improvements have occurred in the treatment of water vapour in models, although detrainment of moisture from clouds remains quite uncertain and discrepancies exist between model water vapour distributions and those observed. It is likely that some of the apparent discrepancy is due to observational error and shortcomings in intercomparison methodology. Models are capable of simulating the moist and very dry regions observed in the tropics and sub-tropics and how they evolve with the seasons and from year to year, indicating that the models have successfully incorporated the basic processes governing water vapour distribution. While reassuring, this does not provide a definitive check of the feedbacks, though the balance of evidence favours a positive clear-sky water vapour feedback of a magnitude comparable to that found in simulations.

Probably the greatest uncertainty in future projections of climate arises from clouds and their interactions with radiation. Cloud feedbacks depend upon changes in cloud height, amount, and radiative properties, including short-wave absorption. The radiative properties depend upon cloud thickness, particle size, shape, and distribution and on aerosol effects. The evolution of clouds depends upon a host of processes, mainly those governing the distribution of water vapour. The physical basis of the cloud parametrizations included into the models has also been greatly improved. However, this increased physical veracity has not reduced the uncertainty attached to cloud feedbacks: even the sign of this feedback remains unknown. A key issue, which also has large implications for changes in precipitation, is the sensitivity of sub-grid scale dynamical processes, turbulent and convective, to climate change. It depends on sub-grid features of surface conditions such as orography. Equally important are microphysical processes, which have only recently been introduced explicitly in the models, and carry major uncertainties. The possibility that models underestimate solar absorption in clouds remains controversial, as does the effect of such an underestimate on climate sensitivity. The importance of the structure of the stratosphere and both radiative and dynamical processes have been recognised, and limitations in representing stratospheric processes add some uncertainty to model results.

Considerable improvements have taken place in modelling ocean processes. In conjunction with an increase in resolution, these improvements have, in some models, allowed a more realistic simulation of the transports and air-sea fluxes of heat and fresh water, thereby reducing the need for flux adjustments in coupled models. These improvements have also contributed to better simulations of natural large-scale circulation patterns such as El Niño-Southern Oscillation (ENSO) and the oceanic response to atmospheric variability associated with the North Atlantic Oscillation (NAO). However, significant deficiencies in ocean models remain. Boundary currents in climate simulations are much weaker and wider than in nature, though the consequences of this fact for the global climate sensitivity are not clear. Improved parametrizations of important sub-grid scale processes, such as mesoscale eddies, have increased the realism of simulations but important details are still under debate. Major uncertainties still exist with the representation of small-scale processes, such as overflows and flow through narrow channels (e.g., between Greenland and Iceland), western boundary currents (i.e., large-scale narrow currents along coastlines), convection, and mixing.

In the Atlantic, the thermohaline circulation (THC) is responsible for the major part of the ocean meridional heat transport associated with warm and saline surface waters flowing northward and cold and fresh waters from the North Atlantic returning at depth. The interplay between the large-scale atmospheric forcing, with warming and evaporation in low latitudes, and cooling and net precipitation at high latitudes, forms the basis of a potential instability of the present Atlantic THC. Changes in ENSO may also influence the Atlantic THC by altering the fresh water balance of the tropical Atlantic, therefore providing a coupling between low and high latitudes. Uncertainty resides with the relative importance of feedbacks associated with processes influencing changes in high latitude sea surface temperatures and salinities, such as atmosphere-ocean heat and fresh water fluxes, formation and transport of sea ice, continental runoff and the large-scale transports in ocean and atmosphere. The Atlantic THC is likely to change over the coming century but its evolution continues to be an unresolved issue. While some recent calculations find little changes in the THC, most projections

suggest a gradual and significant decline of the THC. A complete shut-down of the THC is simulated in a number of models if the warming continues, but knowledge about the locations of thresholds for such a shut-down is very limited. Models with reduced THC appear to be more susceptible for a shut-down. Although a shut-down during the next 100 years is unlikely, it cannot be ruled out.

Recent advances in our understanding of vegetation photosynthesis and water use have been used to couple the terrestrial energy, water and carbon cycles within a new generation of physiologically based land-surface parametrizations. These have been tested against field observations and implemented in General Circulation Models (GCMs) with demonstrable improvements in the simulation of land-atmosphere fluxes. There has also been significant progress in specifying land parameters, especially the type and density of vegetation. Importantly, these data sets are globally consistent in that they are primarily based on one type of satellite sensor and one set of interpretative algorithms. Satellite observations have also been shown to provide a powerful diagnostic capability for tracking climatic impacts on surface conditions; e.g., droughts and the recently observed lengthening of the boreal growing season; and direct anthropogenic impacts such as deforestation. The direct effects of increased carbon dioxide (CO_2) on vegetation physiology could lead to a relative reduction in evapotranspiration over the tropical continents, with associated regional warming over that predicted for conventional greenhouse warming effects. On time-scales of decades these effects could significantly influence the rate of atmospheric CO_2 increase, the nature and extent of the physical climate system response, and ultimately, the response of the biosphere itself to global change. In addition, such models must be used to account for the climatic effects of land-use change which can be very significant at local and regional scales. However, realistic land-use change scenarios for the next 50 to 100 years are not expected to give rise to global scale climate changes comparable to those resulting from greenhouse gas warming. Significant modelling problems remain to be solved in the areas of soil moisture processes, runoff prediction, land-use change, and the treatment of snow and sub-grid scale heterogeneity.

Increasingly complex snow schemes are being used in some climate models. These schemes include parametrizations of the metamorphic changes in snow albedo arising from age dependence or temperature dependence. Recent modelling studies of the effects of warming on permafrost predict a 12 to 15% reduction in near-surface area and a 15 to 30% increase in thickness of the seasonally thawing active layer by the mid-21st century. The representation of sea-ice processes continues to improve with several climate models now incorporating physically based treatments of ice dynamics. The effects of sub-grid scale variability in ice cover and thickness, which can significantly influence albedo and atmosphere-ocean exchanges, are being introduced. Understanding of fast-flow processes for land ice and the role of these processes in past climate events is growing rapidly. Representation of ice stream and grounding line physics in land-ice dynamics models remains rudimentary but, in global climate models, ice dynamics and thermodynamics are ignored entirely.

Climate change may manifest itself both as shifting means as well as changing preference of specific regimes, as evidenced by the observed trend toward positive values for the last 30 years in the NAO index and the climate "shift" in the tropical Pacific in about 1976. While coupled models simulate features of observed natural climate variability such as the NAO and ENSO, suggesting that many of the relevant processes are included in the models, further progress is needed to depict these natural modes accurately. Moreover, because ENSO and NAO are key determinants of regional climate change, and they can possibly result in abrupt and counter-intuitive changes, there has been an increase in uncertainty in those aspects of climate change that critically depend on regional changes.

Possible non-linear changes in the climate system as a result of anthropogenic climate forcing have received considerable attention in the last few years. Employing the entire climate model hierarchy, and combining these results with palaeo-climatic evidence and instrumental observation, has shown that mode changes in all components of the climate system have occurred in the past and may also take place in the future. Such changes may be associated with thresholds in the climate system. Such thresholds have been identified in many climate models and there is an increasing understanding of the underlying processes. Current model simulations indicate that the thresholds may lie within the reaches of projected changes. However, it is not yet possible to give reliable values of such thresholds.

7.1 Introduction

The key problem to be addressed is the response of the climate system to changes in forcing. In many cases there is a fairly direct and linear response and many of the simulated changes fall into that class (Chapter 9). These concern the large-scale general circulations of the atmosphere and ocean, and they are in principle represented in current comprehensive coupled climate models. Such possible large-scale dynamical feedbacks are also influenced by small-scale processes within the climate system. The various feedbacks in the climate system may amplify (positive feedbacks), or diminish (negative feedbacks) the original response. We often approximate the response of a particular variable to a small forcing by a scaling number. A prominent example of such a quantification is the equilibrium global mean temperature increase per Wm^{-2} change in the global mean atmospheric radiative forcing (see Chapter 9, Section 9.2.1).

While many aspects of the response of the climate system to greenhouse gas forcing appear to be linear, regime or mode transitions cannot be quantified by a simple number because responses do not scale with the amplitude of the forcing: small perturbations can induce large changes in certain variables of the climate system. This implies the existence of thresholds in the climate system which can be crossed for a sufficiently large perturbation. While such behaviour has long been known and studied in the context of simple models of the climate system, such thresholds are now also found in the comprehensive coupled climate models currently available. Within this framework, the possibility for irreversible changes in the climate system exists. This insight, backed by the palaeo-climatic record (see Chapter 2, Section 2.4), is a new challenge for global change science because now thresholds have to be identified and their values need to be estimated using the entire hierarchy of climate models.

To estimate the response properly, we must represent faithfully the physical processes in models. Not only must the whole system model perform reasonably well in comparison with observation (both spatial and temporal), but so too must the component models and the processes that are involved in the models. It is possible to tune a model so that some variable appears consistent with that observed, but we must also ask whether it comes out that way for the right reason and with the right variability. By examining how well individual processes are known and can be modelled, we can comment on the capabilities and usefulness of the models, and whether they are likely to be able to properly represent possible non-linear responses of the climate system.

7.1.1 Issues of Continuing Interest

Examples of some processes in the climate system and its components that have been dealt with in the Second Assessment Report (IPCC, 1996) (hereafter SAR) and still are important topics of progress:

- *The hydrological cycle.* Progress has been made in all aspects of the hydrological cycle in the atmosphere, involving evaporation, atmospheric moisture, clouds, convection, and precipitation. Because many facets of these phenomena are sub-grid scale, they must be parametrized. While models reasonably simulate gross aspects of the observed behaviour on several time-scales, it is easy to point out shortcomings, although it is unclear as to how much these affect the sensitivity of simulated climate to changes in climate forcing.

- *Water vapour feedback.* An increase in the temperature of the atmosphere increases its water-holding capacity; however, since most of the atmosphere is undersaturated, this does not automatically mean that water vapour, itself, must increase. Within the boundary layer (roughly the lowest 1 to 2 km of the atmosphere), relative humidity tends to remain fixed, and water vapour does increase with increasing temperature. In the free troposphere above the boundary layer, where the water vapour greenhouse effect is most important, the behaviour of water vapour cannot be inferred from simple thermodynamic arguments. Free tropospheric water vapour is governed by a variety of dynamical and microphysical influences which are represented with varying degrees of fidelity in general circulation models. Since water vapour is a powerful greenhouse gas, increasing water vapour in the free troposphere would lead to a further enhancement of the greenhouse effect and act as a positive feedback; within current models, this is the most important reason for large responses to increased anthropogenic greenhouse gases.

- *Cloud radiation feedback.* Clouds can both absorb and reflect solar radiation (thereby cooling the surface) and absorb and emit long-wave radiation (thereby warming the surface). The compensation between those effects depends on cloud height, thickness and cloud radiative properties. The radiative properties of clouds depend on the evolution of atmospheric water vapour, water drops, ice particles and atmospheric aerosols. These cloud processes are most important for determining radiative, and hence temperature, changes in models. Although their representation is greatly improved in models, the added complexity may explain why considerable uncertainty remains; this represents a significant source of potential error in climate simulations. The range in estimated climate sensitivity of 1.5 to 4.5°C for a CO_2 doubling is largely dictated by the interaction of model water vapour feedbacks with the variations in cloud behaviour among existing models.

- *Sub-grid scale processes in ocean models.* Although improved parametrizations in coarse resolution models are available to represent mixing processes, they do not, in their present form, induce sufficient variability on the broad range of time-scales exhibited by eddy-resolving ocean models. Thus present generations of coarse resolution ocean models may not be able to decide questions about those types of natural variability that are associated with sub-grid scale processes, and increased resolution is highly desirable.

7.1.2 New Results since the SAR

Improved atmospheric and oceanic modules of coupled climate models, especially improved representation of clouds, parametrizations of boundary layer and ocean mixing, and increased grid resolution, have helped reduce and often eliminate the need for flux adjustment in some coupled climate models. This has not reduced the range of sensitivities in projection experiments.

There is a growing appreciation of the importance of the stratosphere, particularly the lower stratosphere, in the climate system. Since the mass of the stratosphere represents only about 10 to 20% of the atmospheric mass, the traditional view has been that the stratosphere can play only a limited role in climate change. However, this view is changing. The transport and distribution of radiatively active constituents, especially water vapour and ozone, are important for radiative forcing. Moreover, waves generated in the troposphere propagate into the stratosphere and are absorbed, so that stratospheric changes alter where and how they are absorbed, and effects can extend downward into the troposphere.

Observational records suggest that the atmosphere may exhibit specific regimes which characterise the climate on a regional to hemispheric scale. Climate change may thus manifest itself both as shifting means as well as changing preference of specific regimes. Examples are the North Atlantic Oscillation (NAO) index, which shows a bias toward positive values for the last 30 years, and the climate "shift" in the tropical Pacific at around 1976.

While considerable advances have been made in improving feedbacks and coupled processes and their depiction in models, the emergence of the role of natural modes of the climate system such as the El Niño-Southern Oscillation (ENSO) and NAO as key determinants of regional climate change, and possibly also shifts, has led to an increase in uncertainty in those aspects of climate change that critically depend on regional changes. It is encouraging that the most advanced models exhibit natural variability that resembles the most important modes such as ENSO and NAO.

The coupled ocean-atmosphere system contains important non-linearities which give rise to a multiplicity of states of the Atlantic thermohaline circulation (THC). Most climate models respond to global warming by a reduction of the Atlantic THC. A complete shut-down of the THC in response to continued warming cannot be excluded and would occur if certain thresholds are crossed. Models have identified the maximum strength of greenhouse gas induced forcing and the rate of increase as thresholds for the maintenance of the THC in the Atlantic ocean, an important process influencing the climate of the Northern Hemisphere. While such thresholds have been found in a variety of fundamentally different models, suggesting that their existence in the climate system is a robust result, we cannot yet determine with accuracy the values of these thresholds, because they crucially depend on the response of the atmospheric hydrological cycle to climate change.

The representation of sea-ice dynamics and sub-grid scale processes in coupled models has improved significantly, which is an important prerequisite for a better understanding of, the current variability in, and a more accurate prediction of future changes in polar sea-ice cover and atmosphere-ocean interaction in areas of deep water formation.

Recent model simulations, including new land-surface parametrizations and field observations, strongly indicate that large-scale changes in land use can lead to significant impacts on the regional climate. The terrestrial carbon and water cycles are also linked through vegetation physiology, which regulates the ratio of carbon dioxide (CO_2) uptake (photosynthesis) to water loss (evapotranspiration). As a result, vegetation water-use efficiency is likely to change with increasing atmospheric CO_2, leading to a reduction in evapotranspiration over densely vegetated areas. Tropical deforestation, in particular, is associated with local warming and drying. However, realistic land-use change scenarios for the next 50 to 100 years are not expected to give rise to global scale climate changes comparable to those resulting from greenhouse gas warming.

7.1.3 Predictability of the Climate System

The Earth's atmosphere-ocean dynamics is chaotic: its evolution is sensitive to small perturbations in initial conditions. This sensitivity limits our ability to predict the detailed evolution of weather; inevitable errors and uncertainties in the starting conditions of a weather forecast amplify through the forecast (Palmer, 2000). As well as uncertainty in initial conditions, such predictions are also degraded by errors and uncertainties in our ability to represent accurately the significant climate processes. In practice, detailed weather prediction is limited to about two weeks.

However, because of the more slowly varying components of the climate system, predictability of climate is not limited to the two week time-scale. Perhaps the most well-known and clear cut example of longer-term predictability is El Niño (see Section 7.6.5) which is predictable at least six months in advance. There is some evidence that aspects of the physical climate system are predictable on even longer time-scales (see Section 7.6). In practice, if natural decadal variability is partially sensitive to initial conditions, then projections of climate change for the 21st century will exhibit a similar sensitivity.

In order to be able to make reliable forecasts in the presence of both initial condition and model uncertainty, it is now becoming common to repeat the prediction many times from different perturbed initial states, and using different global models (from the stock of global models that exist in the world weather and climate modelling community). These so-called multi-model, multi-initial-condition ensembles are the optimal basis of probability forecasts (e.g., of a weather event, El Niño, or the state of the THC).

Estimating anthropogenic climate change on times much longer than the predictability time-scale of natural climate fluctuations does not, by definition, depend on the initial state. On these time-scales, the problem of predicting climate change is one of estimating changes in the probability distribution of climatic states (e.g., cyclonic/anticyclonic weather, El Niño, the THC, global mean temperature) as atmospheric composition is altered in some prescribed manner. Like the initial value problems

mentioned above, estimates of such changes to the probability distribution of climate states must be evaluated using ensemble prediction techniques.

The number of ensemble members required to estimate reliably changes to the probability distribution of a given climatic phenomenon depends on the phenomenon in question. Estimating changes in the probability distribution of localised extreme weather events, which by their nature occur infrequently, may require very large ensembles with hundreds of members. Estimating changes in the probability distribution of large scale frequent events (e.g., the probability of above-average hemispheric mean temperature) requires much smaller ensembles.

An important question is whether a multi-model ensemble made by pooling the world climate community's stock of global models adequately spans the uncertainty in our ability to represent faithfully the evolution of climate. Since the members of this stock of models were not developed independently of one another, such an ensemble does not constitute an independent unbiased sampling of possible model formulations.

7.2 Atmospheric Processes and Feedbacks

7.2.1 Physics of the Water Vapour and Cloud Feedbacks

Any increase in the amount of a greenhouse gas contained in the Earth's atmosphere would reduce the emission of outgoing long-wave radiation (OLR) if the temperature of the atmosphere and surface were held fixed. The climate achieves a new equilibrium by warming until the OLR increases enough to balance the incoming solar radiation. Addition of greenhouse gases affects the OLR primarily because the tropospheric temperature decreases with height. With a fixed temperature profile, increasing the greenhouse gas content makes the higher parts of the atmosphere more opaque to infrared radiation upwelling from below, replacing this radiation with OLR emitted from the colder regions.

Determination of the new equilibrium is complicated by the fact that water vapour is itself a potent greenhouse gas, and the amount and distribution of water vapour will generally change as the climate changes. The atmospheric water vapour content responds to changes in temperature, microphysical processes and the atmospheric circulation. An overarching consideration is that the maximum amount of water vapour air can hold increases rapidly with temperature, in accord with the Clausius-Clapeyron relation. This affects all aspects of the hydrological cycle. Unlike CO_2, water vapour concentration varies substantially in both the vertical and horizontal. An increase in water vapour reduces the OLR only if it occurs at an altitude where the temperature is lower than the ground temperature, and the impact grows sharply as the temperature difference increases. If water vapour at such places increases as the climate warms, then the additional reduction in OLR requires the new equilibrium to be warmer than it would have been if water vapour content had remained fixed. This is referred to as a *positive water vapour feedback.*

Clouds are intimately connected to the water vapour pattern, as clouds occur in connection with high relative humidity, and cloud processes in turn affect the moisture distribution. Clouds affect OLR in the same way as a greenhouse gas, but their net effect on the radiation budget is complicated by the fact that clouds also reflect incoming solar radiation. As clouds form the condensation releases latent heat, which is a central influence in many atmospheric circulations.

The boundary layer is the turbulent, well-mixed shallow layer near the ground, which can be regarded as being directly moistened by evaporation from the surface. In the boundary layer, the increase in water vapour with temperature in proportion with the Clausius-Clapeyron relation is uncontroversial. Observations (e.g., Wentz and Schabel, 2000) clearly show a very strong relation of total column water vapour (precipitable water) with surface and tropospheric temperature. Because the boundary-layer temperature is similar to that of the ground, however, boundary-layer water vapour is not of direct significance to the water vapour feedback. Furthermore, half of the atmospheric water vapour is below 850 mb, so measurements of total column water have limited utility in understanding water vapour feedback. The part of the troposphere above the boundary layer is referred to as the "free troposphere". Water vapour is brought to the free troposphere by a variety of mixing and transport processes, and water vapour feedback is determined by the aggregate effects of changes in the transport and in the rate at which water is removed by precipitation occurring when air parcels are cooled, usually by rising motions.

The complexity of water vapour radiative impact is reflected in the intricate and strongly inhomogeneous patterns of the day-to-day water vapour distribution (Figure 7.1a). The very dry and very moist regions reveal a strong influence of the large-scale dynamical transport. Model simulations exhibit similar patterns (Figure 7.1b), with a notable qualitative improvement at higher resolution (Figure 7.1c). Understanding the dominant transport processes that set up those patterns, and how they can be affected by a modified climate, should help assess the representation of the water vapour feedbacks in the corresponding region found in model simulations.

(i) In the tropical free troposphere, ascent is generally concentrated in intense, narrow, and nearly vertical cumulonimbus towers, with descent occurring slowly over the broad remaining area. The moist regions are broader than the narrow ascending towers and are mostly descending. The vicinity of convective towers is moistened by evaporation of precipitation from the cirrus outflow of the cumulus towers above about 5 km and by the dissipation and mixing of cumulonimbus towers below about 5 km and above the trade wind boundary layer. Cloud coverage thus depends on the detrainment of ice from cumulus towers (Gamache and Houze, 1983). The ice content of the detrained air depends in turn on the efficiency of precipitation within the tower, i.e., condensed water which falls as rain within the towers is no longer available for detrainment. The association of high stratiform cloud cover with high relative humidity was clearly illustrated by Udelhofen and Hartmann (1995), and in the tropics upper-tropospheric humidity (UTH) is tied to the frequency of deep convection (Soden and Fu, 1995).

The tropical dry regions shown in Figure 7.1 are associated with large-scale descent. A number of studies (Sherwood, 1996; Salathe and Hartmann, 1997; Pierrehumbert and Roca, 1998;
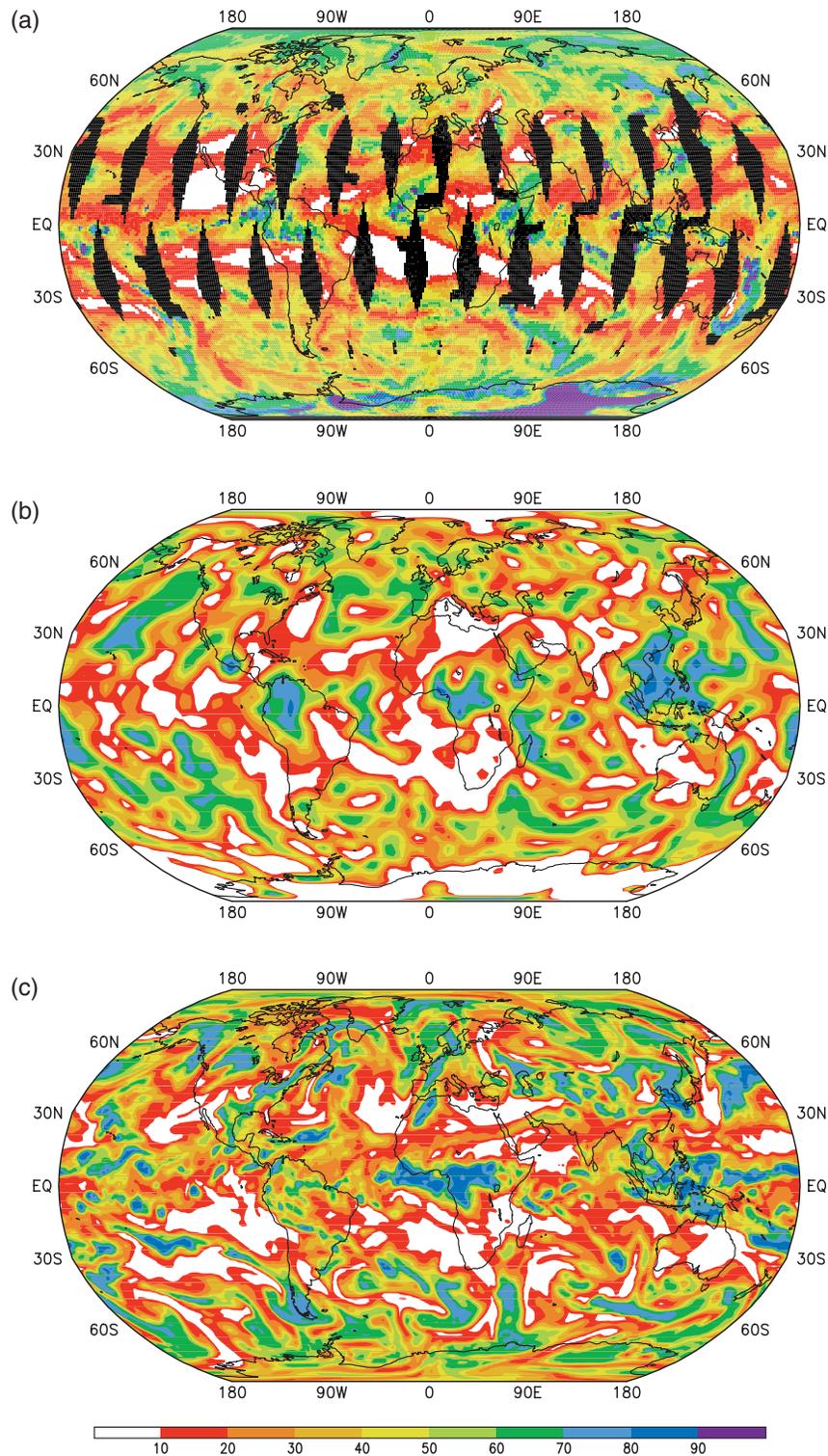
Figure 7.1: Comparison between an observational estimate from satellite radiances and two model simulations of the complex structure of mid-tropospheric water vapour distribution for the date May 5. At any instant, water vapour is unevenly distributed in the atmosphere with very dry areas adjacent to very moist areas. Any modification in the statistics of those areas participates in the atmospheric feedback. The observed small-scale structure of the strong and variable gradients (a) is not well resolved in a simulation with a climate model of the spatial resolution currently used for climate projections (b), but simulated with much better fidelity in models with significantly higher resolution (c). (a): Distribution of mean relative humidity in layer 250 to 600 mb on May 5, 1998, as retrieved from observations on SSM/T-2 satellite (Spencer and Braswell, 1997). Missing data are indicated by black areas and the retrieval is most reliable in the latitude band 30°S to 30°N. (b): Relative humidity at about 400 mb for May 5 of an arbitrary year from a simulation with the GFDL R30L14 atmospheric general circulation model used in the AMIP I simulation (Gates *et al.*, 1999; Lau and Nath, 1999). In small polar areas (about 5% of the globe) some relative humidities are negative (set to zero) due to numerical spectral effects. (c): Relative humidity at 400 mb from the ECHAM4 T106 simulation for May 5 of an arbitrary year (Roeckner *et al.*, 1996; Wild *et al.*, 1998).

Soden, 1998; Dessler and Sherwood, 2000) have shown that the predominant source of water vapour here is large-scale advection from the convective region. Some of the transient moist filaments which account for much of the moisture of the climatologically dry zone can be seen in Figure 7.1a,c. Dry-zone humidity depends on saturation vapour pressure at remote points along the relevant trajectories. The way the water vapour feedback operates in the dry regions is dependent on the manner in which these points change as the climate warms.

The moist regions are also cloudy. In the tropics, water vapour feedback could involve changes in the water vapour content of either the convective or dry regions, or changes in the relative area of the two regions.

(ii) In the extra-tropical free troposphere, convection still plays a role (Hu and Liu, 1998; Kirk-Davidoff and Lindzen, 2000); however, ascent and descent are primarily associated with large-scale wave motions with comparable ascending and descending areas (Yang and Pierrehumbert, 1994; Hu and Liu, 1998). Moisture in the troposphere is directly affected by evaporation, which is a maximum in the sub-tropics, and the boundary-layer reservoir of water vapour that is tapped by extra-tropical waves. Observations confirm that extra-tropical free tropospheric water vapour is mostly not associated with deep convection (Soden and Fu, 1995), though there may still be some influence from the extra-tropical surface via local convection. Condensation in the broad ascending areas leads directly to stratiform clouds.

7.2.1.1 Water vapour feedback

Water vapour feedback continues to be the most consistently important feedback accounting for the large warming predicted by general circulation models in response to a doubling of CO_2. Water vapour feedback acting alone approximately doubles the warming from what it would be for fixed water vapour (Cess *et al.*, 1990; Hall and Manabe, 1999; Schneider *et al.*, 1999; Held and Soden, 2000). Furthermore, water vapour feedback acts to amplify other feedbacks in models, such as cloud feedback and ice albedo feedback. If cloud feedback is strongly positive, the water vapour feedback can lead to 3.5 times as much warming as would be the case if water vapour concentration were held fixed (Hall and Manabe, 1999).

As noted by Held and Soden (2000), the relative sensitivity of OLR to water vapour changes at various locations depends on how one perturbs the water vapour profile; the appropriate choice depends entirely on the nature of the water vapour perturbation anticipated in a changing climate. The sensitivity is also affected by cloud radiative effects, which tend to mask the influence of sub-cloud water vapour on OLR. Incorporating cloud radiative effects and a fixed relative humidity perturbation (argued to be most appropriate to diagnosing GCM water vapour feedback), Held and Soden suggest that OLR is almost uniformly sensitive to water vapour perturbations throughout the tropics. Roughly 55% of the total is due to the free troposphere in the "tropics" (30°N to 30°S) with 35% from the extra-tropics. Allowing for polar amplification of warming increases the proportion of water vapour feedback attributable to the extra-tropics. Of the tropical contribution, about two thirds, or 35% of the global total, is due to the

upper half of the troposphere, from 100 to 500 mb. The boundary layer itself accounts for only 10% of the water vapour feedback globally. Simulations incorporating cloud radiative effects in a doubled CO_2 experiment (Schneider *et al.*, 1999) and a clear-sky analysis based on 15 years of global data (Allan *et al.*, 1999) yield maximum sensitivity to water vapour fluctuations in the 400 to 700 mb layer (see also Le Treut *et al.*, 1994). In a simulation analysed by Schneider *et al.* (1999) extra-tropical water vapour feedback affected warming 50% more than did tropical feedback.

Most of the free troposphere is highly undersaturated with respect to water, so that local water-holding capacity is not the limiting factor determining atmospheric water vapour. Within the constraints imposed by Clausius-Clapeyron alone there is ample scope for water vapour feedbacks either stronger or weaker than those implied by constant relative humidity, especially in connection with changes in the area of the moist tropical convective region (Pierrehumbert, 1999). It has been estimated that, without changes in the relative area of convective and dry regions, a shift of water vapour to lower levels in the dry regions could, at the extreme, lead to a halving of the currently estimated water vapour feedback, but could not actually cause it to become a negative, stabilising feedback (Harvey, 2000).

Attempts to directly confirm the water vapour feedback by correlating spatial surface fluctuations with spatial OLR fluctuations were carried out by Raval and Ramanathan (1989). Their results are difficult to interpret, as they involve the effects of circulation changes as well as direct thermodynamic control (Bony *et al.*, 1995). Inamdar and Ramanathan (1998) showed that a positive correlation between water vapour, greenhouse effect and SST holds for the entire tropics at seasonal time-scales. This is consistent with a positive water vapour feedback, but it still cannot be taken as a direct test of the feedback as the circulation fluctuates in a different way over the seasonal cycle than it does in response to doubling of CO_2.

7.2.1.2 Representation of water vapour in models

General circulation models do not impose a fixed relative humidity. Assumptions built into the models directly govern the relative humidity only in the sparse set of grid boxes that are actively convecting, where the choice of convection scheme determines the humidity. In the case of moist convective adjustment, the relative humidity after convection is explicitly set to a predetermined profile, whereas the mass flux schemes compute a humidity profile based on microphysical assumptions of varying complexity. The relative humidity elsewhere is determined by explicitly resolved dynamical processes, and in fact undergoes marked spatial (e.g., Figure 7.1b,c) and temporal fluctuations. Nonetheless, all models studied to date produce a positive water vapour feedback consistent with the supposition that water vapour increases in such a way as to keep the relative humidity approximately unchanged at all levels (Held and Soden, 2000). The strength of the water vapour feedback is consistent amongst models, despite considerable differences in the treatment of convection and microphysics (Cess *et al.*, 1990).

The "convective region" is potentially a source of modelling errors, since the evaporation of detrained precipitation and other poorly characterised and heavily parametrized processes are

essential to the moistening of the atmosphere. Tompkins and Emanuel (2000) showed that in a single-column model, numerical convergence of the simulated water vapour profile requires a vertical resolution better than 25 mb in pressure (see also Emanuel and Zivkovic-Rothman, 1999). Thus, the apparent lack of sensitivity of water vapour feedback in current GCMs to the way convection is treated may be an artefact of insufficient vertical resolution. An alternative view is that the water vapour flux is vigorous enough to keep the convective region at a substantial fraction of saturation, so that the details of the moistening process do not matter much. In this case the convection essentially extends the boundary layer into the free troposphere, making condensed water abundantly available to evaporation, but in the form of droplets or crystals. Indeed, Dessler and Sherwood (2000) find that satellite observations of tropical water vapour can be understood without detailed microphysical considerations, even in the convective region. Radiosonde observations (Kley *et al.*, 1997) and satellite UTH data (Soden and Fu, 1995) reveal free troposphere relative humidities of 50 to 70% throughout the convective region. Udelhofen and Hartmann (1995) find that moisture decays away from convective systems with a characteristic scale of 500 km, so that convection need not be too closely spaced to maintain a uniformly moistened region. As noted by Held and Soden (2000), the evidence for the opposite view, that convective region air becomes drier as temperature increases, is weak.

This moistening of large-scale tropical subsiding zones by large-scale advection is a process explicitly resolved in models, and in which one can have reasonably high confidence. Care must still be taken with the design of numerical advection methods to avoid spurious transport. In this regard, there has been notable progress since the SAR as models are increasingly using semi-Lagrangian and other advanced advection methods in place of spectral advection of water vapour (Williamson and Rasch, 1994). These methods virtually eliminate spurious transport arising from the need to adjust negative moisture regions, as commonly happens in spectral advection.

In the extra-tropics the ubiquitous large-scale synoptic eddies which dominate moisture transport are explicitly represented in GCMs, and there is reasonably high confidence in simulated mid-latitude water vapour feedback. The eddies maintain a fairly uniform monthly mean relative humidity of 30 to 50% throughout the year (Soden and Fu, 1995; Bates and Jackson, 1997).

Simulation of water vapour variations with natural climate fluctuations such as the annual cycle and El Niño can help provide tests of the verisimilitude of models but may not be sufficient for assessing climate change due to increases in greenhouse gases (Bony *et al.*, 1995). Models are quite successful at reproducing the climatological free troposphere humidity pattern (e.g., Figure 7.1b,c). Model-satellite comparisons of UTH are still at a rather early stage of development; the AMIP simulations did not archive enough fields to provide an adequate understanding of UTH, and there are problems in determining which model level should be compared to the satellite data. Also there are uncertainties in UTH retrievals (see Chapter 2). Caveats notwithstanding, the ensemble mean of the

AMIP simulations shows a moist bias in UTH compared to satellite data, but this result is rendered uncertain by apparent inconsistencies in the computation of model relative humidities for intercomparison purposes. The models studied by AMIP (Bates and Jackson, 1997) appear to show little skill in reproducing the seasonal or interannual variations of convective region UTH, though many show significant correlations between simulated and observed sub-tropical and extra-tropical UTH fluctuations. The latter lends some confidence to the simulated water vapour feedback, as the dry sub-tropics and extra-tropics account for a large part of the feedback. Del Genio *et al.* (1994) found good agreement between the observed seasonal cycle of zonal mean UTH, and that simulated by the GISS model.

Humidity is important to water vapour feedback only to the extent that it alters OLR. Because the radiative effects of water vapour are logarithmic in water vapour concentration, rather large errors in humidity can lead to small errors in OLR, and systematic underestimations in the contrast between moist and dry air can have little effect on climate sensitivity (Held and Soden, 2000). Most GCMs reproduce the climatological pattern of clear-sky OLR very accurately (Duvel *et al.*, 1997). In addition, it has been shown that the CCM3 model tracks the observed seasonal cycle of zonal mean clear-sky OLR to within $5\,\mathrm{Wm^{-2}}$ (Kiehl *et al.*, 1998), the GFDL model reproduces tropical mean OLR fluctuations over the course of an El Niño event (Soden, 1997), and the collection of models studied under the AMIP project reproduces interannual variability of the clear-sky greenhouse parameter with errors generally under 25% for sea surface temperatures (SSTs) under 25°C (Duvel *et al.*, 1997). Errors become larger over warmer waters, owing to inaccuracies in the way the simulated atmospheric circulation responds to the imposed SSTs (which may also not be accurate). The LMD model shows close agreement with the observed seasonal cycle of greenhouse trapping (Bony *et al.*, 1995), but models vary considerably in their ability to track this cycle (Duvel *et al.*, 1997).

Indirect evidence for validity of the positive water vapour feedback in present models can be found in studies of interannual variability of global mean temperature: Hall and Manabe (1999) found that suppression of positive water vapour feedback in the GFDL model led to unrealistically low variability. An important development since the SAR is the proliferation of evidence that the tropics during the Last Glacial Maximum were 2 to 5°C colder than the present tropics. Much of the cooling can be simulated in GCMs which incorporate the observed reduction in CO_2 at the Last Glacial Maximum (see Chapter 8). Without water vapour feedback comparable to that currently yielded by GCMs, there would be a problem accounting for the magnitude of the observed cooling in the tropics and Southern Hemisphere.

7.2.1.3 Summary on water vapour feedbacks

The decade since the First IPCC Assessment Report (IPCC, 1990) has seen progressive evolution in sophistication of thinking about water vapour feedback. Concern about the role of upper-tropospheric humidity has stimulated much theoretical, model diagnostic and observational study. The period since the SAR has seen continued improvement in the analysis of

observations of water vapour from sondes and satellite instrumentation. Theoretical understanding of the atmospheric hydrological cycle has also increased. As a result, observational tests of how well models represent the processes governing water vapour content have become more sophisticated and more meaningful. Since the SAR, appraisal of the confidence in simulated water vapour feedback has shifted from a diffuse concern about upper-tropospheric humidity to a more focused concern about the role of microphysical processes in the convection parametrizations, and particularly those affecting tropical deep convection. Further progress will almost certainly require abandoning the artificial diagnostic separation between water vapour and cloud feedbacks.

In the SAR, a crude distinction was made between the effect of "upper-tropospheric" and "lower-tropospheric" water vapour, and it was implied that lower-tropospheric water vapour feedback was a straightforward consequence of the Clausius-Clapeyron relation. It is now appreciated that it is only in the boundary layer that the control of water vapour by Clausius-Clapeyron can be regarded as straightforward, so that "lower-tropospheric" feedback is no less subtle than "upper-tropospheric". It is more meaningful to separate the problem instead into "boundary layer" and "free tropospheric" water vapour, with the former contributing little to the feedback.

The successes of the current models lend some confidence to their results. For a challenge to the current view of water vapour feedback to succeed, relevant processes would have to be incorporated into a GCM, and it would have to be shown that the resulting GCM accounted for observations at least as well as the current generation. A challenge that meets this test has not yet emerged. Therefore, the balance of evidence favours a positive clear-sky water vapour feedback of magnitude comparable to that found in simulations.

7.2.2 Cloud Processes and Feedbacks

7.2.2.1 General design of cloud schemes within climate models
The potential complexity of the response of clouds to climate change was identified in the SAR as a major source of uncertainty for climate models. Although there has been clear progress in the physical content of the models, clouds remain a dominant source of uncertainty, because of the large variety of interactive processes which contribute to cloud formation or cloud-radiation interaction: dynamical forcing – large-scale or sub-grid scale, microphysical processes controlling the growth and phase of the various hydrometeors, complex geometry with possible overlapping of cloud layers. Most of these processes are sub-grid scale, and need to be parametrized in climate models.

As can be inferred from the description of the current climate models gathered by AMIP (AMIP, 1995; Gates *et al.*, 1999) the cloud schemes presently in use in the different modelling centres vary greatly in terms of complexity, consistency and comprehensiveness. However, there is a definite tendency toward a more consistent treatment of the clouds in climate models. The more widespread use of a prognostic equation for cloud water serves as a unifying framework coupling together the different aspects of the cloud physics, as noted in the

SAR. The evolution of the cloud schemes in the different climate models has continued since then.

The main model improvements can be summarised as follows:

(i) Inclusion of additional conservation equations representing different types of hydrometeors
A first generation of so-called prognostic cloud schemes (Le Treut and Li, 1991; Roeckner *et al.*, 1991; Senior and Mitchell, 1993; Del Genio *et al.*, 1996), has used a budget equation for cloud water, defined as the sum of all liquid and solid cloud water species that have negligible vertical fall velocities. The method allows for a temperature-dependent partitioning of the liquid and ice phases, and thereby enables a bulk formulation of the microphysical processes. By providing a time-scale for the residence of condensed water in the atmosphere, it provides an added physical consistency between the respective simulations of condensation, precipitation and cloudiness. The realisation that the transition between ice and liquid phase clouds was a key to some potentially important feedbacks has prompted the use of two or more explicit cloud and precipitation variables, thereby allowing for a more physically based distinction between cloud water and cloud ice (Fowler *et al.*, 1996; Lohmann and Roeckner, 1996).

(ii) Representation of sub-grid scale processes
The conservation equations to determine the cloud water concentration are written at the scale explicitly resolved by the model, whereas a large part of the atmospheric dynamics generating clouds is sub-grid scale. This is still an inconsistency in many models, as clouds generated by large-scale or convective motions are very often treated in a completely separate manner, with obvious consequences on the treatment of anvils for example. Several approaches help to reconcile these contradictions. Most models using a prognostic approach of cloudiness use probability density functions to describe the distribution of water vapour within a grid box, and hence derive a consistent fractional cover (Smith, 1990; Rotstayn, 1997). An alternative approach, initially proposed by Tiedtke (1993), is to use a conservation equation for cloud air mass as a way of integrating the many small-scale processes which determine cloud cover (Randall, 1995). Representations of sub-grid scale cloud features also require assumptions about the vertical overlapping of cloud layers, which in turn affect the determination of cloud radiative forcing (Jacob and Klein, 1999; Morcrette and Jakob, 2000; Weare, 2000a).

(iii) Inclusion of microphysical processes
Incorporating a cloud budget equation into the models has opened the way for a more explicit representation of the complex microphysical processes by which cloud droplets (or crystals) form, grow and precipitate (Houze, 1993). This is necessary to maintain a full consistency between the simulated changes of cloud droplet (crystal) size distribution, cloud water content, and cloud cover, since the nature, shape, number and size distribution of the cloud particles influence cloud formation and lifetime, the onset of precipitation (Albrecht, 1989), as well as cloud inter-

action with radiation, in both the solar and long-wave bands (Twomey, 1974). Some parametrizations of sub-grid scale condensation, such as convective schemes, are also complemented by a consistent treatment of the microphysical processes (Sud and Walker, 1999).

In warm clouds these microphysical processes include the collection of water molecules on a foreign substance (heterogeneous nucleation on a cloud condensation nucleus), diffusion, collection of smaller drops when falling through a cloud (coalescence), break-up of drops when achieving a certain threshold size, and re-evaporation of drops when falling through a layer of unsaturated air. In cold clouds, ice particles may be nucleated from either the liquid or vapour phase, and spontaneous homogeneous freezing of supercooled liquid drops is also relevant at temperatures below approximately –40°C. At higher temperatures the formation of ice particles is dominated by heterogeneous nucleation of water vapour on ice condensation nuclei. Subsequent growth of ice particles is then due to diffusion of vapour toward the particle (deposition), collection of other ice particles (aggregation), and collection of supercooled drops which freeze on contact (riming). An increase in ice particles may occur by fragmentation. Falling ice particles may melt when they come into contact with air or liquid particles with temperatures above 0°C.

Heterogeneous nucleation of soluble particles and their subsequent incorporation into precipitation is also an important mechanism for their removal, and is the main reason for the indirect aerosol effect. The inclusion of microphysical processes in GCMs has produced an impact on the simulation of the mean climate (Hahmann and Dickinson, 1997).

Measurements of cloud drop size distribution indicate a significant difference in the total number of drops and drop effective radius in the continental and maritime atmosphere, and some studies indicate that inclusion of more realistic drop size distribution may have a significant impact on the simulation of the present climate (Hahmann and Dickinson, 1997).

7.2.2.2 Convective processes

The interplay of buoyancy, moisture and condensation on scales ranging from millimetres to tens of kilometres is the defining physical feature of atmospheric convection, and is the source of much of the challenge in representing convection in climate models. Deep convection is in large measure responsible for the very existence of the troposphere. Air typically receives its buoyancy through being heated by contact with a warm, solar-heated underlying surface, and convection redistributes the energy received by the surface upwards throughout the troposphere. Shallow convection also figures importantly in the structure of the atmospheric boundary layer and will be addressed in Section 7.2.2.3.

Latent heat release in convection drives many of the important atmospheric circulations, and is a key link in the cycle of atmosphere-ocean feedbacks leading to the ENSO phenomenon. Convection is a principal means of transporting moisture vertically, which implies a role of convection in the radiative feedback due to both water vapour and clouds. Convection also in large measure determines the vertical temperature lapse rate of the atmosphere, and particularly so in the tropics. A strong

decrease of temperature with height enhances the greenhouse effect, whereas a weaker temperature decrease ameliorates it. The effect of lapse rate changes on clear-sky water vapour feedback has been studied by Zhang *et al.* (1994), but the significance of the lapse rate contribution (cf. item (5) of the SAR, Technical Summary) has been somewhat exaggerated through a misinterpretation of the paper. In fact the variation in lapse rate effects among the models studied alters the water vapour feedback factor by only 0.25 W/(m^{2}K), or about 10% of the total (Table 1 of Zhang *et al.*, 1994).

There is ample theoretical and observational evidence that deep moist convection locally establishes a "moist adiabatic" temperature profile that, loosely speaking, is neutrally buoyant with respect to ascending, condensing parcels (Betts, 1982; Xu and Emanuel, 1989). This adjustment happens directly at the scale of individual convective clouds, but dynamical processes plausibly extend the radius of influence of the adjustment to the scale of a typical GCM grid box, and probably much further in the tropics, where the lapse rate adjusts close to the moist adiabat almost everywhere. All convective schemes, from the most simple Moist Adiabatic Adjustment to those which attempt a representation of cloud-scale motions (Arakawa and Schubert, 1974; Emanuel, 1991), therefore agree in that they maintain the temperature at a nearly moist adiabatic profile. Moist Adiabatic Adjustment explicitly resets the temperature to the desired profile, whereas mass flux schemes achieve the adjustment to a near-adiabat as a consequence of equations governing the parametrized convective heating field. The constraint on temperature, however, places only a limited constraint on the moisture profile remaining after adjustment, and the performance in terms of moisture, clouds and precipitation may be very variable.

Since the SAR, a variety of simulations of response to CO$_2$ doubling accounting for combinations of different parametrizations have been realised with different models (Colman and McAvaney, 1995; Yao and Del Genio, 1999; Meleshko *et al.*, 2000). The general effects of the convection parametrization on climate sensitivity are difficult to assess because the way a model responds to changes in convection depends on a range of other parametrizations, so results are somewhat inconsistent between models (Colman and McAvaney, 1995; Thompson and Pollard, 1995; Zhang and McFarlane, 1995). There is some indication that the climate sensitivity in models with strong negative cloud feedback is insensitive to convective parametrization whereas models with strong positive cloud feedback show more sensitivity (Meleshko *et al.*, 2000).

7.2.2.3 Boundary-layer mixing and cloudiness

Turbulent motions affect all exchanges of heat, water, momentum and chemical constituents between the surface and the atmosphere, and these motions are also responsible for the mixing processes inside the atmospheric boundary layer. Consequently, the turbulent motions impact on the formation and existence of fog and boundary-layer clouds such as cumulus, stratocumulus and stratus. Cumulus is typically found in fair weather conditions over land and sea, while layers of stratocumulus and stratus can be found in subsidence areas such as the anticyclonic areas in the eastern part of the sub-tropical oceans, or the polar regions.

The atmospheric boundary layer with clouds is typically characterised by a well-mixed sub-cloud layer of order 500 metres, and by a more extended conditionally unstable layer with boundary-layer clouds up to 2 km. The latter layer is very often capped by a temperature inversion. If the clouds are of the stratocumulus or stratus type, then conservative quantities are approximately well mixed in the cloud layer. The lowest part (say 10%) of the sub-cloud layer is known as the surface layer. In this layer the vertical gradients of variables are normally significant, even with strong turbulent mixing. Physical problems associated with the surface layer depend strongly on the type of surface considered (such as vegetation, snow, ice, steep orography) and are treated in the corresponding sub-sections. We note that the surface characteristics do impact on the formation of boundary-layer clouds, because of the turbulent mixing inside the boundary layer.

Atmospheric models have great difficulty in the proper representation of turbulent mixing processes in general. This also impacts on the representation of boundary-layer clouds. At present, the underprediction of boundary-layer clouds is still one of the most distinctive and permanent errors of AGCMs. This has been demonstrated through AMIP intercomparisons by Weare and Mokhov (1995) and also by Weare (2000b). It has a very great importance, because the albedo effect of these clouds is not compensated for by a significant greenhouse effect in both clear-sky and cloudy conditions.

The persisting difficulty in simulation of observed boundary layer cloud properties is a clear testimony of the still inadequate representation of boundary-layer processes. A variety of approaches is followed, ranging from bulk schemes in which the assumption of a well-mixed layer is made *a priori*, to discretised approaches considering diffusion between a number of vertical layers. Here the corresponding diffusion coefficients are being computed from dimensional analysis and observational data fitted to it. The use of algorithms based on the prognostic computation of turbulent kinetic energy and higher-order closure hypotheses is also becoming more common and new schemes continue to be proposed (Abdella and McFarlane, 1997). A critical review and evaluation of boundary-layer schemes was recently made by Ayotte *et al*. (1996). They found that all schemes have difficulty with representing the entrainment processes at the top of even the clear boundary layer.

Important and still open problems include the decoupling between the turbulence at the surface and that within clouds, the non-local treatment of semi-convective cells (thermals) that can transport heat and substances upward, the role of moist physics, and microphysical aspects (Ricard and Royer, 1993; Moeng *et al.*, 1995; Cuijpers and Holtslag, 1998; Grenier and Bretherton, 2001). Several studies (Moeng *et al.*, 1996; Bretherton *et al.*, 1999; Duynkerke *et al.*, 1999) show that column versions of the climate models may predict a reasonable cloud cover in response to observed initial and boundary conditions, but have more difficulty in maintaining realistic turbulent fluxes. The results are also very dependent on vertical resolution and numerical aspects (Lenderink and Holtslag, 2000). This points to the need for new approaches for boundary-layer turbulence, both for clear-sky and cloudy conditions which are not so sensitive to vertical resolution (see also contributions in Holtslag and Duynkerke, 1998).

7.2.2.4 Cloud-radiative feedback processes

Clouds affect radiation both through their three-dimensional geometry and the amount, size and nature of the hydrometeors which they contain. In climate models these properties translate into cloud cover at different levels, cloud water content (for liquid water and ice) and cloud droplet (or crystal) equivalent radius. The interaction of clouds and radiation also involves other parameters (asymmetry factor of the Mie diffusion) which depend on cloud composition, and most notably on their phase. The subtle balance between cloud impact on the solar short-wave (SW) and terrestrial long-wave (LW) radiation may be altered by a change in any of those parameters. In response to any climate perturbation the response of cloudiness thereby introduces feedbacks whose sign and amplitude are largely unknown. While the SAR noted some convergence in the cloud radiative feedback simulated by different models between two successive intercomparisons (Cess *et al.*, 1990, 1995, 1996), this convergence was not confirmed by a separate consideration of the SW and LW components.

Schemes predicting cloudiness as a function of relative humidity generally show an upward displacement of the higher troposphere cloud cover in response to a greenhouse warming, resulting in a positive feedback (Manabe and Wetherald, 1987). While this effect still appears in more sophisticated models, and even cloud resolving models (Wu and Moncrieff, 1999; Tompkins and Emanuel, 2000), the introduction of cloud water content as a prognostic variable, by decoupling cloud and water vapour, has added new features (Senior and Mitchell, 1993; Lee *et al.*, 1997). As noted in the SAR, a negative feedback corresponding to an increase in cloud cover, and hence cloud albedo, at the transition between ice and liquid clouds occurs in some models, but is crucially dependent on the definition of the phase transition within models. The sign of the cloud cover feedback is still a matter of uncertainty and generally depends on other related cloud properties (Yao and Del Genio, 1999; Meleshko *et al.*, 2000).

Most GCMs used for climate simulations now include interactive cloud optical properties. Cloud optical feedbacks produced by these GCMs, however, differ both in sign and strength. The transition between water and ice may be a source of error, but even for a given water phase, the sign of the variation of cloud optical properties with temperature can be a matter of controversy. Analysis from the ISCCP data set, for example, revealed a decrease of low cloud optical thickness with cloud temperature in the sub-tropical and tropical latitudes and an increase at middle latitudes in winter (Tselioudis *et al.*, 1992; Tselioudis and Rossow, 1994). A similar relationship between cloud liquid water path and cloud temperature was found in an analysis of microwave satellite observations (Greenwald *et al.*, 1995). This is opposite to the assumptions on adiabatic increase of cloud liquid water content with temperature, adopted in early studies, and still present in many models. Changes in cloud water path reflect
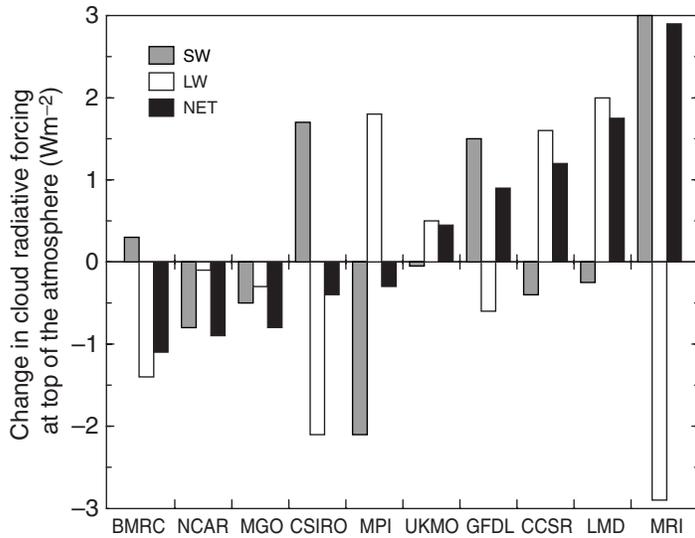
Figure 7.2: Change in the Top of the Atmosphere (TOA) Cloud Radiative Forcing (CRF) associated with a CO_2 doubling (from a review by Le Treut and McAvaney, 2000). The models are coupled to a slab ocean mixed layer and are brought to equilibrium for present climatic conditions and for a double CO_2 climate. The sign is positive when an increase of the CRF (from present to double CO_2 conditions) increases the warming, negative when it reduces it. The contribution of the short-wave (SW, solar) and long-wave (LW, terrestrial) components are first distinguished, and then added to provide a net effect (black bars). Results presented in the diagram are bounded by a 3 Wm^{-2} limit. As in Chapter 8, Table 8.1, the acronyms refer to the atmospheric models of the following institutions: BMRC is the Bureau of Meteorology Research Center (Australia); NCAR is the National Center for Atmospheric Research (USA); CSIRO is the Commonwealth Scientific and Industrial Research Organization (Australia); MPI the Max Planck Institute for Meteorology (Germany); UKMO refers to the model of the Hadley Centre (UK); GFDL is the Geophysical Fluid Dynamics Laboratory (USA); CCSR is the Center for Climate System Research (Japan); LMD is the Laboratoire de Météorologie Dynamique (the corresponding coupled model being referenced as IPSL, France); MRI is the Meteorological Research Institute (Japan). The MGO model appears only in this intercomparison and is the model of the Main Geophysical Observatory (Russia) (see reference in Meleshko *et al.*, 2000).

Figure 7.3: Relationship between simulated global annually averaged variation of net cloud radiative forcing at the top of the atmosphere and precipitable water due to CO_2 doubling produced in simulations with different parametrizations of cloud related processes. Results are from Colman and McAvaney (1995) denoted by triangles, Meleshko *et al.* (2000) denoted by open circles, and Yao and Del Genio (1999) denoted by diamonds.

different effects which may partially compensate, such as changes in cloud vertical extension or cloud water content. The role of low cloud optical thickness dependence on climate was tested in 2×CO_2 experiments using the GISS GCM, in which simulations with fixed or simulated cloud optical properties were compared (Tselioudis *et al.*, 1998). In spite of a low impact on global sensitivity, these results showed a strong cloud impact on the latitudinal distribution of the warming. High latitude warming decreased while low latitude warming increased, resulting in a large decrease in the latitudinal amplification of the warming (by 20% in the Northern Hemisphere and by 40% in the Southern Hemisphere).

Since the SAR, there has been much progress in the use of simplified tropical models to understand the impact of cloud
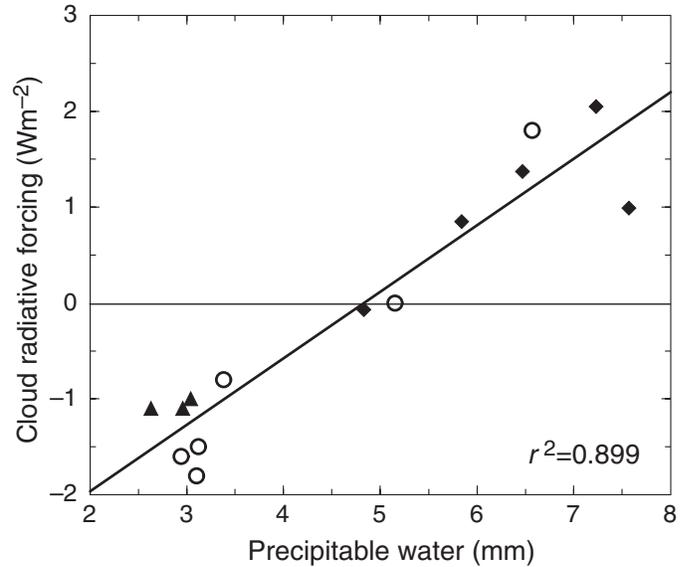
feedbacks, and to address the issue of whether cloud feedbacks impose an upper limit on SST. This problem has been addressed in simplified models that maintain consistency with the whole-tropics energy budget (Pierrehumbert, 1995; Clement and Seager, 1999; Larson *et al.*, 1999). Diagnostic studies have suggested both destabilising (Chou and Neelin, 1999) and stabilising (Lindzen *et al.*, 2001) cloud feedbacks. None of this supports the existence of a strict limitation of maximum tropical SST of the sort proposed by Ramanathan and Collins (1991), which has been criticised on the grounds that it does not respect the whole-tropics energy budget, and that it employs an incorrect means of determining the threshold temperature for convection. It is beyond question that the increased cloudiness prevailing over the warmer portions of the Pacific has a strong effect on the surface energy budget, which is fully competitive with the importance of evaporation. Determination of SST, however, requires a consistent treatment of the top-of-atmosphere energy budget, and cannot be effected with reference to the surface budget alone. This does not preclude the possibility that other cloud feedback mechanisms could have a profound effect on tropical SST, and in no way implies that cloud representation is inconsequential in the tropics. Meehl *et al.* (2000) illustrate this point when they show how a change from a diagnostic prescription of clouds in the NCAR atmospheric GCM to a prognostic cloud liquid water formulation changes the sign of net cloud forcing in the eastern tropical Pacific and completely alters the nature of the coupled model response to increased greenhouse gases.

7.2.2.5 Representation of cloud processes in models
Over the last 10 years, the generalised availability of satellite retrievals (OLR, water path, cloud cover, cloud top temperature) has strongly increased the possibility of assessing clouds simulated by climate models, in spite of remaining uncertainties concerning the vertical structure of the cloud systems, of large importance for all feedback effects. Yet this remains a very difficult task, which may be illustrated by a few figures. Recent simulations of equilibrium climate with a doubling of CO_2 indicate that the induced variation of net cloud radiative forcing short-wave or long-wave, ranges within ± 3 Wm^{-2}, which is a small fraction of the cloud mean long-wave warming (30 to 35 Wm^{-2}) or cloud mean short-wave cooling (45 to 50 Wm^{-2}) (Le Treut and McAvaney, 2000; Figure 7.2). Although most models simulate CRF values within the uncertainty range of the observed values, the discrepancy in terms of response to CO_2 increase is large, both in sign, amplitude, and share between long-wave and short-wave. This disagreement (amplified by the water vapour feedback) reflects the sensitivity of the simulated feedbacks to model formulation (Watterson *et al.*, 1999; Yao and Del Genio, 1999; Meleshko *et al.*, 2000) and is the cause of the large spread in model climate sensitivity (see Figure 7.3; and Chapters 8 and 9). The correct simulation of the mean distribution of cloud cover and radiative fluxes is therefore a necessary but by no means sufficient test of a model's ability to handle realistically the cloud feedback processes relevant for climate change.

Satellite records provide some access to the study of natural climate fluctuations, such as the seasonal or ENSO cycles, which can be used to test the ability of the models to represent different feedbacks. At these time-scales, however, cloud structures are characterised by large shifts in their latitudinal or longitudinal position, as well as changes in their vertical distribution in response to SST changes. Only those latter effects are really relevant to test climate models in the context of climate change. Bony *et al.* (1997) have shown that in the inter-tropical regions, it was possible to isolate them by looking at the dependence of cloud properties on SST for specified dynamical regimes. These regressions are remarkably consistent when carried out with different sets of independent data (ISCCP, ERBE, TOVS, SSMI) and offer a constraining test for models. Similar methodologies are being developed for the mid-latitudes (Tselioudis *et al.*, 2000). It is encouraging, though, that CCM3 has demonstrated considerable accuracy in the reproduction of regional all-sky long-wave and short-wave radiation budgets (Kiehl *et al.*, 1998).

Since the SAR, there has been progress in the qualitative understanding of the complexity of cloud/climate relation. There is also an important and ongoing evolution of the cloud parametrizations included into the models, which is characterised by a greater physical consistency and a greatly enhanced physical content: in particular many models now include a more comprehensive representation of sub-grid scales, convective or turbulent, and explicit microphysics, liquid or ice. Simulation of current climate with those advanced models demonstrate capability to reproduce realistically many features of the cloud radiative forcing and its seasonal variations, for both the solar and terrestrial components.

In spite of these improvements, there has been no apparent narrowing of the uncertainty range associated with cloud feedbacks in current climate change simulations. A straightforward approach of model validation is not sufficient to constrain the models efficiently and a more dedicated approach is needed. This should be favoured by a greater availability of satellite measurements.

7.2.3 Precipitation

Precipitation drives the continental hydrology, and influences the salinity of the ocean. The distribution of the precipitation in space and time, is therefore of key importance. The amount of precipitation also constitutes a measure of the latent heat release within the atmosphere. The long-term global mean precipitation of 984 mm/yr implies a vertically integrated mean heating rate of 78 Wm^{-2} (Arkin and Xie, 1994; Kiehl and Trenberth, 1997). The local precipitation rate on horizontal spatial scales of 1 to 10 km are 10 to 1,000 times the global number so that the associated heating rates often dominate all other effects and strongly influence local and global circulations. Precipitation also acts to remove and transport aerosols and soluble gases both within and below clouds, and thus strongly affects the chemical composition and aerosol distribution. The suspended and precipitating condensates provide sites for aqueous and surface chemical reactions.

The highly variable rain rates and enormous spatial variability makes determination of mean precipitation difficult, let alone how it will change as the climate changes. For instance, a detailed examination of spatial structure of daily precipitation amounts by Osborn and Hulme (1997) shows that in Europe the average separation distance between climate stations where the correlation falls to 0.5 is about 150 km in summer and 200 km in winter. This complexity makes it difficult to model precipitation reliably, as many of the processes of importance cannot be resolved by the model grid (typically 200 km) and so sub-grid scale processes have to be parametrized.

7.2.3.1 Precipitation processes
Precipitation is usually considered to be of stratiform or convective nature, or a mixture of the two. In stratiform precipitation the vertical velocity of air, usually forced by developing low pressure systems, monsoonal circulations, or underlying orography, is comparable to or smaller than the fall speed of snow and ice crystals. Stratiform precipitation dominates in the extra-tropics except over continents in summer, and there is substantial spatial coherency on scales up to and beyond about 100 km. In contrast, convective precipitation systems are associated with vigorous latent-heat-driven vertical circulations on horizontal scales of a few kilometres. Convection is responsible for most of the precipitation in the tropics and middle latitude continents in summer. In many cases, convective and stratiform precipitation interact or occur together, for instance as convective cells are embedded within areas of stratiform precipitation.

7.2.3.2 Precipitation modelling
There is increasing evidence that the use of one or more prognostic cloud water variables for the modelling of stratiform

precipitation is fairly successful in simulating continental and sub-continental scale precipitation distributions, including orographic precipitation, provided the synoptic-scale circulation is properly accounted for. This is the case for numerical weather predictions in the short-term range of 1 to 2 days (Petroliagis *et al.*, 1996), and regional climate models driven by observed lateral boundary conditions (e.g., Jones *et al.*, 1995; Lüthi *et al.*, 1996; Christensen *et al.*, 1998; Giorgi *et al.*, 1998). Cloud schemes that include an explicit cloud water variable and some parametrization of the ice phase (either by carrying an explicit cloud ice variable or by including a temperature-dependent formulation of microphysical conversion rates) appear able to credibly reproduce some of the major features of the observed intensity-frequency relations (Frei *et al.*, 1998; Murphy, 1999).

In contrast, the simulation of convective precipitation, which is fully parametrized, is of substantially poorer quality over continental regions. In a recent intercomparison study that attempted to simulate dry and wet summers over the continental US, large inter-model and model-observation differences were found (Takle *et al.*, 1999), although the larger-scale atmospheric circulation was prescribed. One specific difficulty is the strong diurnal cycle of convective precipitation over land, which is accompanied by the build-up of a well-mixed boundary layer in response to solar heating prior to the onset of convection. Recent studies (Yang and Slingo, 1998; Dai *et al.*, 1999) find that moist convection schemes tend to initiate convection prematurely as compared with the real world, and instability does not build up adequately. Premature cloud formation prevents the correct solar heating from occurring, impacting the development of the well-mixed boundary layer and continental-scale convergence at the surface, which in turn affects the triggering of convection. Scale interactions between convection that is organised by somewhat larger scales also seem to underlie the difficulties all GCMs have in simulating the Madden-Julian Oscillation of intra-seasonal variations in the deep tropics (Slingo *et al.*, 1996).

7.2.3.3 The temperature-moisture feedback and implications for precipitation and extremes

With increasing temperature, the surface energy budget tends to become increasingly dominated by evaporation, owing to the increase in the water holding capacity of the boundary layer. The increase of evaporation is not strictly inevitable (Pierrehumbert, 1999), but it occurs in all general circulation models, though with varying strength. Simulated evapotranspiration and net atmospheric moisture content is also found to increase (Del Genio *et al.*, 1991; Trenberth, 1998), as is observed to be happening in many places (Hense *et al.*, 1988; Gaffen *et al.*, 1992; Ross and Elliot, 1996; Zhai and Eskridge, 1997). Globally there must be an increase in precipitation to balance the enhanced evaporation but the processes by which precipitation is altered locally are not well understood. Over land, enhanced evaporation can occur only to the extent that there is sufficient soil moisture in the unperturbed state. Naturally occurring droughts are likely to be exacerbated by enhanced potential evapotranspiration, which quickly robs soil of its moisture.

Because moisture convergence is likely to be proportionately enhanced as the moisture content increases, it should lead to similarly enhanced precipitation rates. Moreover, the latent heat released feeds back on the intensity of the storms. These factors suggest that, while global precipitation exhibits a small increase with modest surface warming, it becomes increasingly concentrated in intense events, as is observed to be happening in many parts of the world (Karl *et al.*, 1995), including the USA (Karl and Knight, 1998), Japan (Iwashima and Yamamoto, 1993) and Australia (Suppiah and Hennessy, 1998), thus increasing risk of flooding. However, the overall changes in precipitation must equal evaporation changes, and this is smaller percentage-wise than the typical change in moisture content in most model simulations (e.g., Mitchell *et al.*, 1987; Roads *et al.*, 1996). Thus there are implications for the frequency of storms or other factors (duration, efficiency, etc.) that must come into play to restrict the total precipitation. One possibility is that individual storms could be more intense from the latent heat enhancement, but are fewer and farther between (Trenberth, 1998, 1999).

These aspects have been explored only to a limited extent in climate models. No studies deal with true intensity of rainfall, which requires hourly (or higher resolution) data, and the analysis is typically of daily rainfall amounts. Increases in rain intensity and dry periods are simulated along with a general decrease in the probability of moderate precipitation events (Whetton *et al.*, 1993; Cubasch *et al.*, 1995; Gregory and Mitchell, 1995; Mearns *et al.*, 1995; Jones *et al.*, 1997; Zwiers and Kharin, 1998; McGuffie *et al.*, 1999). For a given precipitation intensity of 20 to 40 mm/day, the return periods become shorter by a factor of 2 to 5 (Hennessy *et al.*, 1997). This effect increases with the strength of the event (Fowler and Hennessy, 1995; Frei *et al.*, 1998). However, estimates of precipitation and surface long-wave radiation suggest that the sensitivity of the hydrological cycle in climate models to changes in SST may be systematically too weak (Soden, 2000). Accordingly, it is important that much more attention should be devoted to precipitation rates and frequency, and the physical processes which govern these quantities.

7.2.4 Radiative Processes

7.2.4.1 Radiative processes in the troposphere

Radiative processes constitute the ultimate source and sink of energy in the climate system. They are generally well known, and particularly the clear-sky long-wave transfer, including the absorption properties of most greenhouse gases. Their treatment in atmospheric general circulation models relies on several approximations: the fluxes are computed as averaged quantities over a few spectral intervals, the propagation is limited to the vertical upwelling or downwelling directions, and the role of sub-grid scale features of the clouds or aerosols is essentially neglected. Although this methodology is believed to have only a marginal impact on the accuracy of computed long-wave fluxes, the analysis of satellite, ground-based or aircraft measurements (Cess *et al.*, 1995; Pilewskie and Valero, 1995; Ramanathan *et al.*, 1995) has generated a concern that the radiative algorithms used in climate models could significantly underestimate the atmospheric shortwave absorption. Similar results have been obtained as part of the ARM/ARESE experiment (Valero *et al.*,

1997; Zender *et al.*, 1997). The excess, or "anomalous" observed absorption may reach typical values of about 30 to 40 Wm^{-2}. Its very existence, however, remains controversial and is at odds with other investigations. Li *et al.* (1995) analysed large global data sets from satellite (ERBE) and ground observations (GEBA). They did not find the anomalous absorption except for a few tropical sites over a short period of time. The exception appears to be induced by enhanced absorption due to biomass burning aerosols (Li, 1998). Limited accuracy of the measurements (Imre *et al.*, 1996) and the methodology of analysis (Arking *et al.*, 1996; Stephens, 1996; Barker and Li, 1997) have been raised as possible contributing factors to the finding of the anomalous absorption.

A comparison of the ARM-ARESE measurements with a state of the art radiation code, which uses measured atmospheric quantities as an input, and relies on the same physical assumptions as used in climate models, indicated that the anomalous absorption is larger for cloudy than for clear conditions, and also tends to be larger for visible rather than for near-infrared fluxes (Zender *et al.*, 1997). These two characteristics are consistent with the results of a comparison between the output of the CCM3 general circulation model and observations from Nimbus 7 (Collins, 1998). However, Li *et al.* (1999) analysed all the data sets collected during the ARM/ARESE experiment made by space-borne, air-borne and ground-based instruments and did not find any significant absorption anomaly. They traced the source of controversial findings to be associated with inconsistent measurements made by some air-borne radiometers as used in the studies of Valero *et al.* (1997) and Zender *et al.* (1997) with those from all other instruments. However, other studies (Cess *et al.*, 1999; Pope and Valero, 2000; Valero *et al.*, 2000), that do find a significant absorption anomaly, have further demonstrated that the ARESE data do indeed satisfy a number of consistency tests as well as being in agreement with measurements made by other instruments. Meanwhile, evidence of enhanced cloud absorption has been found from measurements of the MGO aircraft laboratory (Kondratyev *et al.*, 1998). Inclusion of anomalous absorption has been found to improve the representation of atmospheric tides (Braswell and Lindzen, 1998). There finally exists evidence of an effect associated with clear-sky conditions – in the presence of aerosols: models tend to overpredict clear-sky diffusion to the surface (Kato *et al.*, 1997).

The three dimensional nature of the solar radiation diffusion by cloud (Breon, 1992; Cahalan *et al.*, 1994; Li and Moreau, 1996) is unaccounted for by present climate models and may play some role in anomalous absorption. In a recent study using a Monte-Carlo approach to simulate three-dimensional radiative transfer, O'Hirok and Gautier (1998a; 1998b) show that cloud inhomogeneities can increase both the near-infrared gaseous absorption and cloud droplet absorption in morphologically complex cloud fields. The enhancement is caused when photons diffused from cloud edges more easily reach water-rich low levels of the atmosphere and when photons entering the sides of clouds become trapped within the cloud cores. The amplitude of those effects remains limited to an average range of 6 to 15 Wm^{-2}, depending on the solar angle. The inhomogeneities significantly affect the vertical distribution of the heating, though, with

potential consequences on cloud development. Incorporating the effect of cloud inhomogeneities in radiative algorithms may become a necessity, and recent efforts have been made along that path (Oreopoulos and Barker, 1999).

If anomalous absorption turns out to be real, it is an effect that will need to be incorporated into radiation schemes. Evaluation of its importance is hampered by lack of knowledge of a physical mechanism responsible for the absorption, and hence lack of a physical basis for any parametrization. Modelling studies by Kiehl *et al.* (1995) have demonstrated the sensitivity of the simulated climate to changes in the atmospheric absorption. As a radiative forcing, anomalous absorption is fundamentally different from water vapour or CO_2 in that it does not significantly alter the Earth's net radiation budget. Instead, it shifts some of the deposition of solar energy from the ground to the atmosphere (Li *et al.*, 1997), with implications for the hydrological cycle and vertical temperature profile of the atmosphere. Anomalous absorption may not, however, appreciably affect climate sensitivity (Cess *et al.*, 1996).

Model validation is also affected. Many of the data which are used to tune or validate model parametrizations, such as the Liquid Water Path (LWP) or the droplet equivalent radius, are obtained from space measurements by the inversion of radiative algorithms, which ignore cloud inhomogeneities and anomalous absorption. This gives a strong importance to satellite instruments such as POLDER which provide measurements of the same scene at a variety of viewing angles, and provides a good test of the plane-parallel hypothesis in retrievals of cloud quantities.

7.2.4.2 Radiative processes in the stratosphere

The stratosphere lies immediately above the troposphere, with the height of the bounding tropopause varying from about 15 km in the tropics to about 7 km at high latitudes. The mass of the stratosphere represents only about 10 to 20% of the total atmospheric mass, but changes in stratospheric climate are important because of their effect on stratospheric chemistry, and because they enter into the climate change detection problem (Randel and Wu, 1999; Shine and Forster, 1999). In addition there is a growing realisation that stratospheric effects can have a detectable and perhaps significant influence on tropospheric climate.

Solar radiative heating of the stratosphere is mainly from absorption of ultraviolet (UV) and visible radiation by ozone, along with contributions due to the near-infrared absorption by carbon dioxide and water vapour. Depletion of the direct and diffuse solar beams arises from scattering by molecules, aerosols, clouds and surface (Lacis and Hansen, 1974).

The long-wave process consists of absorption and emission of infrared radiation, principally by carbon dioxide, methane, nitrous oxide, ozone, water vapour and halocarbons (CFCs, HFCs, HCFCs, PFCs etc.). The time-scales for the radiative adjustment of stratospheric temperatures is less than about 50 to 100 days.

For CO_2, part of the main 15 micron band is saturated over quite short vertical distances, so that some of the upwelling radiation reaching the lower stratosphere originates from the cold upper troposphere. When the CO_2 concentration is increased, the increase in absorbed radiation is quite small and increased

emission leads to a cooling at all heights in the stratosphere. But for gases such as the CFCs, whose absorption bands are generally in the 8 to 13 micron "atmospheric window", much of the upwelling radiation originates from the warm lower troposphere, and a warming of the lower stratosphere results, although there are exceptions (see Pinnock *et al.*, 1995). Methane and nitrous oxide are in between. In the upper stratosphere, increases in all well-mixed gases lead to a cooling as the increased emission becomes greater than the increased absorption. Equivalent CO_2 is the amount of CO_2 used in a model calculation that results in the same radiative forcing of the surface-troposphere system as a mixture of greenhouse gases (see e.g., IPCC, 1996) but does not work well for stratospheric temperature changes (Wang *et al.*, 1991; Shine, 1993; WMO, 1999).

An ozone loss leads to a reduction in the solar heating, while the major long-wave radiative effects from the 9.6 and 14 micron bands (Shine *et al.*, 1995) produce a cooling tendency in the lower stratosphere and a positive radiative change above (Ramaswamy *et al.*, 1996; Forster *et al.*, 1997). Large transient loadings of aerosols in the stratosphere follow volcanic eruptions (IPCC, 1996) which leads to an increase of the heating in the long-wave. For the solar beam, aerosols enhance the planetary albedo while the interactions in the near-infrared spectrum yield a heating which is about one third of the total solar plus long-wave heating (IPCC, 1996; WMO, 1999). In addition, ozone losses can result from heterogeneous chemistry occurring on or within sulphate aerosols, and those changes produce a radiative cooling (Solomon *et al.*, 1996).

The Antarctic ozone hole is a stratospheric phenomenon with a documented impact on temperature and, during the period 1979 to 1994, ozone decreases very likely contributed a negative radiative forcing of the troposphere-surface that offset perhaps as much as one half of the positive radiative forcing attributable to the increases in CO_2 and other greenhouse gases (Hansen *et al.*, 1997; Shine and Forster, 1999). It appears that most of the observed decreases in upper-tropospheric and lower-stratospheric temperatures were due to ozone decreases rather than increased CO_2 (Ramaswamy *et al.*, 1996; Tett *et al.*, 1996; Bengtsson *et al.*, 1999).

The subject of solar effects on climate and weather (see Section 6.10) has enjoyed a recent resurgence, in part because of observational studies (Labitzke and van Loon, 1997), but more so because of modelling studies that suggest viable mechanisms involving the stratosphere. As solar irradiance changes, proportionally much greater changes are found in the ultraviolet which leads to photochemically induced ozone changes, and the altered UV radiation changes the stratospheric heating rates per amount of ozone present (Haigh, 1996; Shindell *et al.*, 1999a). Including the altered ozone concentrations gave an enhanced tropospheric response provided the stratosphere was adequately resolved.

7.2.5 Stratospheric Dynamics

Waves generated in the troposphere propagate into the stratosphere and are absorbed, so that stratospheric changes alter where and how they are absorbed, and effects can extend downward into the troposphere through a mechanism called "downward control"

(Haynes *et al.*, 1991). The downward propagation of zonal-mean anomalies provides a purely dynamical stratosphere-troposphere link, which may account for the well-documented troposphere-stratosphere anomaly correlations seen in observations (Baldwin *et al.*, 1994; Perlwitz and Graf, 1995). The North Atlantic Oscillation (Section 7.6.4) thus could be coupled with the strength of the wintertime Arctic vortex (Thompson and Wallace, 1998).

The dominant wave-induced forcing in the stratosphere is believed to come from tropospherically generated planetary scale Rossby waves in wintertime. These waves are explicitly resolved in models and data. Thus the meridional mass circulation, although two-celled, is predominantly directed towards the winter pole (e.g., Eluszkiewicz *et al.*, 1996), and leads to a significant warming and weakening of the polar night vortex relative to its radiatively determined state (Andrews *et al.*, 1987). Variability and changes in planetary wave forcing thus lead directly to variability and changes in wintertime polar temperatures, which modulate chemical ozone loss (WMO, 1999).

The principal uncertainties in wave-induced forcing come from gravity waves, which are undetected in analyses, but whose role is inferred from systematic errors in climate models. The most notable such error is the tendency of all atmospheric GCMs to suffer from excessively cold polar temperatures in the winter stratosphere, together with an excessively strong polar night jet, especially in the Southern Hemisphere (Boville, 1995). Enhanced Rayleigh friction improves the results (Manzini and Bengtsson, 1996; Butchart and Austin, 1998), but its physical basis is unclear (Shepherd *et al.*, 1996). The principal forcing of gravity waves arises from unresolved sub-grid scale processes, such as convection, and more physically based gravity wave parametrizations are being developed.

A dominant factor determining the interannual variability of the stratosphere is the quasi-biennial oscillation (QBO). It is driven by wave drag (momentum transport), but it remains unclear exactly which waves are involved (Dunkerton, 1997). Most current atmospheric GCMs do not simulate the QBO and are therefore incomplete in terms of observed phenomena. It appears that QBO-type oscillations are found in models with higher vertical resolution (better than 1 km, Takahashi, 1996; Horinouchi and Yoden, 1998). It is still not clear what aspects of vertical resolution, energy dissipation, and wave spectrum are necessary to generate the QBO in climate models in a self-consistent way.

The meridional mass circulation, known as the Brewer-Dobson circulation, transports chemical species poleward in the stratosphere (Andrews *et al.*, 1987). Air entering the stratosphere in the tropics returns to the troposphere in the extratropics with a time-scale of about five years (Rosenlof, 1995). Current models indicate shorter time-scales (Waugh *et al.*, 1997), but the reasons are not currently well understood. The variation of the height of the troposphere with latitude is also important for meridional transport and troposphere-stratosphere exchange. This is because mid-latitude cross-tropopause mixing is preferentially along isentropic surfaces which are in the troposphere in the tropics but in the stratosphere at higher latitudes. Transport processes in the lowermost stratosphere are important factors affecting tropospheric climate (Pan *et al.*, 1997).

The mean climate and variability of the stratosphere are not well simulated in current models. Because there is increasing evidence of effects of the stratosphere on the troposphere, this increases uncertainty in model results for tropospheric climate change. A key concern is how well mixing on small scales is done in the lowermost stratosphere. While overdue attention is being given to the stratosphere as more resolution in the vertical is added to models, further increases in resolution are desirable.

7.2.6 Atmospheric Circulation Regimes

There is growing evidence that patterns of atmospheric intra-seasonal and interannual variability have preferred states (i.e., local maxima in the probability density function of atmospheric variables in phase space) corresponding to circulation regimes. Using atmospheric data, Corti *et al*. (1999) showed four distinct circulation patterns in the wintertime Northern Hemisphere. These geographical patterns correspond to conventional patterns of low-frequency atmospheric variability which include the so-called "Cold Ocean Warm Land" (COWL; Section 7.6) pattern, the negative Pacific North American pattern, and the so-called negative Arctic Oscillation pattern.

Simplified dynamical models, which represent fundamental aspects of atmospheric circulation, react to external forcing initially by changes in the recurrence frequency of the patterns rather than by changes in the patterns themselves (Palmer, 1999). Therefore, anthropogenically forced climate changes may also be expressed in an altered pattern frequency. It appears that the observed northern hemispheric changes can be associated, to some extent, with a more frequent occurrence of the COWL pattern (Corti *et al.*, 1999), i.e., the horizontal structure of recent climate change is correlated with the horizontal pattern of natural variability.

These results indicate that detailed predictions of anthropogenic climate change require models which can simulate accurately natural circulation patterns and their associated variability, even though the dominant time-scale of such variability may be much shorter than the climate change signal itself. This regime view of climate change has recently been shown in GCM simulations (Monahan *et al.*, 2000).

7.2.7 Processes Involving Orography

The major mountain ranges of the world play an important role in determining the strength and location of the atmospheric jet streams, mainly by generating planetary-scale Rossby waves and through surface drag. Orography acts both through large-scale resolved lifting and diversion of the flow over and around major mountain ranges, and through sub-grid scale momentum transport due to vertically propagating gravity waves at horizontal scales between 10 and 100 km. The limited horizontal resolution of climate GCMs implies a smoothing of the underlying topography which has sometimes been counteracted by enhancing the terrain by using an envelope orography, but this has adverse effects by displacing other surface physical processes. The sub-grid scale momentum transport acts to decelerate the upper-level flow and is included by gravity-wave drag parametrization schemes (e.g., Palmer *et al.*, 1986; Kim, 1996; Lott and Miller, 1997).

No systematic studies are available to assess the impacts of these procedures and schemes on climate sensitivity and variability. The orographic impact is most pronounced in the Northern Hemisphere winter. Gravity wave drag implies a reduction in the strength of the mid-latitude jet stream by almost $20 \ \mathrm{ms^{-1}}$ (Kim, 1996), and alters the amplitude and location of the planetary-scale wave structure (e.g., Zhou *et al.*, 1996). Convective precipitation in models is often spuriously locked onto high topography. Thus the numerical simulation of many key climatic elements, such as rainfall and cloud cover, strongly depends upon orography and is strongly sensitive to the horizontal resolution employed. As such, it is possible that phenomena of climate variability are sensitive to orographic effects and their parametrization (Palmer and Mansfield, 1986). These issues may have potentially important consequences for the planetary-scale distribution of climate change.

7.3 Oceanic Processes and Feedbacks

The ocean influences climate and climate change in various ways. Ocean currents transport a significant amount of heat, usually directed poleward and thus contributing to a reduction of the pole-to-equator temperature gradient; a remarkable exception exists however in the South Atlantic where heat is transported equatorward, i.e. up-gradient, into the North Atlantic. Because of its large heat capacity, ocean heat storage largely controls the time-scales of variability to changes in the ocean-atmosphere system, including the time-scales of adjustment to anthropogenic radiative forcing. The ocean is coupled to the atmosphere primarily through the fluxes of heat and fresh water which are strongly tied to the sea surface temperature (see Section 7.6.1), and also through the fluxes of radiatively active trace gases such as CO_2 (see Chapter 3) which can directly affect the atmospheric radiation balance. All ocean processes which ultimately can influence these fluxes are relevant for climate change. Processes in the ocean surface layer which are associated with seasonal time-scales hence are of obvious relevance. As the budgets in the surface layer depend on the exchange with deeper layers in the ocean, it is also necessary to consider the processes which affect the circulation and water mass distribution in the deep ocean, in particular when the response of the climate system at decadal and longer time-scales is considered. Moreover, processes governing vertical mixing are important in determining the time-scales on which changes of, for example, deep ocean temperature and sea level evolve.

Since the SAR, the assessment of the status of ocean processes in climate models has changed in two ways. On the one hand, advances in model resolution and in the representation of sub-grid scale processes have led to a somewhat improved realism in many model simulations. On the other hand, however, growing evidence for a very high sensitivity of model results to the representation of certain small-scale processes, in particular those associated with the THC, has been found. As a consequence, considerable uncertainties still exist concerning the extent to which present climate models correctly describe the oceanic response to changes in the forcing.

7.3.1 Surface Mixed Layer

The surface mixed layer is directly influenced by the atmospheric fluxes which are connected to the ocean interior by vigorous three-dimensional turbulence. That turbulence is driven primarily by the surface wind stress and convective buoyancy flux, and includes the wave driven Langmuir circulation (e.g., Weller and Price, 1988; McWilliams *et al.*, 1997). As a result, the upper ocean often becomes well mixed.

The heat budget of the mixed layer is determined by horizontal advection, surface heating, entrainment and the vertical heat flux at the mixed-layer base. Entrainment occurs when there is sufficient turbulent energy to deepen the mixed layer and can result in rapid cooling when accompanied by upwelling from Ekman pumping. This pumping velocity at the mixed-layer base results from divergent mixed-layer flow driven by the wind stress. The shallowing of the mixed layer leads to a transfer of water from the mixed layer to the interior of the ocean. The water that passes the deepest mixed-layer depth will not be re-entrained within a seasonal cycle and is subducted. Large subduction rates are found where horizontal gradients in mixed layer depth are large. Thus variations in mixed-layer depth are of primary importance in setting the structure of the interior of the ocean. This process can temporarily shield heat anomalies generated in the mixed layer from the atmosphere. The subduction process itself is relatively well understood (Spall *et al.*, 2000), although the role of sub-grid processes in modifying the subduction process needs further clarification (Hazeleger and Drijfhout, 2000).

The surface buoyancy flux (combined net heat and fresh water flux) effectively drives a cross-isopycnal mass flux by converting mixed-layer water from one density class to another. Waters of intermediate density are transformed into both lighter waters and heavier waters. In general, but especially in the Indian and Pacific Oceans, the thermal and haline contributions are additive in forming light tropical waters, but opposed in forming heavy polar waters. Despite this cancellation about 15 Sv (1 Sverdrup = 1 Sv = $10^6 m^3 s^{-1}$) of North Atlantic Deep Water (NADW) is formed thermally. With more cancellation, less than a few Sverdrups of Antarctic Bottom Water (AABW) is formed in the Southern Ocean. However, nearly 30 Sv of Antarctic Intermediate Water is formed mostly by the haline effect.

In summary, proper parametrization of turbulence in the surface mixed layer is crucial to correctly simulate air-sea exchange, SST and sea ice (e.g., Large *et al.*, 1997; Goosse *et al.*, 1999), and thereby reduce the need for flux adjustments in coupled models. While several schemes are in use (Large and Gent, 1999), a systematic intercomparison of the properties, behaviour and accuracy of these parametrizations is still lacking.

7.3.2 Convection

Open ocean convection occurs every winter at high latitudes when buoyancy loss at the sea surface causes the surface layer to become denser than the water below, and results in highly variable mixing depth as a function of space and time (see recent review by Marshall and Schott, 1999). Convection directly affects the SST locally, and on larger scales indirectly through its effect on water mass properties and circulation. The maximum depth of convection occurs at the end of the cooling season, and depends on the balance between the cumulative air-sea fluxes, including ice-melt and precipitation, and the oceanic advection of buoyancy. During the summer, shallow warm surface mixed layers isolate the newly formed deep water from the atmosphere and mean currents and mesoscale eddies steadily transfer the newly formed deep water into the abyssal ocean.

Deep convective mixing is an essential ingredient of the THC, in particular in the North Atlantic, and is thus important for climate problems. It constitutes a very efficient vertical transfer process, and only a few small regions are needed to offset the slow diffusive buoyancy gain due to vertical (diapycnal) mixing (see also Section 7.3.3; e.g., Winton, 1995). Major sites of known open ocean deep convection are the centre of the Greenland Sea (Schott *et al.*, 1993; Visbeck *et al.*, 1995), Labrador Sea (LabSea Group, 1998) and a small region in the north-western Mediterranean Sea (Schott *et al.*, 1996). However, only the Labrador Sea is in direct contact with the NADW which replenishes the deep waters of the Atlantic, Pacific and Indian Oceans. In the Greenland Sea deep and bottom waters remain local to the Arctic Ocean and deep basins north of Iceland and have no direct influence on the Denmark Strait Overflow (Mauritzen, 1996). Deep water formed in the Mediterranean Sea also never directly outflows through the Strait of Gibraltar. Dense water also forms on the shelf where convection can reach to the sea floor producing a well-mixed layer of dense water. Several mechanisms, such as eddies, flow over canyons and time-varying shelf break fronts, allow the dense water to enter into the deep ocean via descending plumes. This 'shelf convection' is believed to be fairly widespread around the Antarctic continent and is probably the primary mechanism by which AABW is formed (Orsi *et al.*, 1999). AABW is the densest bottom water and penetrates into all of the three major oceans.

The overall effect of open ocean convection is usually parametrized through simple convective-adjustment schemes (Marotzke, 1991) which have been found to work well (Klinger *et al.*, 1996). More advanced schemes have a somewhat increased performance (Paluszkiewicz and Romea, 1997). Lateral exchange between the deep convective centres and the surrounding boundary currents can significantly alter the convective process (Maxworthy, 1997). Within those small regions, deep mixing is affected by mesoscale eddies in two ways: cyclonic eddies provide an additional preconditioning (Legg *et al.*, 1998), and collectively exchange fluid with the periphery of the deep mixed region. Coarse and medium resolution ocean models have shown significantly improved simulations of the deep convective regions when more sophisticated parametrizations of mesoscale eddies were employed (Danabasoglu and McWilliams, 1995; Visbeck *et al.*, 1997). In particular the unrealistic widespread convective mixing (>500 m) over much of the Southern Ocean was significantly reduced.

Shelf plume convection is more difficult to represent in coarse resolution climate models. The problem is challenging because shelf convection is heavily influenced by the details of the bathymetry, coastal fronts and mesoscale eddies

(Gwarkiewicz and Chapman, 1995), as well as entrainment of the ambient water (Baringer and Price, 1997). Several different attempts have been made to parametrize its overall effect (e.g., Beckmann and Döscher, 1997; Killworth and Edwards, 1999). Most ocean models have, however, not yet implemented such schemes and ventilate, e.g., the Southern Ocean by means of extensive open ocean (polynya) convection. The effect on the sensitivity of the current coupled climate models to forcings which involve changes in the convective processes is not known.

The convective activity in the Greenland and Labrador Seas varies inversely on decadal time-scales (see Chapter 2, Section 2.2.2.5). The switch of the convective activity from the Greenland Sea to the Labrador Sea has been attributed to changes in the index of the North Atlantic Oscillation (Dickson *et al.*, 1996). The magnitude of the corresponding change in THC intensity is, however, controversial. While model results suggest moderate fluctuations (10 to 15%), it has been claimed from analysis of hydrographic observations that these changes might be much larger, with heat transport changes of more than 0.3 PW at 48°N, and in excess of 0.5 PW at 36°N (Koltermann *et al.*, 1999).

In summary, the representation of oceanic convection in current climate models is satisfactory to simulate the convection changes observed over the last decades. It is, however, not certain that current schemes will work equally well in situations that involve substantial changes in the THC.

7.3.3 Interior Ocean Mixing

Diapycnal mixing across density surfaces provides the main way to warm the cold deep waters which are formed by convection and sink at high latitudes, thus allowing them to rise through the thermocline and complete the lower limb of the "conveyor belt". Diapycnal mixing is an essential part of the ocean circulation, in particular the THC, and can affect surface conditions and climate change on decadal to centennial and longer time-scales.

The processes leading to mixing in the main thermocline involve random internal wave breaking (Gregg, 1989; Polzin *et al.*, 1995), and to some degree also double-diffusive mixing (St. Laurent and Schmitt, 1999). Diffusivities in most of the main thermocline are typically of the order 10^{-5} m^{2}s^{-1} or less (Gregg, 1989; Ledwell *et al.*, 1993), whereas diffusivities of an order of magnitude larger are required to close the THC (Munk, 1966). Recent observations in the deep ocean have, however, found that turbulence is greatly enhanced 1,000 to 2,000 m above the bottom in regions of rough bottom topography (Polzin *et al.*, 1997), with mixing rates reaching values of 1 to 3×10^{-4} m^{2}s^{-1} (Ledwell *et al.*, 2000). The most likely cause is internal waves generated by tidal flows over kilometre-scale bathymetric features. In addition to tidal-driven mixing, the calculations of Munk and Wunsch (1998) indicate that wind-driven mixing in the Antarctic Circumpolar Current contributes substantially. Preliminary estimates of mixing rates based on the internal wave parametrization suggest that the wind-driven mixing is more uniformly distributed throughout the water column (Polzin and Firing, 1997). Whereas the classical assumption of uniform mixing and

upwelling led to an expectation of poleward interior flow in the deep ocean, the new data suggest downwelling in the interior, with upwelling confined to the many ocean bottom fracture zone valleys perpendicular to the ridge axis (Ledwell *et al.*, 2000).

Evidence for a significant role for double diffusion in ocean mixing has emerged. The "salt finger" and "diffusive convection" processes transfer heat and salt at different rates resulting in a density transport against its mean gradient. New data suggest that salt fingers may have a somewhat subtle role over widespread areas of the sub-tropical gyres (St. Laurent and Schmitt, 1999). The implications of widespread double diffusion for the general circulation are, however, controversial. Gargett and Holloway (1992) found in a model study with a simplistic representation of double-diffusive mixing that there were dramatic changes in the circulation and water masses. Recent studies using a more conservative parametrization of double-diffusion suggest modest though still significant changes in the circulation (Zhang *et al.*, 1998).

Diapycnal mixing in the ocean is usually associated with energy conversions, and parametrizations are often based on energy arguments. In their most simple form, these suggest formulating mixing coefficients in terms of stability frequency and/or Richardson number. Double-diffusive mixing has been included in a few models only to very a limited extent. The higher mixing rates found in the abyssal ocean over rough topography have so far not been included in the vertical mixing scheme of coupled climate models, but have been used with some effect on the deep circulation in ocean models (e.g., Hasumi and Suginohara, 1999).

The sensitivity of climate model results to the mixing parametrization is not fully clear. In a state of thermohaline equilibrium, the intensity of the meridional overturning circulation should be strongly dependent on the average internal mixing rate, and in ocean-only models the meridional overturning circulation often varies with a certain power of the average mixing rate (Zhang *et al.*, 1999a). Some models indicate, however, that significant transports may be involved in wind-driven flows along isopycnals which outcrop in different hemispheres. The buoyancy changes are confined to the surface mixed layers, and little or no interior mixing is required. The scaling laws and dynamics of such flows have yet to be clarified, but they do raise the possibility of a meridional heat transport independent of the interior mixing rate.

In summary, the uncertainties associated with interior ocean mixing parametrizations are likely to be small for climate projections over a few decades but could be considerable over longer time scales.

7.3.4 Mesoscale Eddies

Mesoscale eddies in the ocean have a scale of 50 to 100 km, and correspond dynamically to high and low pressure systems in the atmosphere. The role of eddies for climate change arises from their influence on the circulation by (i) transporting and mixing temperature and salinity, (ii) exchanging (usually extracting) potential energy from the mean flow, and (iii) exchanging momentum with the mean flow (in both directions). Eddy

processes are of primary importance for the dynamics of intense western boundary currents, through the exchange of momentum and energy via instability and/or rectification processes, and also influence the dynamics of the Southern Ocean. The eddy contribution to the meridional transport of heat and fresh water is small in many regions but cannot be ignored on the global scale. Long lived, propagating eddies such as Agulhas rings determine a major part of the inter-basin exchange between Indian and South Atlantic Oceans. The decaying rings provide a source of warm salty water important for the global thermohaline circulation (de Ruijter *et al.*, 1999), and variations in that exchange may generate THC variations.

Considerable progress has been made in recent years with the parametrization of eddies in climate models of coarse and medium resolution (cf., Chapter 8, Table 8.1) which do not explicitly represent eddies. New schemes are based on eddy dynamics and the physics of baroclinic instability. Lateral eddy mixing of tracers such as potential temperature and salinity is mainly directed along isopycnals, and has a small effect on the dynamics but is important for water mass properties. The traditional mixing along horizontal surfaces which is still used in several climate models leads to unrealistic upwelling in the western boundary current (Boening *et al.*, 1995) and strongly resolution-dependent simulations of meridional overturning and heat transport (Roberts and Marshall, 1998). Isopycnal mixing is natural in models with an isopycnal vertical co-ordinate, for other models a stable and conservative algorithm for isopycnal rotation of the diffusion tensors is now available (Griffies *et al.*, 1998).

The dynamical effects of baroclinic instability are now frequently parametrized as an additional eddy advection of tracers (Gent *et al.*, 1995). With this parametrization, the northward heat transport in the North Atlantic Ocean is less dependent on resolution, and matches the observational estimates much better. Aspects of the Southern Hemisphere circulation are also improved by this parametrization. Theoretical studies (e.g., Killworth, 1997) suggest somewhat different formulations based on down-gradient mixing of potential vorticity. The strengths of isopycnal mixing and eddy-induced advection are usually described empirically through coefficients which are constant or dependent on grid size. For modelling climate change, it is, however, imperative to relate these coefficients to properties of the mean flow (Visbeck *et al.*, 1997).

The parametrization of exchange of eddy momentum with the mean flow remains a challenge. Some studies suggest a substantial eddy influence on the mean barotropic flow based on the interaction of a statistical eddy field with bottom topography (Eby and Holloway, 1994; Merryfield and Holloway, 1997). However, due to the near-geostrophy of ocean currents, it is possible that these processes are not as critical as the sub-grid scale effects on tracers for the overall quality of ocean model solutions.

In summary, while the effects of ocean eddies for climate change are likely to be moderately small, a quantitative assessment will require coupled simulations with eddy-permitting ocean models.

7.3.5 Flows over Sills and through Straits

The water mass structure in the deep ocean is largely dominated by the flows across a few shallow sills and through straits. The role of such flows for climate change arises from their influence on the THC which in turn can affect surface conditions. Once water has crossed a sill, it descends the continental slope as a dense gravity current and provides the water source for the downstream basin. The water mass properties are determined by the entrainment of and mixing with ambient water (Baringer and Price, 1997). For the NADW which is at the heart of the sinking branch of the global conveyor, the overflow of cold water across the Greenland-Iceland-Scotland ridge is the principal source. Observations show intense flow with speeds up to 1 m/s, in a layer of less than 100 m thickness above the bottom and within 20 km of the continental slope. Model calculations suggest that an interruption of this overflow would lead to a breakdown of the Atlantic THC and the associated heat transport within less than a decade (Döscher *et al.*, 1994). In the past decades the overflow appears to have been fairly steady. Another prominent feature is the Indonesian Throughflow which has substantial contributions to the variability of the THC and heat transport in the Indian Ocean (Godfrey, 1996).

In coarse and medium resolution climate models, the overflow across the Greenland-Iceland-Scotland ridge has been found to be highly sensitive to the precise geometry used. For example, changes in topography by as little as one grid cell resulted in gross changes not only to the amount of cross-ridge flux but also to its location, and to the composition of the water mass actually crossing the sill. Thus, a 50% change in heat flux at the Greenland-Iceland-Scotland ridge latitude could be achieved in a model by the addition or subtraction of a single grid box (Roberts and Wood, 1997). Even eddy-permitting simulations give flows through sills which are very sensitive to model details (Willebrand *et al.*, 2001). The physical processes involve hydraulic control and are not properly represented in climate models, and it is unclear whether a situation with substantial overflow changes can be modelled correctly. Parametrizations for the flux across a sill are only available for the simplest process models (Killworth, 1994; Pratt and Chechelnitsky, 1997) that do not include mixing or unsteadiness, both of which are known to be important at sills (Spall and Price, 1998).

Climate models which are based on depth co-ordinates obtain far too much mixing near a sill. This is caused by both poor mixing parametrizations in such models and by excessive diapycnal mixing resulting from the 'staircase'-like representation of bottom topography. As a result, water mass structure downstream of a sill is poorly represented in climate models. Isopycnic models are free of this erroneous mixing, and addition of Richardson number dependent mixing to such models results in realistic tongues of dense water moving downslope, mixing at a rate consistent with observations (Hallberg, 2000). A promising new development is the explicit description of the turbulent bottom boundary layer in climate models which yields more realistic flow of dense water down slopes (Beckmann and Döscher, 1997; Killworth and Edwards, 1999).

In summary, the uncertainties in the representation of the flows across the Greenland-Iceland-Scotland ridge limit the ability of models to simulate situations that involve a rapid change in the THC.

7.3.6 Horizontal Circulation and Boundary Currents

The horizontal circulation in ocean gyres contributes to the meridional transports of heat and fresh water in the climate system (see Section 7.6.2), and therefore is of immediate relevance for climate change. Much of that transport occurs through Western Boundary Currents (WBCs) such as the Gulf Stream, Kuroshio, Agulhas Current and others which are prominent elements of the ocean circulation. These currents are mainly driven by the wind, and have a typical width of 50 km. Once a WBC has left the continental slope, it is characterised by recirculation regimes and strong mesoscale variability. The dynamical influence of the WBCs on the less vigorous interior circulation is not fully understood. Their pathways are, however, crucial in determining the location of the sub-polar front which separates the warm waters of the sub-tropics from the colder sub-polar waters. The lower branch of the THC is also dominated by deep WBCs. In the Atlantic, these are concentrated within 30 km of the continental slope, and are accompanied by substantial recirculation and variability (Lee *et al.*, 1996).

The width and strength of boundary currents in climate models are very sensitive to resolution, they become stronger and narrower as the resolution is increased, provided that at the same time the sub-grid scale transports are also reduced. For example, a recent simulation for the North Atlantic using a grid resolution of 1/10° (equivalent to 11 km or better) indicates that features such as the width, location and variability of boundary currents, the eddy field and its statistics, as well as regional current features are in rather good agreement with observations (Smith *et al.*, 2000). On the other hand, in non-eddy-resolving climate models, boundary currents are quite unrealistic, they lack the observed sharp fronts and recirculation regimes and hence miss the associated air-sea heat fluxes and their dynamical influence on mid-ocean circulation. The effect of having weaker and wider boundary currents for the model's climate and climate sensitivity has so far not been systematically evaluated.

7.3.7 Thermohaline Circulation and Ocean Reorganisations

In the Atlantic Ocean, the THC is responsible for the relatively mild climate in Western Europe (see Section 7.6.1). While palaeo-oceanographic analyses suggest that the Atlantic THC has been relatively stable for the last 8,000 years, a series of large and rapid climatic changes during the last Ice Age has been reconstructed from numerous palaeoclimatic archives (see Chapter 2, Section 2.4). Based on the presently available evidence, these changes are best explained by major reorganisations involving the THC (Broecker, 1997; Stocker and Marchal, 2000). Changes of the THC, due to natural variability or slowly changing surface forcing, thus have an important effect on the climate on a regional to hemispheric scale, and numerous model studies since the SAR have investigated potential changes in
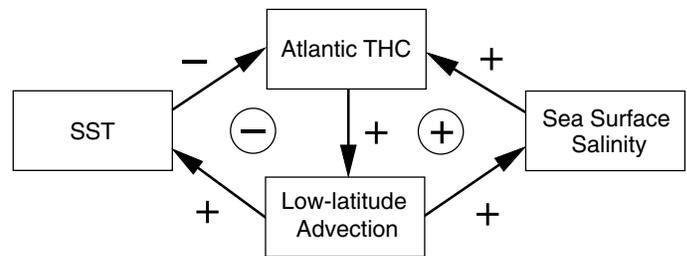

Figure 7.4: Idealised schematics of two advective feedback loops involving the thermohaline circulation (THC). The signs attached to the arrows indicate the correlation between changes in the quantity of the outgoing box with that of the ingoing box, e.g., warmer sea surface temperatures (SST) lead to weaker THC. Resulting correlations of a loop are circled and they indicate whether a process is self-reinforced (positive sign) or damped (negative sign). A stabilising loop (left) is associated with changes in SST due to changes in the advection of heat. This loop may give rise to oscillations. The second loop (right) is due to the influence of advection of low latitude salty waters into the areas of deep water formation. The resulting correlation is positive and the loop may therefore cause instabilities.

THC and elucidated the underlying mechanisms and their impact on the climate system.

Generally, in high latitudes the ocean loses heat and gains fresh water (precipitation and continental runoff) which has opposite effects on the density of ocean water. In addition, the density of sea water is influenced by the supply of warm and salty water from the low latitudes which constitutes the positive feedback maintaining the Atlantic THC (Figure 7.4). This balance is influenced by the surface fluxes of heat and fresh water, i.e., precipitation, evaporation, continental runoff and sea-ice formation, all processes that are likely to change in the future. Some models also suggest an influence of Southern Ocean wind on the Atlantic THC (Toggweiler and Samuels, 1995).

The response of the THC to a perturbation depends on the relative strength of further feedbacks. Reduced convection and advective heat transport into a region lead to colder SSTs which counteracts the effect of salinity on density and thus limits the strength of the destabilising oceanic feedbacks (Figure 7.4). The atmospheric heat transport compensates for parts of the changes in ocean heat transport and is a key factor in determining the stability of the THC (Zhang *et al.*, 1993; Mikolajewicz and Maier-Reimer, 1994). Atmospheric moisture transport among basins provides another feedback (Schiller *et al.*, 1997). Model results suggest that in the presence of overflow between Greenland and Iceland the THC is not very sensitive to changes in the atmosphere-ocean fluxes (Lohmann and Gerdes, 1998).

It is likely that sea ice also has an effect on the stability of the THC: decreased THC and hence oceanic heat transport leads to more sea ice formation (Schiller *et al.*, 1997). Formation of sea-ice tends to increase the density of sea water both through brine rejection and cooling of the overlying air via increased surface albedo and enhanced insulation. Increased export of sea ice from these areas represents a significant fresh water transport over long distances which can decrease deep water formation, thus representing a positive feedback. A reliable estimate of the net

effect of sea ice on the stability of the THC is hampered by the still crude representation of sea ice in most current climate models and the resulting unrealistic simulation of sea-ice distributions. A negative feedback contributing to a stabilisation of the THC was recently proposed by Latif *et al.* (2000). They suggested that during El Niño conditions fresh water export from the tropical Atlantic via the atmosphere is enhanced; this tendency is also found in observations (Schmittner *et al.*, 2000). This implies an increased supply of saltier waters towards the northern North Atlantic which facilitates deep water formation, hence a stabilising process for the THC; the opposite effect occurs for La Niña conditions.

A special concern are possible reductions of the Atlantic THC caused by warming and freshening of high latitude surface water associated with global warming (Manabe and Stouffer, 1993; Stocker and Schmittner, 1997). Both the high latitude warming and an enhanced poleward transport of moisture in the atmosphere contribute to the reduction of water density in the formation regions of NADW. However, it is not clear which of these two processes is the more important (Dixon *et al.*, 1999; Mikolajewicz and Voss, 2000). Most coupled climate models indicate a reduction in the meridional overturning circulation, a measure of the THC, from 10 to 50% in response to increasing CO_2 concentration in the atmosphere for the next 100 years (see Chapter 9). A notable exception is one coupled climate model (Latif *et al.*, 2000), but this result must be corroborated with other comprehensive climate models that are capable of resolving well both ENSO and the THC processes.

A less likely, but not impossible, scenario is a complete shutdown of the THC, which would have a dramatic impact on the climate around the North Atlantic. A complete shut-down requires the passing of a critical threshold and may be an irreversible process because of multiple equilibria of the THC. Multiple equilibria have been reported by the entire ocean and climate model hierarchy ranging from simple models (Stommel, 1961; Stocker and Wright, 1991), uncoupled OGCMs (Bryan, 1986; Marotzke and Willebrand, 1991; Weaver and Hughes, 1994) to fully coupled ocean-atmosphere GCMs (Manabe and Stouffer, 1988). The structure of the oceanic reorganisation beyond the threshold, simulated in models of different complexity, is robust: the Atlantic THC ceases (Manabe and Stouffer, 1993; Schmittner and Stocker, 1999), which leads to a reduction in the meridional heat transport in the Atlantic, and hence a regional cooling counteracts the temperature increase. It depends on the model's climate sensitivity whether the combined effect results in a net warming or net cooling in the regions most affected by the meridional heat transport of the Atlantic THC. In addition, such reorganisations would have a profound impact on the north-south distribution of the warming and precipitation (Schiller *et al.*, 1997), on sea level rise (see Chapter 11, Section 11.5.4.1; Knutti and Stocker, 2000), and on the biogeochemical cycles (see Chapter 3, Section 3.7.2; Joos *et al.*, 1999).

Model simulations with different climate models have found a complete shut-down of the THC when the global atmospheric temperature increases by an amount between 3.7 and 7.4°C (Manabe and Stouffer, 1993; Stocker and Schmittner, 1997; Dixon *et al.*, 1999). It is however not clear whether the climate system possesses a threshold in this range, as the values depend on the response of the hydrological cycle to the warming and the parametrizations of mixing processes in the ocean. Furthermore, the rate of temperature increase also determines stability: the THC is less stable under faster perturbations (Stocker and Schmittner, 1997; Stouffer and Manabe, 1999). Model simulations further suggest that the proximity to the threshold depends on the strength of the THC: a weaker THC is more likely to shut down completely (Tziperman, 2000).

In summary, a reduction of the Atlantic THC is a likely response to increased greenhouse gas forcing based on currently available model simulations. Uncertainties in the model simulation of the hydrological cycle, the vertical transport of heat in the ocean interior and the parametrization of deep water formation processes, however, translate directly to uncertainties regarding the stability and future evolution of the THC. While none of the current projections with coupled models exhibit a complete shutdown of the THC during the next 100 years (see Chapter 9, Figure 9.21), one cannot exclude the possibility that such thresholds lie in the range of projected climate changes. Furthermore, since natural variability in the climate system is not fully predictable, it follows that there are inherent limitations to predicting transitions and thresholds.

7.4 Land-Surface Processes and Feedbacks

The net radiation absorbed by the continents is partitioned mainly into sensible and latent (evapotranspiration) heat fluxes whose release back into the atmosphere directly influences local air temperature and humidity and thence other climate system variables. In any given locale, soil moisture availability and vegetation state largely determine the fraction of net radiation that is used for evapotranspiration, as well as the photosynthetic and respiration rates. Thus, realistic modelling of land surface-atmosphere interactions is essential to realistic prediction of continental climate and hydrology. In doing this, attention must be paid to the links between vegetation and the terrestrial energy, water and carbon cycles, and how these might change due to eco-physiological responses to elevated CO_2 and changes in land use.

7.4.1 Land-Surface Parametrization (LSP) Development

The exchanges of energy, momentum, water, heat and carbon between the land surface and the atmosphere must be more realistically and accurately calculated in the next generation of coupled models (Sellers *et al.*, 1997). Fluxes of the first four quantities, traditionally defined as physical climate system variables, are routinely parametrized in Numerical Weather Prediction (NWP) models and climate models as functions of the surface albedo, aerodynamic roughness length and surface "moisture availability" (Betts *et al.*, 1998; Viterbo *et al.*, 1999). These land-surface properties can all be defined as functions of the type and density of the local vegetation, and the depth and physical properties of the soil. The first generation of land-surface parametrizations (LSPs) developed in the 1970s took little account of these relationships, and were replaced by biophysically realistic models, complete with supporting vegetation and soil databases, which led
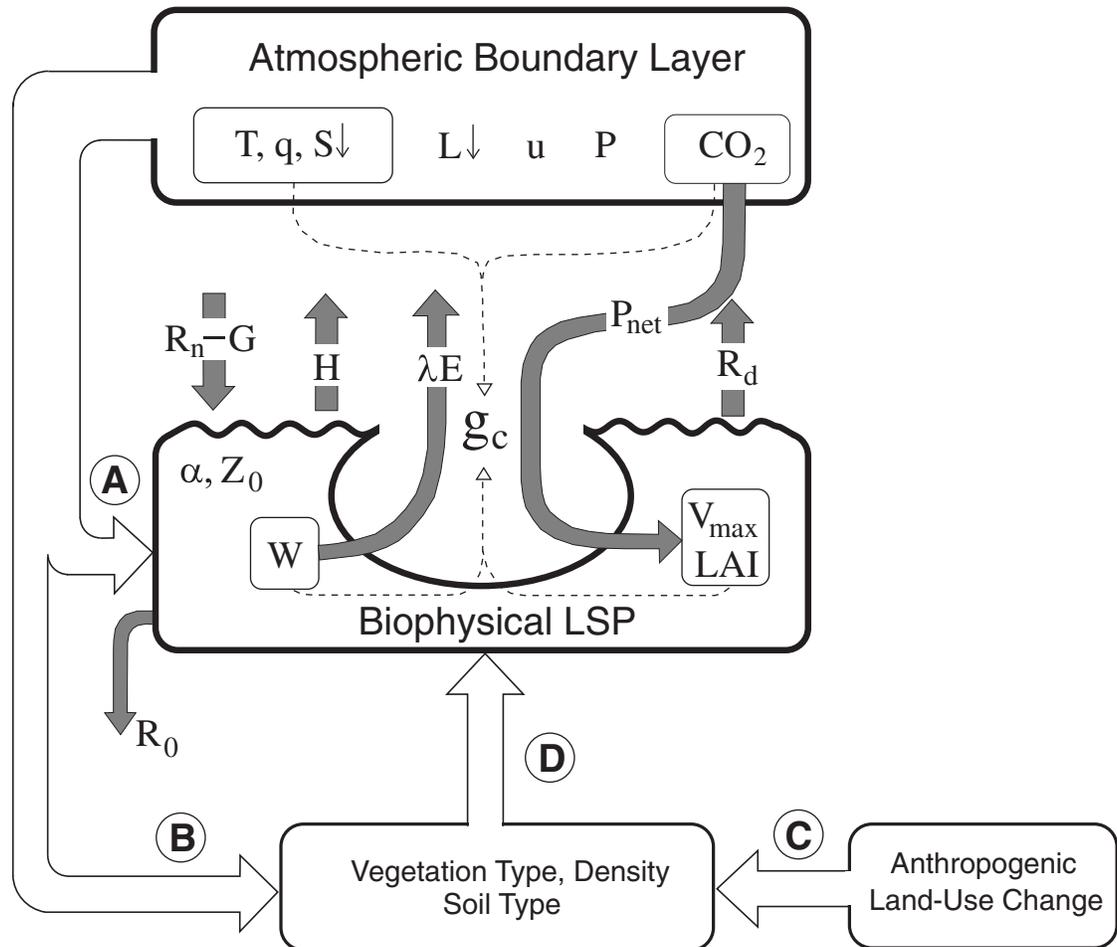
Figure 7.5: Schematic showing relationships between a simulation of the Atmospheric Boundary Layer (ABL), a Land-Surface Parametrization (LSP), vegetation and soil properties, and anthropogenic change. Interactions are shown by broad white arrows marked with capital letters, fluxes by grey arrows, and dependencies by dotted lines. (A) Diurnal-seasonal interactions between the ABL and the LSP; the ABL variables of air temperature, humidity, downward short-wave radiation, downward long-wave radiation, wind speed and precipitation (T, q, $S\downarrow$, $L\downarrow$, u, P) are used to force the LSP which calculates net radiation minus ground heat, sensible heat, and latent heat fluxes (R_n–G, H, λE), which in turn feed back to the atmosphere. Three surface parameters in the LSP are critical to these calculations: Albedo and surface roughness (α, Z_0) determine the radiative balance and turbulent exchange regime, and in third generation LSPs, the canopy conductance term, g_c (equivalent to the summation of all the leaf stomatal conductances) determines the vegetation evapotranspiration rate (λE) and net photosynthetic rate (P_{net}). On time-scales of minutes to hours, g_c is a direct function of T, q, $S\downarrow$, CO_2 concentration and soil moisture (W). Increasing CO_2 concentration can act to significantly reduce g_c and hence limit λE. The maximum value of g_c is determined by parameters related to vegetation density or leaf area index (LAI), and biochemical capacity (V_{max}). Long-term climatic forcing (B) and land-use change (C) can alter the vegetation type and density, soil properties and ecosystem respiration rates, R_d, by which carbon is returned to the atmosphere from the vegetation and soil. (D) Changes in vegetation properties affect V_{max} and LAI, and changes in soil properties affect soil moisture (W) and runoff (R_0).

to significant improvements in NWP and climate model perform-ance in the 1980s and early 1990s. However, these second genera-tion models incorporated only empirical descriptions of the evapotranspiration process, by which water is taken up from the soil by plant roots and released into the atmosphere through tiny pores in leaf surfaces called stomata, while CO_2 is drawn from the atmosphere into leaf interiors for photosynthesis through these same stomata. Research has shown that living plants appear to actively control stomatal widths (conductance) in response to changes in water vapour and CO_2 concentration to optimise the ratio of water vapour losses to CO_2 uptake, and simple, robust models of the photosynthesis-conductance system in plant leaves have been constructed based on this idea, see Figure 7.5 (Farquhar *et al.*, 1980; Collatz *et al.*, 1991; Sellers *et al.*, 1992a). These models have been parametrized and verified at the leaf level, and can also be scaled up to describe vegetation canopy processes at regional scales using satellite data. These third generation LSPs, published in the late 1990s, thus combine consistent descriptions of the physical climate system transfer processes for energy, momentum, water and heat, with the biophysics of photosynthesis (Bonan, 1995; Sellers *et al.*, 1996c; Dickinson *et al.*, 1998). Why is this important?

Photosynthesis and respiration are climatically sensitive and exhibit interannual variations following climate variations (Dai and Fung, 1993; Francey *et al.*, 1995; Goulden *et al.*, 1996; Myneni *et al.*, 1997; Randerson *et al.*, 1997; Xiao *et al.*, 1998; Randerson *et al.*, 1999; Tian *et al.*, 1999). Furthermore, there appears to have been a net enhancement of terrestrial photosynthesis over respiration over the last two decades, according to inverse modelling results (Tans *et al.*, 1990; Ciais *et al.*, 1995; Keeling *et al.*, 1995; Denning *et al.*, 1996a,b; Randerson *et al.*, 1999); and isotopic analyses (Fung *et al.*, 1997). While disagreements remain about the longitudinal distribution (Rayner and Law, 1999) and the processes responsible for this uptake (Holland *et al.*, 1997a; Field and Fung, 1999; Houghton and Hackler, 1999), these results indicate that changes in the terrestrial carbon balance could be a significant factor in determining future trajectories of atmospheric CO_2 concentration and thus the rate and extent of global warming; see further discussion in Chapter 3. The third generation LSPs have incorporated advances in our understanding of how green plants function, how they alter isotopic fractions of gases they come into contact with, and how they interact with radiation to produce distinctive signatures that can be observed by remote sensing satellites (Tucker *et al.*, 1986; Sellers *et al.*, 1992a; Myneni *et al.*, 1995). As a result, LSPs can now be used to calculate mutually consistent land-atmosphere fluxes of energy, heat, water and carbon (Denning *et al.*, 1996a,b; Randall *et al.*, 1996).

Photosynthesis and stomatal conductance also exhibit strong diurnal variation, and improved representation of this has led to better simulation of the diurnal variation of surface heat and water fluxes and hence more realistic forcings for boundary-layer dynamics and convection (Denning *et al.*, 1996a; Randall *et al.*, 1996). These physiologically driven variations in the surface fluxes have a direct influence on the diurnal surface air temperature range in continental interiors and are directly sensitive to changes in atmospheric CO_2 concentration (Collatz *et al.*, 2000). Furthermore, increasing atmospheric CO_2 is likely to have a direct effect on vegetation stomatal function through feedbacks in the photosynthesis-conductance system. Increased CO_2 concentrations allow vegetation to maintain the same photosynthetic rate with a lower evapotranspiration rate. In a recent GCM study, tropical photosynthesis and transpiration rates were calculated to change only slightly under a CO_2 concentration of 700 ppm, while the additional surface net radiation due to global warming was mainly returned to the atmosphere as sensible heat flux, boosting warming over the tropical continents by 0.4 to 0.9°C above the direct greenhouse warming of 1.7°C (Sellers *et al.*, 1996a). It has been hypothesised that this effect may be partially countered by increased vegetation growth (Betts *et al.*, 1997), but it is not clear to what extent this would be significant in already densely vegetated areas such as the tropical forests. To what extent can we trust these new models and their predictions?

The third generation LSPs combine biology and atmospheric physics in an economical and plausible way and require fewer parameters than their empirical predecessors (Bonan, 1995; Sellers *et al.*, 1996c; Dickinson *et al.*, 1998). Equally important, these models provide more opportunities for parameter calibration, constraint, process sub-model validation and "upscaling" algorithm verification through comparison with observations. This is because a powerful range of carbon-related and physiological fluxes and variables may be added to the physical climate system parameters conventionally used for LSP validation (Colello *et al.*, 1998; Delire and Foley, 1999). It has also been found that the leaf-level physiological photosynthesis-conductance models developed and tested under laboratory and field conditions can be spatially integrated to describe processes over large areas using routine satellite observations. Over the last few years, satellite measurements have been used to construct global data sets of vegetation type and other surface parameters at monthly time resolution and one degree spatial resolution or better (Sellers *et al.*, 1996b). Most importantly, these data sets are globally consistent in that they are primarily based on one type of satellite sensor and one set of interpretative algorithms. Satellite observations also provide a powerful diagnostic capability for tracking climatic impacts on surface conditions; e.g., droughts and the recently observed lengthening of the boreal growing season; and direct anthropogenic impacts, e.g., deforestation. Validation of the process models, upscaling methodologies and the satellite algorithms used to define global parameter fields, has been achieved through a series of large-scale field experiments (Andre *et al.*, 1986; Sellers *et al.*, 1992b; Bolle *et al.*, 1993; Goutorbe, 1994; Sellers *et al.*, 1995). In every environment studied so far (mid-latitude grassland and forest, boreal forest, arid zones) these methods have been used to calculate regional land-atmosphere flux fields that concur with satellite observations and fluxes measured by surface rigs and low flying aircraft (Cihlar *et al.*, 1992; Desjardins *et al.*, 1992; Sellers *et al.*, 1992c).

The field experiments have provided other significant benefits to the modelling community: LSPs in NWP models have been enhanced, leading to direct improvements in precipitation and cloudiness prediction over the continents (Beljaars *et al.*, 1996; Betts *et al.*, 1996), and large biases in some NWP surface parameter fields, for example winter albedo in the boreal forest, have been corrected (Betts *et al.*, 1998). Climate modellers have similarly used the results from field experiments to improve process sub-models (Shao and Henderson-Sellers, 1996), global parameter sets (Sellers *et al.*, 1996b), and to develop better methods for dealing with land-surface spatial heterogeneity (Avissar, 1998; Avissar *et al.*, 1998). Model validation and intercomparison tests have used field experiment data sets to baseline the performance of LSPs within a rigorous intercomparison framework (see Chapter 8, Section 8.5.4).

While there has been considerable success in upscaling process sub-models and parameter sets to describe continental-scale fluxes and states, there remain some difficult areas, notably the treatment of heterogeneous landscapes, soil water transport and catchment hydrology (see Section 7.4.3); the treatment of snow (see Section 7.5.1); and the coupling of LSPs with atmospheric boundary-layer models (see Section 7.2). Sophisticated scaling methodologies are needed to deal with the many non-linear components in these systems and accurate, realistic modelling of these processes on a large scale is likely to remain a challenge for some time to come.

Global biogeochemical models have been developed independently of LSPs to investigate carbon cycling by the terrestrial biosphere (e.g., Field *et al.*, 1995; Foley *et al.*, 1996, 1998; Cao and Woodward, 1998; Kicklighter *et al.*, 1998; see also Chapter 3). Biogeochemical models are now being coupled with LSPs so that a complete, internally consistent carbon balance can be performed along with conventional surface energy balance calculations (see also Section 7.4.2). Changes in the isotopic fractions of key gases as a result of interactions with the vegetation physiology can also be calculated (Ciais *et al.*, 1997; Fung *et al.*, 1997; Randerson and Thompson, 1999) and preliminary work is under way to calculate dry deposition rates and thus refine calculations of the global tropospheric budget of O_3 and reactive N-species within LSPs.

The eventual result should be powerful, internally consistent, model combinations that will be capable of simulating the influence of the physical climate system on the terrestrial carbon cycle, and *vice versa*. This kind of model will be important for realistic simulation of the global climate out beyond a few decades, during which carbon cycle-climate interactions could significantly influence the rate of atmospheric CO_2 increase, the nature and extent of the physical climate system response, and ultimately, the response of the biosphere itself to global change. Furthermore, the performance of such models can be checked, or constrained, by a combination of conventional physical climate system observations, atmospheric gas and isotope fraction concentrations, and satellite data.

Many scientific and technical problems must be solved to achieve these goals. Sections 7.4.2, 7.4.3 and 7.5.1 cover some particular issues that will be important for the construction of realistic, accurate LSPs in the future.

7.4.2 Land-Surface Change

Climate and carbon cycle simulations extending over more than a few decades must take account of land-surface change for two main reasons. First, changes in the physical character of the land surface can affect land-atmosphere exchanges of radiation, momentum, heat and water (see Figure 7.5 and the simulation studies discussed below). These effects must be allowed for within climate simulations or analyses to avoid confusion with the effects of global warming. Second, changes in vegetation type, density and associated soil properties usually lead to changes in terrestrial carbon stocks and fluxes that can then directly contribute to the evolution of atmospheric CO_2 concentration. Therefore, any historical analysis of the atmospheric CO_2 record must estimate these contributions to avoid inaccurate attribution of carbon sinks or sources. Similarly, model simulations extending over the next 50 to 100 years should allow for significant perturbations to the atmospheric carbon budget from changes in terrestrial ecosystems (Woodwell *et al.*, 1998; see also Chapter 3).

There are two types of land-surface change; direct anthropogenic change, such as deforestation and agriculture; and indirect change, where changes in climate or CO_2 concentration force changes in vegetation structure and function within biomes, or the migration of biomes themselves. With respect to direct anthropogenic change, population growth in the developing countries and the demand for economic development worldwide has led to regional scale changes in vegetation type, vegetation fraction and soil properties (Henderson-Sellers *et al.*, 1996; Ramankutty and Foley, 1998). Such changes can now be continuously monitored from space, and the satellite data record extends back to 1973. Large-scale deforestation in the humid tropics (South America, Africa and Southeast Asia) has been identified as an important ongoing process, and its possible impact on climate has been the topic of several field campaigns (Gash *et al.*, 1996), and modelling studies (for example, Nobre *et al.*, 1991; Lean *et al.*, 1996; Xue and Shukla, 1996; Zhang *et al.*, 1996a; Hahmann and Dickinson, 1997; Lean and Rowntree, 1997). Some significant extra-tropical impacts have also been identified in several model experiments (e.g., Sud *et al.*, 1996; Zhang *et al.*, 1996b). Replacement of tropical forest by degraded pasture has been observed to reduce evaporation, and increase surface temperature; these effects are qualitatively reproduced by most models. However, large uncertainties still persist about the impact of large-scale deforestation on the hydrological cycle over the Amazon in particular. Some numerical studies point to a reduction of moisture convergence while others tend to increase the inflow of moisture into the region. This lack of agreement occurs during the rainy season and reflects our poor understanding of the interaction of convection and land-surface processes (Polcher, 1995; Zhang *et al.*, 1997a), in addition to the effects of differences between the formulations in the land-surface schemes, their parameter fields, and the host GCMs used in the studies.

Other simulation work has indicated that the progressive cultivation of large areas in the East and Midwest USA over the last century may have induced a regional cooling of the order of 1 to 2°C due to enhanced evapotranspiration rates and increased winter albedo (Bonan, 1999). Snow-vegetation albedo effects significantly influence the near-surface climate; assignment of an open snow albedo value to the winter boreal forest in an NWP led to the prediction of air temperatures that were 5 to 10°C too low over large areas of Canada (Betts *et al.*, 1998). Work has also been done on the interaction between Sahelian vegetation and rainfall that suggests that the persistent rainfall anomaly observed there in the 1970s and 1980s could be related to land-surface changes (Claussen, 1997; Xue, 1997). All these studies indicate that large-scale land-use changes can lead to significant regional climatic impacts. However, it is unlikely that the aggregate of realistic land-use changes over the next 50 to 100 years will contribute to global scale climate changes comparable to those resulting from the warming associated with the continuing increase in greenhouse gases.

Changes to the land surface resulting from climate change or increased CO_2 concentration are likely to become important over the mid- to long term. For example, the extension of the growing season in high latitudes (Myneni *et al.*, 1997) will probably result in increases in biomass density, biogeochemical cycling rates, photosynthesis, respiration and fire frequency in the northern forests, leading to significant changes in albedo, evapotranspiration, hydrology and the carbon balance of the zone (Bonan *et al.*, 1992; Thomas and Rowntree, 1992; Levis *et al.*, 1999). There

have been several attempts to calculate patterns of vegetation type and density as a function of climate (e.g., Zeng *et al.*, 1999); most of these have made use of climate predictions to calculate the future steady-state distribution of terrestrial biomes but some have attempted to model transitional cases (Ciret and Henderson-Sellers, 1998).

However, over the next 50 to 100 years, it is more likely that changes in vegetation density and soil properties within existing biome borders will make a greater contribution to modifying physical climate system and carbon cycle processes than any large-scale biogeographical shifts. In some cases, soil physical and chemical properties will limit the rate at which biomes can "migrate"; for example, colonisation of the tundra by boreal forest species is likely to be slowed by the lack of soil. Climate-vegetation relations are discussed further in Chapter 8, Section 8.5.5 with respect to past climates.

At present, only limited global data sets for LSPs are available and these need to be further improved. A comprehensive land-use/land cover data set, providing a global time-series of vegetation and soil parameters over the last two centuries at GCM resolution, would be a very useful tool to separate land-use change impacts on regional climate from global scale warming effects. Additionally, for both historical analyses and future projections, there is a need for interactive vegetation models that can simulate changes in vegetation parameters and carbon cycle variables in response to climate change. These proposed fourth generation models are just beginning to be designed and implemented within climate models.

7.4.3 Land Hydrology, Runoff and Surface-Atmosphere Exchange

Soil moisture conditions directly influence the net surface energy balance and determine the partitioning of the surface heat flux into sensible and latent contributions, which in turn control the evolution of the soil moisture distribution. There have been studies of the importance of soil moisture anomalies for episodes of drought (Atlas and Wolfson, 1993) and flooding (Beljaars *et al.*, 1996; Giorgi *et al.*, 1996), and the impact of initial soil moisture conditions on mid-latitude weather (Betts *et al.*, 1996; Schär *et al.*, 1999). Results from other GCM studies (e.g., Milly and Dunne, 1994; Bonan, 1996; Ducharne *et al.*, 1996) and regional and global water budgets analyses (e.g., Brubaker *et al.*, 1993; Brubaker and Entekhabi, 1996) have deepened our appreciation of the importance of land-surface hydrology in the regional and global energy and water exchanges. In relation to climate change, such mechanisms are relevant since they might lead to, or intensify, a reduction in summer soil moisture in mid- and high latitude semi-arid regions under doubled CO_2 conditions (Wetherald and Manabe, 1999). Most of these studies reported some impact of soil conditions upon land precipitation during episodes of convective activity, and there is observational evidence from lagged correlation analysis between soil moisture conditions and subsequent precipitation over Illinois that this mechanism is active in mid-latitudes (Findell and Eltahir, 1997). The formulation of surface runoff and baseflow has been calculated to have an indirect but strong impact on the surface energy balance (Koster and Milly, 1997).

The feedback mechanisms between soil moisture conditions and precipitation are particularly relevant to climate change studies since they may interact with, and determine the response to, larger-scale changes in atmospheric circulation, precipitation and soil moisture anomalies. The modelling of soil moisture-climate interactions is complicated by the range of time-scales involved, as soil moisture profiles can have a "memory" of many months, and the interaction of vertical soil moisture transfers with the larger-scale horizontal hydrology. Work is continuing to improve the realism of vertical water transfers, the effect of soil water on evapotranspiration rates, and the parametrization of sub-grid scale variability in land hydrological components (e.g., Avissar and Schmidt, 1998; Wood *et al.*, 1998). To date, there have been few attempts to describe the effects of within-grid horizontal transfers of water, but there has been success in connecting river routing schemes to GCMs (Dümenil *et al.*, 1997; see also Chapter 8, Section 8.5.4.2). Development in this area has lagged significantly behind that of vegetation canopy processes, despite the fact that the former are critical to a land-surface scheme's overall performance.

7.5 Cryosphere Processes and Feedbacks

The cryosphere, comprising snow and ice within the Earth system, introduces forcings that can affect oceanic deep water formation and feedbacks that can amplify climate variability and change. Important feedbacks involve: (i) the dependence of surface albedo on the temperature, depth and age of ice and snow; (ii) the influence of melt/freeze processes on sea surface salinity and deep-water formation. Palaeoclimatic evidence (Chapter 2, Section 2.4), indicating that extreme climate excursions have been induced by cryospheric processes, as well as recent observations that Arctic sea ice has decreased significantly in both extent and thickness (see Box 7.1), motivates the addition of this new section to the TAR.

7.5.1 Snow Cover and Permafrost

The presence of snow and ice adds complexity to surface energy and water balance calculations due to changes in surface albedo and roughness and the energies involved in phase changes and heat transfer within the snow/soil profile (Slater *et al.*, 1998a; Viterbo *et al.*, 1999). The parametrizations of snow processes have received significant attention since the SAR and more complex snow schemes are now used in some climate models (Loth *et al.*, 1993; Verseghy *et al.*, 1993; Lynch-Stieglitz, 1994). These models include advanced albedo calculations based on snow age or temperature and may explicitly model the metamorphism of snow as well as representing liquid water storage and wind-blown snow. Douville *et al.* (1995), Yang *et al.* (1997), Loth *et al.* (1993) and Slater *et al.* (1998b) examined the ability of snow modules within specific land-surface schemes to simulate snow cover. An offline evaluation of many schemes by Schlosser *et al.* (2000) focused on how successfully current land-surface schemes simulated snow over an 18 year period; they found considerable scatter in the simulation of snow and no evidence that the ability to simulate cold climate hydrology was related to scheme complexity.

Permafrost, defined as any soil/rock material that remains frozen throughout two or more consecutive years, underlies almost 25% of the exposed land surface in the Northern Hemisphere (Zhang *et al.*, 1999b). The uppermost layer of ground above permafrost, which experiences seasonal thawing, is called the active layer. The most distinct feature of land-atmosphere interactions in permafrost regions is that mass exchange is usually limited to this relatively shallow active layer, with complex transfers of heat by conduction and percolation across the ice/water interface. Recent modelling studies indicate that by the middle of the 21st century, climatic warming may result in a 12 to 15% reduction of the near-surface permafrost area and a 15 to 30% increase of the active layer thickness (Anisimov and Nelson, 1996, 1997; Anisimov *et al.*, 1997). Because of the latent heat involved, thawing of ice-rich permafrost under the changing climatic conditions will be slow, while the reaction of the active layer will be very fast.

There are two major longer term feedbacks between climate and permafrost: release of greenhouse gases from thawing permafrost (Goulden *et al.*, 1998; see also Chapter 4, Section 4.2) and changes in the vegetation associated with the thickening of the active layer. The first contributes directly to the global radiative forcing, while the second alters parameters of the radiation balance and surface hydrology.

7.5.2 Sea Ice

Sea ice plays an important role in moderating heat exchange between the ocean and atmosphere at high latitudes, especially by controlling the heat flux through openings in the ice. Sea ice also interacts with the broader climate system via the ice albedo feedback, which amplifies projected climate warming at high latitudes, and by oceanic feedbacks involving ice growth and melt and the fresh water balance at the ocean surface (Curry and

Webster, 1999; Lewis, 2000) Two feedbacks associated with sea ice are illustrated in Figure 7.6.

The Arctic Ocean sea-ice cover evolves from a highly reflective snow covered surface with few openings in May to a decaying sea-ice cover, mottled with melt ponds and interrupted by frequent openings in July. The seasonal changes in mean albedo in the central Arctic, from roughly 0.8 in May to 0.5 in mid-August, are known to within about ± 0.06 to 0.08. The mean spatial pattern in each summer month features lower albedos in the central Arctic and values 0.1 to 0.2 higher along the ice margins, but the spatial evolution of the pattern in any given year is variable. Averages observed at Soviet North Pole drifting stations, from 1950 to 1991, tend to be higher than satellite-based estimates (Marshunova and Mishin, 1994). Albedo depends on wavelength of radiation and on type and thickness of ice; however, ice type and thickness become unimportant if the snow cover exceeds 3 cm water equivalent. The representation of sea-ice albedo in AGCMs may take account of fractional snow cover, specified or predicted sea-ice thickness, ice surface temperature and the fraction of openings and puddles (Barry, 1996). Most models treat visible and near-infrared spectral ranges but there is still a wide variety of snow and ice albedo parametrizations among atmospheric and ocean GCMs. Important new data sets on puddle albedos (Morassutti and LeDrew, 1996) and the temporal evolution of melt pond coverage (Fetterer and Untersteiner, 1998) will enable more realistic albedo formulations to be developed.

Since the SAR, several coupled climate models have incorporated an explicit treatment of openings in sea ice, often in conjunction with ice dynamics. This is typically effected by partitioning a model grid cell into ice-free and ice-covered fractions. However, sub-grid scale variability in ice thickness, not represented in these schemes, can have a potentially important influence on sea-ice mass balance (Schramm *et al.*, 1997), ice/ocean fluxes of heat and fresh water (Holland *et al.*, 1997b) and the sensitivity of sea ice to thermodynamic perturbations (Holland and Curry, 1999). Recent advances in modelling the thickness distribution function make representing sub-grid scale variability, and the accompanying effects, feasible in global climate simulations (Bitz *et al.*, 2001). Other developments since the SAR include updated parametrizations of snow ageing and associated albedo changes and the implementation in some models of a multi-layer formulation of heat conduction through the ice. Snow plays a particularly important role in sea-ice thermodynamics by modifying the surface albedo, reducing thermal conductivity (and hence ice growth rates), and in some locations causing submergence and surface flooding of ice. Considerable effort continues to be devoted to the development and testing of improved physically based parametrizations suitable for use in such models. Recent field experiments, most notably SHEBA (Randall *et al.*, 1998; Perovich *et al.*, 1999), have provided observational data particularly suited to evaluating climate model parametrizations of sea-ice thermodynamic processes and initial attempts at this are underway. Although sea-ice thermodynamic processes are crudely approximated in many coupled climate models (see Chapter 8, Section 8.5.3), it is unclear how these approximations contribute to errors in climate model simulations.
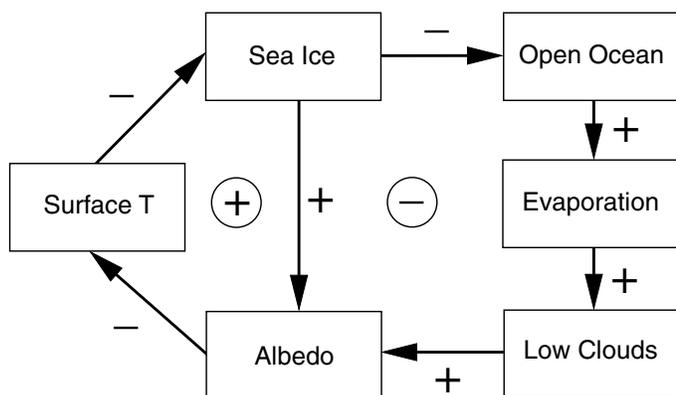
Figure 7.6: Idealised feedback loops involving sea ice. The signs attached to the arrows indicate the correlation between changes in the quantity of the outgoing box with that of the ingoing box, e.g., more sea ice leads to larger albedo. Resulting correlations of a loop are circled and they indicate whether a process is self-reinforced (positive sign) or damped (negative sign). Generally, resulting negative correlations can lead to oscillations, whereas resulting positive correlations may lead to instabilities. The classical ice-albedo effect is shown in the left loop, a feedback involving the overlying atmosphere is on the right.

Box 7.1: Sea ice and climate change.

Sea-ice processes:
Sea ice in the Arctic and around Antarctica responds directly to climate change and may, if properly monitored, become increasingly important for detecting climate change. Although sea ice covers only about 5% of the Earth's surface, its extent and thickness have important influences in the coupled atmosphere-ocean system. Increasing the understanding of these processes and representing them more realistically in climate models is important for making more reliable climate change projections. Several processes associated with sea ice are climatically relevant. The sea-ice albedo effect is an important contributor to the amplification of projected warming at high latitudes. Albedo decreases if the extent of sea ice is reduced and more ocean surface is exposed, resulting in increased heat absorption and hence warming. Melting of snow and the formation of melt-water ponds also reduces albedo and alters the radiation balance. Changes in sea-ice thickness and lead (open water) fraction modify the heat transfer from the ocean: thinner sea ice and more leads result in enhanced heat loss from the exposed ocean thus further warming the atmosphere. Changes in cloud cover may influence how large this effect really is. A principal mechanism for dense water formation in the ocean around Antarctica and in shelf regions of the Arctic is the rejection of brine as sea water freezes. Changes in sea-ice formation alter the properties and formation rates of ocean deep water and therefore have an influence on the water mass structure that reaches far beyond the area of sea ice. Finally, ice export from the Arctic represents an important southward flux of fresh water which influences the density structure of the upper ocean in the Nordic, Labrador and Irminger Seas.

Observations of sea ice:
Observations of sea-ice extent and concentration (the fraction of local area covered by ice) are based primarily on satellite data available since the late 1970s. Sea-ice thickness is also important in assessing possible changes in the amount of sea ice; however, thickness observations are more difficult to make. For the Arctic, thickness data come primarily from sonar measurements from submarines and a few oceanographic moorings. Although limited, the observations indicate statistically significant decreases in ice extent and thickness over the past few decades, with Arctic sea-ice extent declining at a rate of about 3% per decade since the late 1970s. Sea-ice retreat in the Arctic spring and summer over the last few decades is consistent with an increase in spring temperature, and to a lesser extent, summer temperatures at high latitudes. Thickness data show a near 40% decrease in the summer minimum thickness of Arctic sea ice over approximately the last 30 years. Estimates using independent methods for the winter, but over a much shorter period, also suggest thickness reductions, but at a markedly slower rate. However, due to limited sampling, uncertainties are difficult to estimate, and the influence of decadal to multi-decadal variability cannot yet be assessed.

While Arctic sea-ice extent and thickness have clearly decreased in the last 20 years, changes in Antarctic sea-ice extent have been insignificant. The earlier part of the data set indicates somewhat greater ice extents in the early 1970s, and indirect evidence from historical records also points to more northerly sea-ice margins in the 1930s and 1940s. Warming over much of Antarctica has only been about 0.5°C over the last 50 years with the notable exception of the Antarctic Peninsula where temperatures have increased by about 2°C for reasons that remain unclear.

Sea-ice modelling and projection:
Sea ice is particularly difficult to simulate in climate models because it is influenced directly by both the atmosphere (temperature, radiation, wind) and the ocean (heat transport and mixing, and surface currents), and because many of the relevant processes require high grid resolution or must be parametrized. Recent coupled climate models include a sea-ice component that incorporates openings in the ice, often in conjunction with ice dynamics (motion and deformation). Furthermore, updated parametrizations of snow ageing and associated albedo changes and multi-layer formulations of heat conduction through the ice and overlying snow cover are being implemented in some models. Although many thermodynamic processes are crudely approximated, it is unclear how these approximations contribute to errors in climate model simulations. Sea-ice dynamics is important in determining local ice thickness and export of sea ice from the formation areas, but despite the rather mature status of physically based sea-ice dynamics models, only a few of the current coupled climate models include such a component. Coupled model simulations of the seasonal cycle of sea-ice coverage in both hemispheres exhibit large deviations from the limited observational data base, as illustrated in Chapter 8, and current research is aimed at improving model performance.

Coupled model projections of the future distribution of sea ice differ quantitatively from one to another as shown in Chapter 9. However, they agree that sea-ice extent and thickness will decline over the 21st century as the climate warms. Box 7.1, Figure 1 illustrates this with annual mean Arctic ice extent results from two coupled models. The simulations of ice extent decline over the past 30 years are in good agreement with the observations, lending confidence to the subsequent projections which show a substantial decrease of Arctic sea-ice cover leading to roughly 20% reduction in annual mean Arctic sea-ice extent by the year 2050.
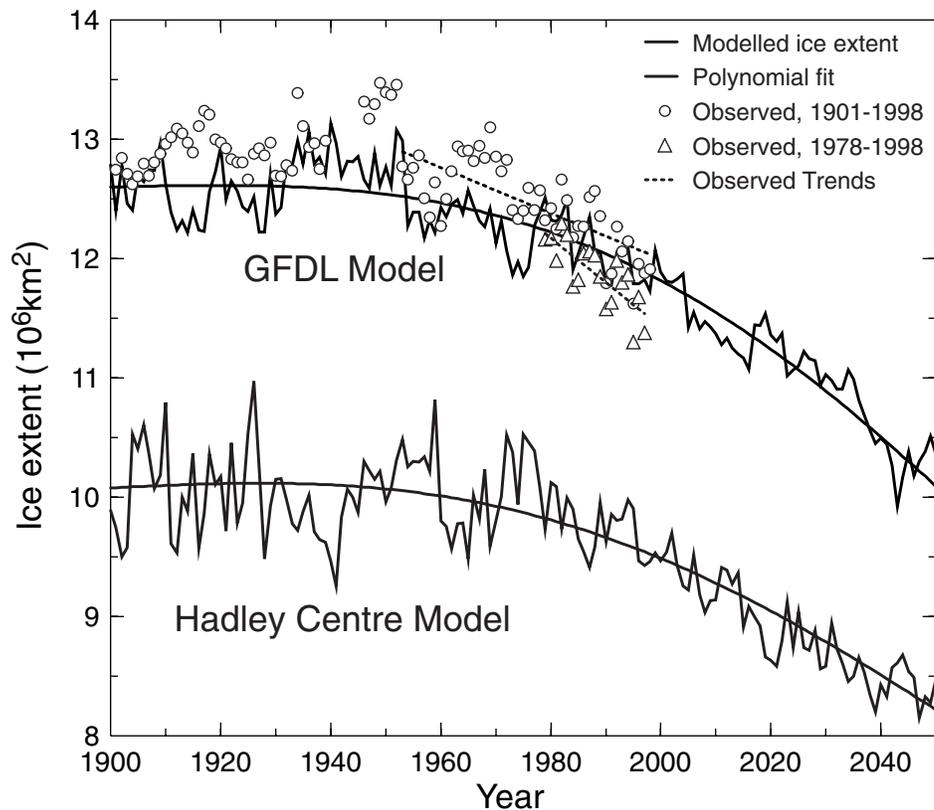
Box 7.1, Figure 1: Observed and modelled variations of annual averages of Northern Hemisphere sea-ice extent (10^6 km^2). Observed data for 1901 to 1998 are denoted by open circles (Chapman and Walsh, 1993, revised and updated) and for 1978 to 1998 by open triangles (Parkinson *et al.*, 1999, updated). The modelled sea-ice extents are from the GFDL and Hadley Centre climate model runs forced by observed CO_2 and aerosols. Modelled data are smoothed by a polynomial fit. Sea-ice extent in these models was determined as the area which had a thickness exceeding 2 cm. This criterion was determined to yield the best agreement with the observed mean during 1953 to 1998; this choice also reproduces the seasonal cycle realistically. Figure from Vinnikov *et al.* (1999).

Ice motion is driven by wind and ocean currents and resisted by ice-ocean drag and internal ice stresses. The representation of internal stresses is the primary distinguishing feature among ice dynamics models. Sensitivity experiments with stand alone sea-ice models (Hibler, 1984; Pollard and Thompson, 1994; Arbetter *et al.*, 1997) indicate that inclusion of ice dynamics can alter the modelled sensitivity of the ice cover to climatic perturbations. An assessment of sea-ice dynamic schemes suited to use in global climate models has been undertaken by the ACSYS Sea-Ice Model Intercomparison Project (SIMIP) (Lemke *et al.*, 1997), which has initially focused on the evaluation of sea-ice rheologies (the relationship between internal stresses and deformation). Results are summarised in Kreyscher *et al.* (1997) and indicate that the elliptical yield curve, viscous-plastic scheme of Hibler (1979) generally outperforms the other schemes evaluated in terms of comparisons to observed ice drift statistics, ice thickness and Fram Strait outflow. Clearly, the effects of ice-related fresh water transports and of other potentially important processes influenced by ice dynamics are not included in climate models which ignore ice motion (see Chapter 8, Section 8.5.3). The

effect on climate sensitivity remains to be assessed. Since the SAR, progress has been made at improving the efficiency of numerical sea-ice dynamic models, making them more attractive for use in coupled climate models (Hunke and Dukowicz, 1997; Zhang and Hibler, 1997).

The high latitude ocean fresh water budget is dominated by cryospheric processes. These include growth, melt and transport of sea ice, glacial melt, snowfall directly on ice and its subsequent melt and the runoff of snow melt water from adjacent land. Decadal-scale oscillations in atmospheric circulation may result in changes of the distribution of precipitation over watersheds that empty into the Arctic Ocean as well as of the snow cover on sea ice itself. The various components of the Arctic fresh water budget are reviewed in detail in Lewis (2000). Fresh water transport by sea ice is becoming increasingly important in coupled climate models as the trend toward eliminating flux adjustments requires explicit representation of this type of redistribution of the fresh water entering the ocean's surface.

Transport of sea ice through Fram Strait has long been implicated in modulating sea surface salinity and deep water

formation in the North Atlantic (Dickson *et al.*, 1988; Belkin *et al.*, 1998). Recent modelling studies show that wind forcing dominates the variability in ice outflow (Hakkinen, 1993; Harder *et al.*, 1998; Hilmer *et al.*, 1998) and suggest that decadal-scale oscillations in atmospheric circulation are reflected in overall ice transport patterns (Proshutinsky and Johnson, 1997; Polyakov *et al.*, 1999). Net export of ice from the Arctic Ocean to the North Atlantic amounts to an annual loss of roughly 0.4 m of fresh water (Vinje *et al.*, 1998), which is offset by net ice growth. The salt released by this ice growth is in turn largely offset by inflow of fresher Pacific water, via the Bering Strait, and river runoff, maintaining a stable stratification. Changes in ice outflow, such as might arise under a changing climate, could alter the distribution of fresh water input to the Arctic and North Atlantic, with consequences for ocean circulation, heat transport and carbon cycling.

Around Antarctica, ice transport primarily exports fresh water from coastal regions where it is replaced by net ice growth. The salt released by this growth contributes directly to Antarctic deep water production (Goosse *et al.*, 1997; Legutke *et al.*, 1997; Stössel *et al.*, 1998; Goosse and Fichefet, 1999). However, the details of how salt released by freezing sea ice is distributed in the water column can have a substantial impact on water mass formation and circulation (Duffy and Caldeira, 1997; Legutke *et al.*, 1997; Duffy *et al.*, 1999) and hence on heat and carbon sequestration in a changing climate.

7.5.3 Land Ice

Ice stream instability, ice shelf break-up and switches in routing and discharge of glacial melt water present themselves as mechanisms for altering the surface salinity of oceans and inducing changes in the pattern and strength of the THC. There are positive and negative feedbacks associated with changing land ice masses (Figure 7.7). In coupled climate models, all these cryospheric processes are represented simply as surface fresh water inputs to the ocean (see Chapter 8, Section 8.5.4.2).
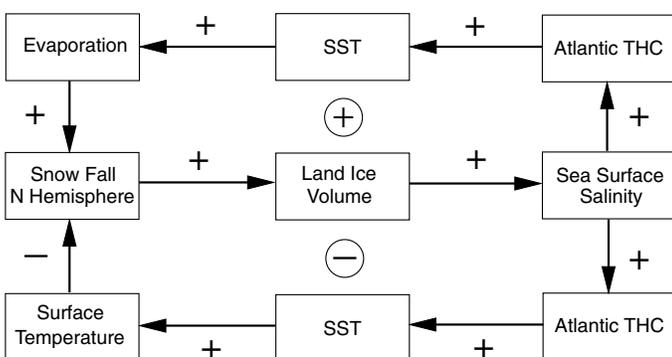

Figure 7.7: Feedback loops associated with land ice masses. Changes in their volume affect the salt balance at the sea surface and may influence the thermohaline circulation (THC). While there is palaeo-climatic evidence that this has happened often during the last Ice Age, the above processes are unlikely to play a major role for future climate change.

Ice sheets are continental scale masses of fresh water ice formed by the burial and densification of snow. They can be divided into areas that are grounded on the land surface, either below or above sea level, and areas that are afloat. Grounded parts of ice sheets exhibit slow and fast modes of flow. The slow sheet-flowing component is the more prevalent but the fast stream-flowing component can account for most of the ice discharge. Switching between slow and fast modes of flow may occur thermally, mechanically or hydrologically and is suggestive of "surging", a known cyclic instability of certain glaciers (Kamb *et al.*, 1985; Bindschadler, 1997). The slow-flow process for ice sheets is internal creep and the fast-flow processes relevant to ice streams are bottom sliding, enhanced creep and sub-glacial sediment deformation (Alley, 1989; Iken *et al.*, 1993; Engelhardt and Kamb, 1998). The factors controlling onset, discharge and width of ice streams are subject to poorly understood geological, topographic, thermal and hydrological controls (Clarke and Echelmeyer, 1996; Anandakrishnan and Alley, 1997; Bindschadler, 1997; Anandakrishnan *et al.*, 1998; Bell *et al.*, 1998; Jacobson and Raymond, 1998).

Although in GCMs the albedo of land ice is typically fixed, satellite observations could be used to remove this limitation; the melt area, as identified from satellite passive microwave observations (Mote *et al.*, 1993; Abdalati and Steffen, 1995), and AVHRR-derived albedo estimates can now be mapped (Stroeve *et al.*, 1997). Land ice dynamics and thermodynamics, ignored in current coupled GCMs, respond to changes in the temperature and balance of accumulation and melt at upper and lower surfaces. These boundary conditions involve couplings to the atmosphere, ocean and lithosphere. Ice sheet models typically represent atmospheric boundary conditions using simple elevation-based parametrizations. However, results obtained for Antarctica using this approach (Huybrechts and Oerlemans, 1990; Fastook and Prentice, 1994) compare favourably with those using more comprehensive AGCM-derived boundary conditions (Thompson and Pollard, 1997). Predictive models of future evolution must incorporate past ice-mass variations because ice sheets continue to respond to climate change for several thousand years. Time-scales complicate the inclusion of land ice in existing coupled climate models, and it is usual in these models to regard land ice as passive, providing only a static boundary for the atmosphere. Models of ocean circulation seldom incorporate explicit treatments of melt water inputs from land ice.

Models simulate the coupled evolution of ice sheet flow, form and temperature. The flow law in Glen (1955) is commonly adopted but such models must employ a poorly justified flow enhancement factor to correctly capture the height-to-width ratios of ice sheets. In general, these models perform well in inter-comparison exercises (Huybrechts *et al.*, 1996; Payne *et al.*, 2000), but there is uncertainty in the predicted thermal structure and bottom melting conditions. This constitutes a potentially serious shortcoming because several models of ice sheet instability invoke thermal trigger mechanisms (MacAyeal, 1992). Ice stream flow models are limited by the current knowledge of the controlling physical processes. Outstanding issues involve the relative importance of bottom drag and lateral drag (Whillans and

van der Veen, 1993; MacAyeal *et al.*, 1995) and the representation of fast-flow and water-transport processes (Fowler and Schiavi, 1998; Hindmarsh, 1998; Tulaczyk *et al.*, 1998). Recently, coupled models of the evolution of ice streams within ice sheets have been developed (Marshall and Clarke, 1997) which incorporate the crucial processes of ice stream onset (Bell *et al.*, 1998) and margin migration (van der Veen and Whillans, 1996).

Floating margins of ice sheets are called ice shelves, the largest of which are found in West Antarctica and mediate the transfer of ice between fast-flowing ice streams and the Southern Ocean. Break-up of one or both of the large West Antarctic ice shelves, either associated with ice stream instability or independent of it, cannot be discounted and would be considerably more probable than complete disintegration of the West Antarctic ice sheet (Bentley, 1998; see also Chapter 11, Section 11.3.3). Such an event would be accompanied by a large increase in iceberg flux to the Southern Ocean and uncertain effects on the production of AABW and ocean circulation. Different ice shelf models compare well (MacAyeal *et al.*, 1996); however, the stability of grounding lines remains an issue and could significantly influence the behaviour of numerical models (Hindmarsh, 1993). The suggestion that the grounding line is inherently unstable (Thomas and Bentley, 1978) is not supported by more recent modelling studies (Muszynski and Birchfield, 1987; Huybrechts and Oerlemans, 1990; Hindmarsh, 1993). However, this issue has yet to be resolved.

Megafloods of water stored beneath ice sheets have been postulated (Shaw *et al.*, 1996) but the subject is controversial. The estimated total volume of lake water beneath Antarctica is equivalent to 10 to 35 mm of sea level rise (Dowdeswell and Siegert, 1999) but the simultaneous release of all this stored water is unlikely. The timing would be unpredictable and climate impacts, if any, would be associated with the effect of the fresh water pulse on AABW formation. Modelling such phenomena is beyond the scope of existing ice dynamics models. Although progress has been made in the understanding of ice stream processes, there are still many unanswered questions and representation of ice stream and grounding line physics in land-ice dynamics models remains rudimentary.

7.6 Processes, Feedbacks and Phenomena in the Coupled System

This section deals with some of the processes and feedbacks in the coupled atmosphere-ocean system; those involving land and the cryosphere are dealt with in Sections 7.4 and 7.5, respectively. Increasingly, natural modes of variability of the atmosphere and the atmosphere-ocean system are also understood to play key roles in the climate system and how it changes, and thus the teleconnections which are believed to be most important for climate change are briefly discussed.

7.6.1 Surface Fluxes and Transport of Heat and Fresh Water

Fundamental issues in the global climate system are the relative amounts of heat and fresh water carried by the oceans and the atmosphere to balance the global heat and water budgets.

Because the top-of-the-atmosphere radiation largely determines the distribution of net energy on the Earth, the fluid components of the climate system, the atmosphere and ocean, transport heat and energy from regions of surplus to regions of deficit, with the total heat transport constrained. In the SAR a major problem with atmospheric models was that their surface fluxes with the ocean and the implied oceanic heat transports did not agree with the quite uncertain observational estimates and the biggest problem was clearly with clouds. The result was that all coupled models of the current climate either had a bias in their simulation of the mean state or that a "flux adjustment" was employed to keep the mean state close to that observed. Although some recent coupled ocean-atmosphere models (Boville and Gent, 1998; Gordon *et al.*, 2000) do not have adjustments to the modelled surface heat, water and momentum fluxes (see Chapter 8, Section 8.4.2), the drift in surface climate is small. This implies that the surface air-sea heat and water fluxes calculated by the model are reasonably consistent with the simulated ocean heat and fresh water transports. However, only comparison with flux values of known accuracy can verify the predicted fluxes, and thereby increase confidence in the modelled physical processes.

The role of the oceans in maintaining the global heat and water budgets may be assessed using bulk formulae, residual and direct (hydrographic) methods. Direct measurements of the sensible and latent heat fluxes have led to improved parametrizations (Fairall *et al.*, 1996; Weller and Anderson, 1996; Godfrey *et al.*, 1998), but large 20 to 30% uncertainties amounting to several tens of Wm^{-2} remain (DeCosmo *et al.*, 1996; Gleckler and Weare, 1997). Recent global air-sea flux climatologies based on ship data and bulk formulae (da Silva *et al.*, 1994; Josey *et al.*, 1999) exhibit an overall global imbalance; on average the ocean gains heat at a rate of about 30 Wm^{-2}. This was adjusted by globally scaling the flux estimates (da Silva *et al.*, 1994), but spatially uniform corrections are not appropriate (Josey *et al.*, 1999). While satellites give data over all ocean regions (e.g., Schulz and Jost, 1998; Curry *et al.*, 1999), and precipitation estimates over the oceans are only viable using satellites (Xie and Arkin, 1997), their accuracy is still unknown. Overall, surface evaporation minus precipitation (E–P) estimates are probably accurate to no better than about 30%.

In the residual method the atmospheric energy transport is subtracted from the top-of-the-atmosphere radiation budget to derive the ocean heat transport. Until fairly recently, the atmospheric poleward transport estimates were too small and led to overestimates of the ocean transports. This has improved with local applications of global numerical atmospheric analyses based on four dimensional data assimilation (Trenberth and Solomon, 1994; Keith, 1995). With reanalysis of atmospheric observations, more reliable atmospheric transports are becoming available (Table 7.1). Sun and Trenberth (1998) show that large interannual changes in poleward ocean heat transports are inferred with El Niño events in the Pacific. The moisture budget estimates of E–P are generally superior to those computed directly from E and P estimates from the model used in the assimilation (e.g., Trenberth and Guillemot, 1998) and are probably to be preferred to bulk flux estimates, given the inaccuracy of bulk estimates of P.

In the direct method the product of ocean velocity and

temperature measured over the boundaries is integrated to determine the ocean heat transport divergence for the volume. While it deals with ocean circulation and the mechanisms of ocean heat transport, estimates could only be made at a few locations where high quality observations were available and assumptions, such as geostrophic velocity estimates, are reasonable. Most of the recent estimates are for the Atlantic Ocean (see Table 7.1), for which there is general agreement that there is northward ocean heat transport at all latitudes. It is generally understood that this northward heat transport is associated with the THC in which NADW is formed in the polar and sub-polar North Atlantic and subsequently flows southward as a deep western boundary current into the Southern Ocean. In the North Pacific Ocean at 10°N (Wijffels et al., 1996), the northward heat flux of 0.7 ± 0.5 PW (1 PetaWatt = 1 PW = 10^{15} W) is due primarily to a shallow Ekman upper thermocline cell. It is estimated that a 6 Sv change in Ekman transport, which is comparable to the differences among existing climatologies, would cause a 0.4 PW change in meridional heat transport. For the South Pacific (Koshlyakov and Sazhina, 1996; Tsimplis et al., 1998) and Indian oceans (Robbins and Toole, 1997) the determination of ocean heat transport is hampered by uncertainties in the size of the Indonesian Throughflow and in the Agulhas Current transports (Beal and Bryden, 1997), and the estimates of northward heat transport across 30°S in the Indian Ocean range from –0.4 to –1.3 PW (Robbins and Toole, 1997; Macdonald, 1998). Macdonald (1998) and Macdonald and Wunsch (1996) have made a global inverse analysis of selected high quality hydrographic sections covering all ocean basins taken prior to the World Ocean Circulation Experiment (WOCE) observational period to produce meridional heat transports (Table 7.1). For the heat fluxes, results from the methods are beginning to converge. While some new direct ocean fresh water transport measure-

ments (Saunders and King, 1995) indicate that the South Atlantic receives adequate excess precipitation to supply the cross equatorial flux of fresh water for North Atlantic excess evaporation, this runs contrary to previous estimates (Wijffels et al., 1992) and the recent atmospheric moisture budget results (Trenberth and Guillemot, 1998).

The latest results of the zonal mean ocean heat transports computed from (i) observational data as residuals, (ii) models run without flux adjustments and (iii) direct measurements agree within error estimates (Table 7.1). This suggests that the models are now converging on the correct values for the zonally averaged heat fluxes. However, significant regional biases and compensating errors in the radiative and turbulent fluxes still exist (Doney et al., 1998; Gordon et al., 2000). The coupled model fresh water flux estimates are more problematic. For example, the inter-tropical convergence zone may become skewed and spuriously migrate from one hemisphere to the other, seriously distorting the precipitation fields (e.g., Boville and Gent, 1998).

The compatibility and improvements of the ocean and atmospheric heat transports in models is evidently the primary reason why coupled runs can now be made without flux adjustments (Gregory and Mitchell, 1997). This is due to a better representation of key processes in both atmosphere and ocean components of climate models, and improved spatial resolution. These key processes include, in the atmosphere, convection, boundary-layer physics, clouds, and surface latent heat fluxes (Hack, 1998), and in the ocean, boundary layer and mesoscale eddy mixing processes (Doney et al., 1998; Large and Gent, 1999). However, while simulated SSTs generally agree well with observations (deviations of less than 2°C), there are large areas where consistent errors of SST occur in the models (e.g., too cold in the North Pacific; too warm in coastal upwelling regions, see Chapter 8, Figure 8.1a). These point to processes that must be

Table 7.1: *Ocean heat transport estimates, positive northwards in PetaWatts (1 PetaWatt = 1 PW = 10^{15}W), from analyses of individual hydrographic sections from pre WOCE sections (Macdonald, 1998), indirect methods (Trenberth et al., 2001), and years 81 to 120 of the HadCM3 (UKMO) coupled model (Gordon et al., 2000) and from the CSM 1.0 (NCAR) (Boville and Gent, 1998). Typical error bars are ±0.3 PW. For the Atlantic the sections are: 55°N (Bacon, 1997), 24°N (Lavin et al., 1998), 14°N (Klein et al., 1995), 11°S (Speer et al., 1996), and at 45°S (Saunders and King, 1995). For the Pacific: 47°N (Roemmich and McCallister, 1989), 24°N (Bryden et al., 1991), 10°N (Wijffels et al., 1996). Because of the Indonesian throughflow, South Pacific and Indian Ocean transports make most sense if combined.*

Atlantic	Sections	Macdonald	Trenberth	HadCM3	CSM 1.0
55°N	0.28	–	0.29	–	0.63
48°N	–	0.65	0.41	0.54	0.81
24°N	1.27	1.07	1.15	1.14	1.31
14°N	1.22	–	1.18	–	1.27
11°N	–	1.39	1.15	1.12	1.21
11°S	0.60	0.89	0.63	–	0.65
23°S	–	0.33	0.51	0.67	0.61
45°S	0.53	–	0.62	0.64	–
Pacific					
47°N	−0.09	−0.08	−0.06	0.17	0.11
24°N	0.76	0.45	0.73	0.50	0.69
10°N	0.70	0.44	0.85	0.68	0.87
Pacific + Indian					
32°S	–	−1.34	−1.14	−1.19	−1.13

improved in future models. For instance, stratocumulus decks are not well simulated in coupled models, resulting in significant deviations of SST from the observed (see Chapter 8, Figure 8.1a and Section 8.4.2 for a discussion).

7.6.2 Ocean-atmosphere Interactions

There is no clear separation between the wind-driven circulation and the THC (see Section 7.3.6) because they interact with each other on several time-scales. While there is a great deal of empirical evidence that the ocean and sea surface temperatures co-vary with the atmosphere, this may only indicate that the atmosphere forces the ocean, and it does not necessarily signify a feedback or a truly coupled process that contributes to the variability. Moreover, it is very difficult to establish such coupling from observational studies. This topic was not dealt with thoroughly by the SAR. In the tropics there is clear evidence of the ocean forcing the atmosphere, such as in El Niño (see Section 7.6.5). In the extra-tropics much of what can be seen is accountable through fairly random wind variations; essentially stochastic forcing of the ocean is converted into low frequency ocean variability and gives a red spectrum in oceanic temperatures and currents up to the decadal time-scale (Hasselmann, 1976; Hall and Manabe, 1997). Feedback to the atmosphere is not involved. In the spatial resonance concept (Frankignoul and Reynolds, 1983) there is still no feedback from the ocean to the atmosphere, but oceanic quantities may exhibit a spectral peak through an advective time-scale (Saravanan and McWilliams, 1998) or Rossby wave dynamics time-scale (Weng and Neelin, 1998). In coupled air-sea modes, such as those proposed by Latif and Barnett (1996) for the North Pacific and by Groetzner *et al.* (1998) for the North Atlantic, there is a feedback from the ocean to the atmosphere. Spectral peaks are found in both the ocean and the atmosphere, and the period of the oscillation is basically determined by the adjustment time of the sub-tropical gyre to changes in the wind stress curl.

Coupled models indicate that, in mid-latitudes, the predominant process is the atmosphere driving the ocean as seen by the surface fluxes and as observed, yet when an atmospheric model is run with specified SSTs, the fluxes are reversed in sign, showing the forcing of the atmosphere from the now infinite heat capacity of the ocean (implied by specified SSTs). Recent ensemble results (Rodwell *et al.*, 1999; Mehta *et al.*, 2000) have been able to reproduce the decadal North Atlantic atmospheric variations from observed SSTs but with much reduced amplitude. Bretherton and Battisti (2000) suggest that this is consistent with a predominant stochastic driving of the ocean by the atmosphere with some modest feedback on the atmosphere, and that the signal only emerges through ensemble averaging.

In the extra-tropics, a key question remains the sensitivity of the mid-latitude atmosphere to surface forcing from sea ice and sea surface temperature anomalies. Different modelling studies with similar surface conditions yield contradictory results (e.g., Robertson *et al.*, 2000a,b). The crude treatment of processes involving sea ice, oceanic convection, internal ocean mixing and eddy-induced transports and the coarse resolution of most coupled climate models, adds considerably to the uncertainty.

7.6.3 Monsoons and Teleconnections

The weather and climate around the world in one place is generally strongly linked to that in other places through atmospheric linkages. In the tropics and sub-tropics, large-scale overturning in the atmosphere, which is manifested as the seasonal monsoon variations, links the wet summer monsoons to the dry subsiding regions usually in the tropics and sub-tropics of the winter hemisphere. Throughout the world, teleconnections link neighbouring regions mainly through large-scale, quasi-stationary atmospheric Rossby waves. A direct consequence of these linkages is that some regions are wetter and/or hotter than the prevailing global scale changes, while half a wavelength away the regions may be dryer and/or cooler than the global pattern. Moreover, because of the way these patterns set up relative to land and ocean, they can alter the global mean changes. In addition, errors in models (such as in convection in the tropical Pacific) can be manifested non-locally through teleconnections, e.g., in the North Pacific SSTs (see Figure 8.1a), although other processes are also involved.

The term "monsoon" is now generally applied to tropical and sub-tropical seasonal reversals in both the atmospheric circulation and associated precipitation. These changes arise from reversals in temperature gradients between continental regions and the adjacent oceans with the progression of the seasons. The dominant monsoon systems in the world are the Asian-Australian, African and the American monsoons. As land heats faster than ocean in summer, heated air rises and draws moist low-level maritime air inland where convection and release of latent heat fuel the monsoon circulation. For the Asian monsoon, a regional meridional temperature gradient extending from the tropical Indian Ocean north to mid-latitude Asia develops prior to the monsoon through a considerable depth of the troposphere (Webster *et al.*, 1998). To a first order, the stronger this meridional temperature gradient, the stronger the monsoon. Thus land-surface processes, such as soil moisture and snow cover in Asia can influence the monsoon and, along with SST variations, may induce quasi-biennial variability (Meehl, 1997). Additionally, large-scale forcing associated with tropical Pacific SSTs influences monsoon strength through the large-scale east-west overturning in the atmosphere. Anomalously cold (warm) Pacific SSTs often are associated with a strong (weak) monsoon, though these connections are somewhat intermittent.

Some teleconnections arise simply from natural preferred modes of the atmosphere associated with the mean climate state and the land-sea distribution. Several are directly linked to SST changes (Trenberth *et al.*, 1998). The most prominent are the Pacific-North American (PNA) and the North Atlantic Oscillation (NAO; see Section 7.6.4) in the Northern Hemisphere, and both account for a substantial part of the pattern of northern hemispheric temperature change, especially in winter (Hurrell, 1996), in part through the "cold ocean warm land" (COWL) pattern (Wallace *et al.*, 1995; Hurrell and Trenberth, 1996) (see

Chapter 2). Although evidently a prominent mode of the atmosphere alone, the PNA is also influenced by changes in ENSO (see Section 7.6.5). Thompson and Wallace (1998, 2000) suggest that the NAO may be the regional manifestation of an annular (zonally symmetric) hemispheric mode of variability characterised by a seesaw of atmospheric mass between the polar cap and the middle latitudes in both the Atlantic and Pacific Ocean basins and they call this the Arctic Oscillation (AO). A similar, even more zonal structure is dominant in the Southern Hemisphere (Trenberth *et al.*, 1998) (the Southern Annular Mode, sometimes called the Antarctic Oscillation, AAO). The vertical structure of both AO and AAO extends well into the stratosphere (Perlwitz and Graf, 1995; Thompson and Wallace, 1998).

In the Atlantic, an important emerging coupled mode of variability is the so-called tropical Atlantic dipole, which involves variations of opposite sign in the sea level pressure field across the equatorial Atlantic and corresponding variations in the ITCZ location. Given the background SST and wind fields, anomalous SSTs of opposite sign across the equatorial region are apt to alter the surface winds in such a way as to enhance or reduce evaporative cooling of the ocean and reinforce the original SST pattern (Carton *et al.*, 1996; Chang *et al.*, 1997). The ocean provides a decadal time-scale to the coupled interactions.

Dominant large-scale patterns of ocean-atmosphere interactions are also found in the tropical Indian Ocean (Saji *et al.*, 1999; Webster *et al.*, 1999). They have characteristics similar to El Niño and are associated with large east-west SST changes and a switch of the major tropical convection areas from Africa to Indonesia. There are indications that this atmosphere-ocean process is somewhat independent of ENSO and represents a natural mode of the tropical Indian Ocean.

The vital processes for improved monsoon simulation in models are those associated with the hydrological cycle, especially in the tropics. These include convection, precipitation and other atmospheric processes (see Section 7.2) as well as land surface processes (see Section 7.4), and interactions of the atmosphere with complex topography and with the ocean. The difficulties in assembling all of these elements together has led to problems in simulating mean precipitation as well as interannual monsoon variability, although improvements are evident (Webster *et al.*, 1998, and see Chapter 8, Section 8.7.3).

For teleconnections and regional climate patterns, not only are there demanding requirements on simulating the variations in tropical SSTs that drive many of the interannual and longer-term fluctuations through latent heating in the associated tropical precipitation, but results also depend on the mean state of the atmosphere through which Rossby waves propagate. Feedbacks from changes in storm tracks, and thus momentum and heat transports by transient atmospheric disturbances, as well as interactions with changed land-surface soil moisture from precipitation changes and interactions with extra-tropical oceans are critical. While there is scope for further improvements, great strides have been made in modelling all these aspects in the recent years.

7.6.4 North Atlantic Oscillation and Decadal Variability

The NAO is the dominant pattern of wintertime atmospheric circulation variability over the extra-tropical North Atlantic (Hurrell, 1995), and has exhibited decadal variability and trends (see Chapter 2, Section 2.6). There is strong evidence indicating that much atmospheric circulation variability in the form of the NAO arises from internal atmospheric processes (Saravanan, 1998; Osborn *et al.*, 1999). During winters when the stratospheric vortex is stronger than normal, the NAO (and AO) tends to be in a positive phase suggesting an interaction and perhaps even a downward influence from the stratosphere to the troposphere (see Sections 7.2.5 and 7.6.3; Baldwin and Dunkerton, 1999). The recent trend in the NAO/AO could possibly thus be related to processes which are known to affect the strength of the stratospheric polar vortex such as tropical volcanic eruptions (Kodera, 1994; Kelly *et al.*, 1996), ozone depletion, and changes in greenhouse gas concentrations resulting from anthropogenic forcing (Shindell *et al.*, 1999b).

It has long been recognised that fluctuations in SST are related to the strength of the NAO, and Dickson *et al.* (1996, 2000) have shown a link to the ocean gyre and thermohaline circulations. The leading mode of SST variability over the North Atlantic during winter is associated with the NAO. During high NAO years anomalous SSTs form a tri-polar pattern with a cold anomaly in the sub-polar region, a warm anomaly in the middle latitudes, and a cold sub-tropical anomaly (e.g., Deser and Blackmon, 1993), consistent with the spatial form of the anomalous surface fluxes associated with the NAO pattern (Cayan, 1992). This indicates that SST is responding to atmospheric forcing on seasonal time-scales (Deser and Timlin, 1997). However, GCM simulations suggest that SST in the North Atlantic can, in turn, have a marked effect on NAO (see Section 7.6.2). Winter SST anomalies were observed to spread eastward along the path of the Gulf Stream and North Atlantic Current with a transit time-scale of a decade (Sutton and Allen, 1997). These SST anomalies reflect anomalies in the heat content of the deep winter mixed layers that when exposed to the atmosphere in winter (Alexander and Deser, 1995) could affect the NAO, imprinting the advective time-scale of the gyre on the atmosphere (McCartney *et al.*, 1996). Moreover, similar processes were identified in coupled GCM integrations (Groetzner *et al.*, 1998; Timmermann *et al.*, 1998; Delworth and Mann, 2000) where changes in SST due to oceanic processes (gyre advection or thermohaline circulation) affected the NAO. This, in turn, leads to changes in heat and fresh water fluxes, and in wind stress forcing of the oceanic circulation. Oceanic response to such changes in the forcing produced a negative feedback loop, leading to decadal oscillations. However, the role of these mechanisms is yet to be established.

Watanabe and Nitta (1999) have suggested that high latitude snow cover on land is responsible for decadal changes in the NAO. Changes in sea-ice cover in both the Labrador and Greenland Seas as well as over the Arctic also appear to be well correlated with the NAO (Deser *et al.*, 2000). Such changes may also affect the atmosphere because of the large changes in sensible and latent heat fluxes along the ice edge.

Box 7.2: Changes in natural modes of the climate system.

Observed changes in climate over the Northern Hemisphere in winter reveal large warming over the main continental areas and cooling over the North Pacific and North Atlantic. This "cold ocean – warm land" pattern has been shown to be linked to changes in the atmospheric circulation, and, in particular, to the tendency in the past few decades for the North Atlantic Oscillation (NAO) to be in its positive phase. Similarly, the Pacific-North American (PNA) teleconnection pattern has been in a positive phase in association with a negative Southern Oscillation index or, equivalently, the tendency for El Niño-Southern Oscillation (ENSO) to prefer the warm El Niño phase following the 1976 climate shift (Chapter 2). Because of the differing heat capacities of land and ocean, the "cold ocean-warm land" pattern has amplified the Northern Hemisphere warming. A fingerprint of global warming from climate models run with increasing greenhouse gases indicates greater temperature increases over land than over the oceans, mainly from thermodynamic (heat capacity and moisture) effects. This anthropogenic signal is therefore very similar to that observed, although an in-depth analysis of the processes involved shows that the dynamical effects from atmospheric circulation changes are also important. In other words, the detection of the anthropogenic signal is potentially masked or modified by the nature of the observed circulation changes, at least in the northern winter season. The detection question can be better resolved if other seasons are also analysed (Chapter 12). Attribution of the cause of the observed changes requires improved understanding of the origin of the changes in atmospheric circulation. In particular, are the observed changes in ENSO and the NAO (and other modes) perhaps a consequence of global warming itself?

There is no simple answer to this question at present. Because the natural response of the atmosphere to warming (or indeed to any forcing) is to change large-scale waves, some regions will warm while others cool more than the hemispheric average, and counterintuitive changes can be experienced locally. Indeed, there are preferred modes of behaviour of the atmospheric circulation, sometimes manifested as preferred teleconnection patterns (see this chapter) that arise from the planetary waves in the atmosphere and the distribution of land, high topography, and ocean. Often these modes are demonstrably natural modes of either the atmosphere alone or the coupled atmosphere-ocean system. As such, it is also natural for modest changes in atmospheric forcing to project onto changes in these modes, through changes in their frequency and preferred sign, and the evidence suggests that changes can occur fairly abruptly. This is consistent with known behaviour of non-linear systems, where a slow change in forcing or internal mechanisms may not evoke much change in behaviour until some threshold is crossed at which time an abrupt switch occurs. The best known example is the evidence for a series of abrupt climate changes in the palaeoclimate record apparently partly in response to slow changes in sea level and the orbit of the Earth around the Sun (Milankovitch changes, see Chapter 2). There is increasing evidence that the observed changes in the NAO may well be, at least in part, a response of the system to observed changes in sea surface temperatures, and there are some indications that the warming of tropical oceans is a key part of this (see this chapter for more detail). ENSO is not simulated well enough in global climate models to have confidence in projected changes with global warming (Chapter 8). It is likely that changes in ENSO will occur, but their nature, how large and rapid they will be, and their implications for regional climate change around the world are quite uncertain and vary from model to model (see this chapter and Chapter 9). On time-scales of centuries, the continuing increase of greenhouse gases in the atmosphere may cause the climate system to cross a threshold associated with the Atlantic thermohaline circulation: beyond this threshold a permanent shut-down of the thermohaline circulation results (see this chapter and Chapter 9).

Therefore, climate change may manifest itself both as shifting means as well as changing preference of specific regimes, as evidenced by the observed trend toward positive values for the last 30 years in the NAO index and the climate "shift" in the tropical Pacific about 1976. While coupled models simulate features of observed natural climate variability such as the NAO and ENSO, suggesting that many of the relevant processes are included in the models, further progress is needed to depict these natural modes accurately. Moreover, because ENSO and NAO are key determinants of regional climate change, and they can possibly result in abrupt changes, there has been an increase in uncertainty in those aspects of climate change that critically depend on regional changes.

7.6.5 El Niño-Southern Oscillation (ENSO)

The strongest natural fluctuation of climate on interannual time-scales is the El Niño-Southern Oscillation (ENSO) phenomenon, and ENSO-like fluctuations also dominate decadal time-scales (sometimes referred to as the Pacific decadal oscillation). ENSO originates in the tropical Pacific but affects climate conditions globally. The importance of changes in ENSO as the climate changes and its potential role in possible abrupt shifts have only recently been appreciated. Observations and modelling of ENSO are addressed in Chapters 2, 8 and 9; here the underlying processes are discussed. Observational and modelling results suggest that more frequent or stronger ENSO events are possible in the future. Because social and ecological systems are particularly vulnerable to rapid changes in climate, for the next decades, these may prove of greater consequence than a gradual rise in mean temperature.

7.6.5.1 ENSO processes

ENSO is generated by ocean-atmosphere interactions internal to the tropical Pacific and overlying atmosphere. Positive temperature anomalies in the eastern equatorial Pacific (characteristic of an El Niño event) reduce the normally large sea surface temperature difference across the tropical Pacific. As a consequence, the trade winds weaken, the Southern Oscillation index (defined as the sea level pressure difference between Tahiti and Darwin) becomes anomalously negative, and sea level falls in the west and rises in the east by as much as 25 cm as warm waters extend eastward along the equator. At the same time, these weakened trades reduce the upwelling of cold water in the eastern equatorial Pacific, thereby strengthening the initial positive temperature anomaly. The weakened trades also cause negative off-equatorial thermocline depth anomalies in the central and western Pacific. These anomalies propagate westward to Indonesia, where they are reflected and propagate eastward along the equator. Thus some time after their generation, these negative anomalies cause the temperature anomaly in the east to decrease and change sign. The combination of the tropical air-sea instability and the delayed negative feedback due to sub-surface ocean dynamics can give rise to oscillations (for a summary of theories see Neelin *et al.*, 1998). Two of these feedbacks are schematically illustrated in Figure 7.8. Beyond influencing tropical climate, ENSO seems to have a global influence: during and following El Niño, the global mean surface temperature increases as the ocean transfers heat to the atmosphere (Sun and Trenberth, 1998).

The shifts in the location of the organised rainfall in the tropics and the associated latent heat release alters the heating patterns of the atmosphere which forces large-scale waves in the atmosphere. These establish teleconnections, especially the PNA and the southern equivalent, the Pacific South American (PSA) pattern, that extend into mid-latitudes altering the winds and changing the jet stream and storm tracks (Trenberth *et al.*, 1998), with ramifications for weather patterns and societal impacts around the world.
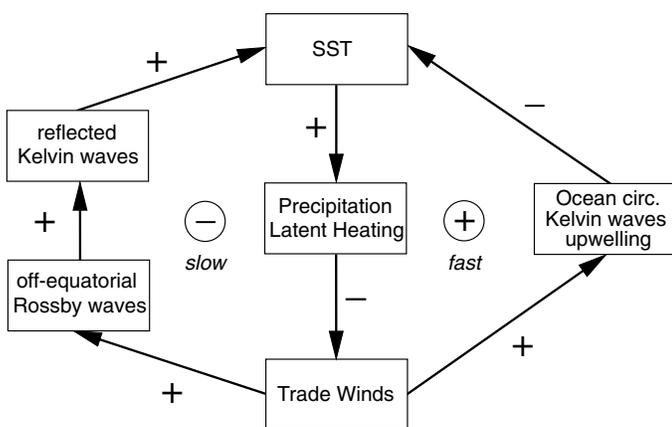

Figure 7.8: Simplified principal feedback loops active in El Niño-Southern Oscillation (ENSO). The fast loop (right) gives rise to an instability responsible for the development of an El Niño, the slow loop (left) tends to dampen and reverse the anomalies, so that together, these processes excite oscillations.

Another related feedback occurs in the sub-tropics. The normally cold waters off the western coasts of continents (such as California and Peru) encourage the development of extensive low stratocumulus cloud decks which block the Sun, and this helps keep the ocean cold. A warming of the waters, such as during El Niño, eliminates the cloud deck and leads to further sea surface warming through solar radiation. Kitoh *et al.* (1999) found that this mechanism could lead to interannual variations in the Pacific Ocean without involving equatorial ocean dynamics. Currently, stratocumulus decks are not well simulated in coupled models, resulting in significant deviations of SST from the observed (see Chapter 8, Figure 8.1).

Indices of ENSO for the past 120 years (Figure 7.9), indicate that there is considerable variability in the ENSO cycle in the modern record. This variability has been variously attributed to: (i) stochastic forcing due to weather and other high-frequency "noise", and the Madden-Julian intra-seasonal oscillation in particular; (ii) deterministic chaos arising from internal non-linearities of the tropical Pacific ENSO system; (iii) forcing within the climate system but external to the tropical Pacific, and (iv) changes in exogenous forcing (see Neelin *et al.*, 1998 and references therein). Palaeo-proxies, archaeological evidence, and instrumental data (see Chapter 2) all indicate variations in ENSO behaviour over the past centuries, and throughout the Holocene. Much of this variability appears to be internal to the Earth's climate system, but there is evidence that the rather weak forcing due to orbital variations may be responsible for a systematic change to weaker ENSO cycles in the mid-Holocene (Sandweiss *et al.*, 1996; Clement *et al.*, 1999; Rodbell *et al.*, 1999). However, it appears that the character of ENSO can change on a much faster time-scale than that of small amplitude insolation change imposed by the Earth's varying orbit. The inference to be drawn from observed ENSO variability is that small forcings are able to cause large alterations in the behaviour of this non-linear system.

Following the apparent climate "shift" in the tropical Pacific around 1976 (Graham, 1994; Trenberth and Hurrell, 1994) (Figure 7.9), which is part of the recent tropical Pacific warming, the last two decades are characterised by relatively more El Niño variability, including the two strongest El Niño events (1982/83 and 1997/98) in the 130 years of instrumental records and a long-lasting warm spell in the early 1990s (Trenberth and Hoar, 1997; see Wunsch, 1999, and Trenberth and Hurrell, 1999, for a discussion on statistical significance). The tropical Pacific warming may be linked to anthropogenic forcing (Knutson and Manabe, 1998), but attribution is uncertain in view of the strong natural variability observed (Latif *et al.*, 1997; Zhang *et al.*, 1997b) and the inability of models to fully simulate ENSO realistically.

Whereas the above discussion has dealt with processes on multiple time-scales, separation of the time-scales into inter-annual (periods less than a decade) and inter-decadal (Zhang *et al.*, 1997b) show quite similar patterns. More focused equatorial signals occur on interannual time-scales, and are identifiable with the equatorial dynamically active waves in the ocean, while the lower-frequency variations, called the Pacific Decadal Oscillation (PDO), have relatively a somewhat larger expression in mid-latitudes of both hemispheres, but with an "El Niño-like" pattern. Because the patterns are highly spatially correlated and
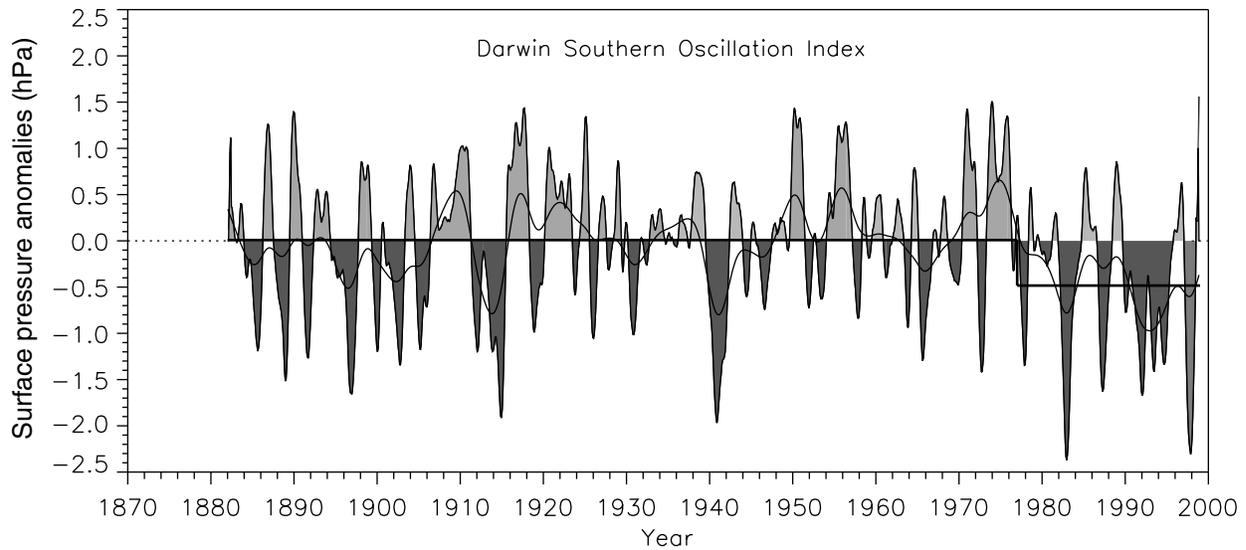
Figure 7.9: Darwin Southern Oscillation Index (SOI) represented as monthly surface pressure anomalies in hPa. Data cover the period from January 1882 to December 1998. Base period climatology computed from the period January 1882 to December 1981. The step function fit is illustrative only, to highlight a possible shift around 1976 to 1977.

thus not orthogonal, there is no unique projection onto them at any one time and they should not be considered independently.

In the tropics, it has been difficult for models to simulate all of the important processes correctly, and errors exist in the mean state of the tropical Pacific and the variability (see Chapter 8, Section 8.7.1). It is unlikely that it is possible to simulate the mean annual cycle correctly without simulating realistic ENSO events, as ENSO alters the mean state through rectification effects. For example, it is known that some regions only receive rainfall during an El Niño event. Hence it would be impossible to simulate correct rainfall in these regions without also simulating El Niño. Moreover, ENSO events are phase-locked to the annual cycle and changes in the mean state alter ENSO variability. In the Zebiak and Cane (1991) model the tropical east Pacific SST is systematically cooler during the "weak ENSO" regime than during the "strong ENSO" regime. Cloud radiative forcing feedbacks, such as the interactions between stratus regimes and ocean temperature, are poorly simulated, and the greenhouse effects of clouds versus their possible brightening with climate change are very uncertain.

Model studies have shown that greenhouse gas forcing is likely to change the statistics of ENSO variability, but the character of the change is model dependent. A comprehensive simulation suggests that greenhouse warming may induce greater ENSO activity marked by larger interannual variations relative to the warmer mean state (Timmermann *et al.*, 1999). More El Niños would increase the probability of certain weather regimes which favour COWL patterns associated with increased hemispheric mean surface temperatures (Hurrell, 1996; Corti *et al.*, 1999). The positive feedbacks involved in ENSO imply that small errors in simulating the relevant processes can be amplified. Yet increasing evidence suggests that ENSO plays a fundamental role in global climate and its interannual variability, and increased credibility in both regional and global climate

projections will be gained once realistic ENSOs and their changes are simulated.

7.6.5.2 *ENSO and tropical storms*
Any changes in ENSO as the climate changes will impact the distribution and tracks of tropical cyclones (including intense storms such as hurricanes and typhoons). During an El Niño, for example, the incidence of hurricanes typically decreases in the Atlantic and far western Pacific and Australian regions, but increases in the central and eastern Pacific (Lander, 1994). Thus it should be recognised that decreases in one area may be offset by increases in another area because of the global connectivity of the tropical atmospheric circulation. Global warming from increasing greenhouse gases in the atmosphere suggests increased convective activity but there is a possible trade-off between individual versus organised convection. While increases in sea surface temperatures favour more and stronger tropical cyclones, increased isolated convection stabilises the tropical troposphere and this in turn suppresses organised convection making it less favourable for vigorous tropical cyclones to develop (Yoshimura *et al.*, 1999). Thus changes in atmospheric stability (Bengtsson *et al.*, 1996) and circulation may produce offsetting tendencies (e.g., Royer *et al.*, 1998). General circulation models of the atmosphere (see Chapter 8, Section 8.8.4) do not resolve the scales required to properly address this issue; for instance, moist convection and hurricanes are not resolved adequately.

7.7 Rapid Changes in the Climate System

Small changes in the climate system can be sufficiently understood by assuming linear relationships between variables. However, many climate processes are non-linear by nature, and conclusions based on linear models and processes may in these

cases no longer be valid. Non-linearity is a prerequisite for the existence of thresholds in the climate system: small perturbations or changes in the forcing can trigger large reorganisations if thresholds are passed. The result is that atmospheric and oceanic circulations may change from one regime to another. This could possibly be manifested as rapid climate change.

There is no clear definition of "rapid climate change". In general, this notion is used to describe climate changes that are of significant magnitude (relative to the natural variability) and occur as a shift in the mean or variability from one level to another. In order to distinguish such changes from "extreme events", a certain persistence of the change is required. Among the classical cases are spontaneous transitions from one preferred mode to another or transitions triggered by slowly varying forcing. This occurs in non-linear systems which have multiple equilibria (Lorenz, 1993). Evidence for the possibility of such transitions can be found in palaeoclimatic records (see Chapter 2, Section 2.4; and Stocker, 2000), in observations of changes in large-scale circulation patterns from the instrumental record (see Section 7.6.5.1), and contemporary observations of regional weather patterns (e.g., Corti *et al.*, 1999).

Here, we briefly summarise non-linear changes that have captured attention in the recent literature and that have been assessed in this chapter:

• The Northern Hemispheric atmospheric circulation exhibits different regimes that are associated with the North Atlantic Oscillation. Recent analyses of observations suggest that relatively rapid regime changes are possible (see Section 7.2.6) and that they may have happened frequently in the past (Appenzeller *et al.*, 1998). Several studies suggest that the recent changes may be a response to anthropogenic forcing, but our understanding of the processes generating NAO is not sufficient to have confidence in whether this is the case.

• Observed variability of ENSO suggests that a transition to more frequent El Niño occurred around 1976 (see Section 7.6.5.1). Current understanding of ENSO processes does not yet permit a distinction as to the extent this is a response to anthropogenic forcing versus part of the long-term natural variability of the tropical atmosphere-ocean system, or both (see also Chapter 2, Section 2.6.2).

• Results from most climate models suggest that the Atlantic thermohaline circulation slows down in response to global warming; some models simulate a complete shut-down if certain thresholds are passed (see Section 7.3.6 and Chapter 9,

Section 9.3.4.3). Such a shut-down is in general not abrupt but evolves on a time-scale which is determined by the warming, i.e., a few decades to centuries. Processes for such an evolution are increasingly understood. As model resolution increases and high latitude processes are better represented in these models (sea ice, topography), additional feedbacks influencing the Atlantic THC will be investigated and their relative importance must be explored. This will lead to a better quantification of the overall stability of the THC.

• Large polar ice masses, ice shelves or even complete ice sheets may be destabilised by sea level rise (see Section 7.5 and Chapter 11, Section 11.3.3), thereby contributing to further sea level rise.

• Warming in the high latitudes may lead to significant reductions in sea ice and associated feedbacks may accelerate this development (see Box 7.1).

• Large-scale and possibly irreversible changes in the terrestrial biosphere and vegetation cover are thought to have occurred in the past when anthropogenic perturbation was negligible (e.g., the development of the Saharan desert, Claussen *et al.*, 1999). These changes may be interpreted as non-linear changes triggered by slow changes in external forcing and thus cannot be excluded to occur in the future. Knowledge on these phenomena, however, is not advanced yet.

Reducing uncertainty in climate projections also requires a better understanding of these non-linear processes which give rise to thresholds that are present in the climate system. Observations, palaeoclimatic data, and models suggest that such thresholds exist and that transitions have occurred in the past. The occurrence of such transitions can clearly not be excluded in a climate that is changing. On the contrary, model simulations indicate that such transitions lie within the range of changes that are projected for the next few centuries if greenhouse gas concentrations continue to increase. A particular concern is the fact that some of these changes may even be irreversible due to the existence of multiple equilibrium states in the climate system.

Comprehensive climate models in conjunction with sustained observational systems, both *in situ* and remote, are the only tool to decide whether the evolving climate system is approaching such thresholds. Our knowledge about the processes, and feedback mechanisms determining them, must be significantly improved in order to extract early signs of such changes from model simulations and observations.

References

Abdalati, W. and K. Steffen, 1995: Passive microwave-derived snow-melt regions on the Greenland ice sheet. *Geophys. Res. Lett.,* **22**, 787-790.

Abdella, K. and N. McFarlane, 1997: A new second-order turbulence closure scheme for the planetary boundary layer. *J. Atm. Sci.,* **54**, 1850-1867.

Albrecht, B., 1989: Aerosols, cloud microphysics and fractional cloudiness. *Science,* **245**, 1227-1230.

Alexander, M.A. and C. Deser, 1995: A mechanism for the recurrence of winter time midlatitude SST anomalies. *J. Phys. Oceanogr.,* **25**, 122-137.

Allan, R.P., K.P. Shine, A. Slingo and J.A. Pamment, 1999: The dependence of clear-sky outgoing long-wave radiation on surface temperature and relative humidity. *Quart. J. Roy. Met. Soc.,* **125**, 2103-2126.

Alley, R.B., 1989: Water-pressure coupling of sliding and bed deformation: II. Velocity-depth profiles. *J. Glaciol.,* **35**, 119-129.

AMIP, 1995: *Proceedings of the First International AMIP Scientific Conference* [Gates, W. L. (ed.)]. World Meteorological Organization, Geneva.

Anandakrishnan, S. and R.B. Alley, 1997: Stagnation of ice stream C, West Antarctica, by water piracy. *Geophys. Res. Lett.,* **24**, 265-268.

Anandakrishnan, S., D.D. Blankenship, R.B. Alley and P.L. Stoffa, 1998: Influence of subglacial geology on the position of a West Antarctic ice stream from seismic observations. *Nature,* **394**, 62-65.

Andre, J.C., J.P. Goutorbe and A. Perrier, 1986: HAPEX/MOBILHY: A hydrologic atmospheric experiment for the study of water budget and evaporation flux at the climate scales. *Bull. Am. Met. Soc.,* **67**, 138-144.

Andrews, D.G., J.R. Holton and C.B. Leovy, 1987: *Middle Atmosphere Dynamics.* Academic Press, Florida. Chapter 2.

Anisimov, O.A. and F.E. Nelson, 1996: Permafrost distribution in the northern hemisphere under scenarios of climatic change. *Glob. Planet. Change,* **14**, 59-72.

Anisimov, O.A. and F.E. Nelson, 1997: Permafrost zonation and climate change: results from transient general circulation models. *Clim. Change,* **35**, 241-258.

Anisimov, O.A., N.I. Shiklomanov and F.E. Nelson, 1997: Effects of global warming on permafrost and active-layer thickness: results from transient general circulation models. *Glob. Planet. Change,* **61**, 61-77.

Appenzeller, C., T.F. Stocker and M. Anklin, 1998: North Atlantic oscillation dynamics recorded in Greenland ice cores. *Science,* **282**, 446-449.

Arakawa, A. and W.H. Schubert, 1974: Interaction of a cumulus cloud ensemble with the large-scale environment. Part I. *J. Atm. Sci.,* **31**, 674-701.

Arbetter, T.E., J.A. Curry, M.M. Holland and J.A. Maslanik, 1997: Response of sea-ice models to perturbations in surface heat flux. *Ann. Glaciol.,* **25**, 193-197.

Arkin, P.A. and P. Xie, 1994: The Global Precipitation Climatology Project: First algorithm intercomparison project. *Bull. Am. Met. Soc.,* **75**, 401-420.

Arking, A., M.-D. Chou and W.L. Ridgway, 1996: On estimating the effects of clouds on atmospheric absorption based on flux observations above and below cloud level. *Geophys. Res. Lett.,* **23**, 829-832.

Atlas, R.M. and N. Wolfson, 1993: The effect of SST and soil moisture anomalies on GLA model simulations of the 1988 U.S. summer drought. *J. Clim.,* **6**, 2034-2048.

Avissar, R., 1998: Which type of soil-vegetation-atmosphere transfer scheme is needed for general circulation models: a proposal for a higher-order scheme. *J. Hydrol.,* **212**, 136-154.

Avissar, R. and T. Schmidt, 1998: An evaluation of the scale at which ground-surface heat flux patchiness affects the convective boundary layer using large-eddy simulations. *J. Atm. Sci.,* **55**, 2666-2689.

Avissar, R., E.W. Eloranta, K. Gurer and G.J. Tripoli, 1998: An evaluation of the large-eddy simulation option of the regional atmospheric modeling system in simulating a convective boundary layer: a FIFE case study. *J. Atm. Sci.,* **55**, 1109-1130.

Ayotte, K.W., P.P. Sullivan, A. Andren, S.C. Doney, A.A.M. Holtslag, W.G. Large, J.C. McWilliams, C.-H. Moeng, M. Otte, J.J. Tribbia and J.C. Wyngaard, 1996: An evaluation of neutral and convective planetary boundary-layer parameterization relative to large eddy simulations. *Bound.-Lay. Meteorol.,* **79**, 131-175.

Bacon, S., 1997: Circulation and fluxes in the North Atlantic between Greenland and Ireland. *J. Phys. Oceanogr.,* **27**, 1420-1435.

Baldwin, M.P. and T.J. Dunkerton, 1999: Propagation of the Arctic Oscillation from the stratosphere to the troposphere. *J. Geophys. Res.,* **104**, 30937-30946.

Baldwin, M.P., X. Cheng and T.J. Dunkerton, 1994: Observed correlations between winter-mean tropospheric and stratospheric circulation anomalies. *Geophys. Res. Lett.,* **21**, 1141-1144.

Baringer, M.O. and J.F. Price, 1997: Mixing and spreading of the Mediterranean outflow. *J. Phys. Oceanogr.,* **27**, 1654-1677.

Barker, H.W. and Z. Li, 1997: Interpreting shortwave albedo-transmittance plots: True or apparent anomalous absorption. *Geophys. Res. Lett.,* **24**, 2023-2026.

Barry, R.G., 1996: The parameterization of surface albedo for sea ice and its snow cover. *Prog. Phys. Geogr.,* **20**, 63-79.

Bates, J.J. and D.L. Jackson, 1997: A comparison of water vapor observations with AMIP 1 simulations. *J. Geophys. Res.,* **102**, 21837-21852.

Beal, L.M. and H.L. Bryden, 1997: Observations of an Agulhas Undercurrent. *Deep-Sea Res. I,* **44**, 1715-1724.

Beckmann, A. and R. Döscher, 1997: A method for improved representation of dense water spreading over topography in geopotential-coordinate models. *J. Phys. Oceanogr.,* **27**, 581-591.

Beljaars, A.C.M., P. Viterbo, M.J. Miller and A.K. Betts, 1996: The anomalous rainfall over the United States during July 1993: Sensitivity to land-surface parameterization and soil-moisture anomalies. *Mon. Wea. Rev.,* **124**, 362-383.

Belkin, I.M., S. Levitus, J. Antonov and S.-A. Malmberg, 1998: "Great Salinity Anomalies" in the North Atlantic. *Prog. Oceanogr.,* **41**, 1-68.

Bell, R.E., D.D. Blankenship, C.A. Finn, D.L. Morse, T.A. Scambos, J.M. Brozena and S.M. Hodge, 1998: Influence of subglacial geology on the onset of a West Antarctic ice stream from aerogeophysical observations. *Nature,* **394**, 58-62.

Bengtsson, L., M. Botzet and M. Esch, 1996: Will greenhouse gas-induced warming over the next 50 years lead to higher frequency and greater intensity of hurricanes? *Tellus,* **48A**, 57-73.

Bengtsson, L., E. Roeckner and M. Stendel, 1999: Why is the global warming proceeding much slower than expected? *J. Geophys. Res.,* **104**, 3865-3876.

Bentley, C.R., 1998: Rapid sea-level rise from a West Antarctic ice-sheet collapse: a short-term perspective. *J. Glaciol.,* **44**, 157-163.

Betts, A.K., 1982: Saturation point analysis of moist convective overturning. *J. Atm. Sci.,* **39**, 1484-1505.

Betts, A.K., J.H. Ball, A.C.M. Beljaars, M.J. Miller and P.A. Viterbo, 1996: The land-surface atmosphere interaction: A review based on observational and global modeling perspectives. *J. Geophys. Res.,* **101**, 7209-7225.

Betts, A.K., P. Viterbo, A.C.M. Beljaars, H.L. Pan, S.Y. Hong, M. Goulden and S. Wofsy, 1998: Evaluation of land-surface interaction in ECMWF and NCEP/NCAR reanalysis models over grassland (FIFE) and boreal forest (BOREAS). *J. Geophys. Res.,* **103**, 23079-23085.

Betts, R.A., P.M. Cox, S.E. Lee and F.I. Woodward, 1997: Contrasting physiological and structural vegetation feedbacks in climate change simulations. *Nature,* **387**, 796-799.

Bindschadler, R., 1997: Actively surging West Antarctic ice streams and

their response characteristics. *Ann. Glaciol.,* **24**, 409-414.

Bitz, C.M., M.M. Holland, A.J. Weaver and M. Eby, 2001: Simulating the ice-thickness distribution in a coupled climate model. *J. Geophys. Res.,* **106**, 2441-2464.

Boening, C.W., W.R. Holland, F.O. Bryan, G. Danabasoglu and J.C. McWilliams, 1995: An overlooked problem in model simulations of the thermohaline circulation and heat transport in the Atlantic Ocean. *J. Clim.,* **8**, 515-523.

Bolle, H.-J., J.-C. Andre, J.L. Arrue, H.K. Barth, P. Bessemoulin, A. Brasa, H.A.R. de Bruin, J. Cruces, G. Dugdale, E.T. Engman, D.L. Evans, R. Fantechi, F. Fiedler, A. van de Griend, A.C. Imeson, A. Jochum, P. Kabat, T. Kratzsch, J.-P. Lagouarde, I. Langer, R. Llamas, E. Lopez-Baeza, J. Melia Miralles, L.S. Muniosguren, F. Nerry, J. Noilhan, H.R. Oliver, R. Roth, S.S. Saatchi, J. Sanchez Diaz, M. de Santa Olalla, W.J. Shuttleworth, H. Sogaard, H. Stricker, J. Thornes, M. Vauclin and D. Wickland, 1993: EFEDA: European field experiment in a desertification threatened area. *Ann. Geophys.,* **11**, 173-189.

Bonan, G.B., 1995: Land-atmosphere CO_2 exchange simulated by a land surface process model coupled to an atmospheric general circulation model. *J. Geophys. Res.,* **100**, 2817-2831.

Bonan, G.B., 1996: Sensitivity of a GCM simulation to subgrid infiltration and surface runoff. *Clim. Dyn.,* **12**, 279-285.

Bonan, G.B., 1999: Frost followed the plow: Impacts of deforestation on the climate of the United States. *Ecol. Appl.,* **9**, 1305-1315.

Bonan, G.B., D. Pollard and S.L. Thompson, 1992: Effects of boreal forest vegetation on global climate. *Nature,* **359**, 716-718.

Bony, S., J.-P. Duvel and H. Le Treut, 1995: Observed dependence of the water vapor and clear-sky greenhouse effect on sea surface temperature: comparison with climate warming experiments. *Clim. Dyn.,* **11**, 307-320.

Bony, S., K.M. Lau and Y.C. Sud, 1997: Sea surface temperature and large-scale circulation influences on tropical greenhouse effect and cloud radiative forcing. *J. Clim.,* **10**, 2055-2077.

Boville, B.A., 1995: Middle atmosphere version of CCM2 (MACCM2): annual cycle and interannual variability. *J. Geophys. Res.,* **100**, 9017-9039.

Boville, B.A. and P.R. Gent, 1998: The NCAR climate system model, version one. *J. Clim.,* **11**, 1115-1130.

Braswell, W.D. and R.S. Lindzen, 1998: Anomalous short wave absorption and atmospheric tides. *Geophys. Res. Lett.,* **25**, 1293-1296.

Breon, F., 1992: Reflectance of broken cloud fields: Simulation and parameterization. *J. Atm. Sci.,* **49**, 1221-1232.

Bretherton, C.S. and D.S. Battisti, 2000: An interpretation of the results from atmospheric general circulation models forced by the time history of the observed sea surface temperature distribution. *Geophys. Res. Lett.,* **27**, 767-770.

Bretherton, C.S., M.K. McVean, P. Bechtold, A. Chlond, W.R. Cotton, J. Cuxart, H. Cuijpers, M. Khairoutdinov, B. Kosovic, D. Lewellen, C.-H. Moeng, P. Siebesma, B. Stevens, D.E. Stevens, I. Sykes and M.C. Wyant, 1999: An intercomparison of radiatively-driven entrainment and turbulence in a smoke cloud, as simulated by different numerical models. *Quart. J. Roy. Met. Soc.,* **125**, 391-423.

Broecker, W.S., 1997: Thermohaline circulation, the Achilles heel of our climate system: will man-made CO_2 upset the current balance? *Science,* **278**, 1582-1588.

Brubaker, K.L. and D. Entekhabi, 1996: Analysis of feedback mechanisms in land-atmosphere interaction. *Water Resour. Res.,* **32**, 1343-1357.

Brubaker, K.L., D. Entekhabi and P.S. Eagleson, 1993: Estimation of continental precipitation recycling. *J. Clim.,* **6**, 1077-1089.

Bryan, F., 1986: High-latitude salinity effects and interhemispheric thermohaline circulations. *Nature,* **323**, 301-304.

Bryden, H.L., D.H. Roemmich and J.A. Church, 1991: Ocean heat transport across 24N in the Pacific. *Deep-Sea Res.,* **38**, 297-324.

Butchart, N. and J. Austin, 1998: Middle atmosphere climatologies from

the troposphere-stratosphere configuration of the UKMO's unified model. *J. Atm. Sci.,* **55**, 2782-2809.

Cahalan, R.F., W. Ridgeway, W.J. Wiscombe, S. Gollmer and Harshvardhan, 1994: Independent pixel and Monte Carlo estimates of stratocumulus albedo. *J. Atm. Sci.,* **51**, 3776-3790.

Cao, K.K. and F.I. Woodward, 1998: Dynamic responses of terrestrial ecosystem carbon cycling to global climate change. *Nature,* **393**, 249-252.

Carton, J.A., X. Cao, B.S. Giese and A.M. da Silva, 1996: Decadal and interannual SST variability in the tropical Atlantic. *J. Phys. Oceanogr.,* **26**, 1165-1175.

Cayan, D.R., 1992: Latent and sensible heat flux anomalies over the northern oceans: the connection to monthly atmospheric circulation. *J. Clim.,* **5**, 354-369.

Cess, R.D., G.L. Potter, J.P. Blanchet, G.J. Boer, A.D.D. Genio, M. Deque, V. Dymnikov, V. Galin, W.L. Gates, S.J. Ghan, J.T. Kiehl, A.A. Lacis, H. Le Treut, Z.X. Li, X.-Z. Liang, B.J. McAvaney, V.P. Meleshko, J.F.B. Mitchell, J.-J. Morcrette, D.A. Randall, L. Rikus, E. Roeckner, J.F. Roer, U. Schlese, D.A. Sheinin, A. Slingo, A.P. Sokolov, K.E. Taylor, W.M. Washington, R.T. Wetherald, I. Yagai and M.-H. Zhang, 1990: Intercomparison and interpretation of climate feedback processes in 19 atmospheric general circulation models. *J. Geophys. Res.,* **95**, 16601-16615.

Cess, R.D., M. Zhang, P. Minnis, L. Corsetti, E.G. Dutton, B.W. Forgan, D.P. Garber, W.L. Gates, J.J. Hack, E.F. Harrisson, X. Jing, J.T. Kiehl, C.N. Long, J.-J. Morcrette, G.L. Potter, V. Ramanathan, B. Subasilar, C.H. Whitlock, D.F. Young and Y. Zhou, 1995: Absorption of solar radiation by clouds: Observations versus models. *Science,* **267**, 496-499.

Cess, R.D., M.H. Zhang, W.J. Ingram, G.L. Potter, V. Alekseev, H.W. Barker, E. Cohen-Solal, R.A. Colman, D.A. Dazlich, A.D. Del Genio, M.R. Dix, V. Dymnikov, M. Esch, L.D. Fowler, J.R. Fraser, V. Galin, W.L. Gates, J.J. Hack, J.T. Kiehl, H. LeTreut, K.K.-W. Lo, B.J. McAvaney, V.P. Meleshko, J.-J. Morcrette, D.A. Randall, E. Roeckner, J.-F. Royer, M.E. Schlesinger, P.V. Sporyshev, B. Timbal, E.M. Volodin, K.E. Taylor, W. Wang and R.T. Wetherald, 1996: Cloud feedback in atmospheric general circulation models: An update. *J. Geophys. Res.,* **101**, 12791-12794.

Cess, R.D., M.H. Zhang, F.P.J. Valero, S.K. Pope, A. Bucholtz, B. Bush, C.S. Zender and J. Vitko, 1999: Absorption of solar radiation by the cloudy atmosphere: Further interpretations of collocated aircraft measurements. *J. Geophys. Res.,* **104**, 2059-2066.

Chang, P., L. Ji and H. Li, 1997: A decadal climate variation in the tropical ocean from thermodynamic air-sea interactions. *Nature,* **385**, 516-518.

Chapman, W.L. and J.E. Walsh, 1993: Recent variations of sea ice and air temperature in high latitudes. *Bull. Am. Met. Soc.,* **74**, 33-48.

Chou, C. and J.D. Neelin, 1999: Cirrus detrainment-temperature feedback. *Geophys. Res. Lett.,* **26**, 1295-1298.

Christensen, O.B., J.H. Christensen, B. Machenhauer and M. Botzet, 1998: Very high-resolution regional climate simulations over Scandinavia - Present climate. *J. Clim.,* **11**, 3204-3229.

Ciais, P., P.P. Tans, J.W.C. White, M. Trolier, R.J. Francey, J.A. Berry, D.R. Randall, P.J. Sellers, J.G. Collatz and D.S. Schimel, 1995: Partitioning of ocean and land uptake of CO_2 as inferred by $\delta^{13}C$ measurements from the NOAA Climate Monitoring and Diagnostics Laboratory Global Air Sampling Network. *J. Geophys. Res.,* **100**, 5051-5070.

Ciais, P., A.S. Denning, P.P. Tans, J.A. Berry, D.A. Randall, G.J. Collatz, P.J. Sellers, J.W.C. White, M. Trolier, H.A.J. Meijer, R.J. Francey, P. Monfray and M. Heimann, 1997: A three-dimensional synthesis study of delta O-18 in atmospheric CO_2. 1. Surface fluxes. *J. Geophys. Res.,* **102**, 5857-5872.

Cihlar, J., P.H. Carmori, P.H. Schuepp, R.L. Desjardins and J.I. Macpherson, 1992: Relationship between satellite-derived vegetation

indices and aircraft-based CO_2 measurements. *J. Geophys. Res.,* **97**, 18515-18521.

Ciret, C. and A. Henderson-Sellers, 1998: Sensitivity of global vegetation models to present-day climate grassland simulated by global climate models. *Glob. Biogeochem. Cyc.,* **11**, 1141-1169.

Clarke, T.S. and K. Echelmeyer, 1996: Seismic-reflection evidence for a deep subglacial trough beneath Jakobshavns Isbrae, West Greenland. *J. Glaciol.,* **43**, 219-232.

Claussen, M., 1997: Modeling bio-geophysical feedbacks in the African and Indian monsoon region. *Clim. Dyn.,* **13**, 247-257.

Claussen, M., C. Kubatzki, V. Brovkin, A. Ganopolski, P. Hoelzmann and H.-J. Pachur, 1999: Simulation of an abrupt change in Saharan vegetation in the mid-Holocene. *Geophys. Res. Lett.,* **26**, 2037-2040.

Clement, A. and R. Seager, 1999: Climate and the tropical oceans. *J. Clim.,* **12**, 3383-3401.

Clement, A., R. Seager and M.A. Cane, 1999: Orbital controls on tropical climate. *Paleoceanogr.,* **14**, 441-455.

Colello, G.D., C. Grivet, P.J. Sellers and J.A. Berry, 1998: Modeling of energy, water and CO_2 flux in a temperate grassland ecosystem with SiB2: May-October 1987. *J. Atm. Sci.,* **55**, 1141-1169.

Collatz, G.J., J.T. Ball, C. Grivet and J.A. Berry, 1991: Physiological and environmental regulation of stomatal conductance, photosynthesis and transpiration: A model that includes a laminar boundary layer. *Agric. For. Meteorol.,* **54**, 107-136.

Collatz, G.J., L. Bounoua, S.O. Los, D.A. Randall, I.Y. Fung and P.J. Sellers, 2000: A mechanism for the influence of vegetation on the response of the diurnal temperature range to a changing climate. *Geophys. Res. Lett.,* **27**, 3381-3384.

Collins, W.G., 1998: Complex quality control of significant level rawinsonde temperature. *J. Atmos. Oc. Tech.,* **15**, 69-79.

Colman, R.A. and B.J. McAvaney, 1995: Sensitivity of the climate response of the atmospheric general circulation model to changes in convective parameterization and horizontal resolution. *J. Geophys. Res.,* **100**, 3155-3172.

Corti, S., F. Molteni and T.N. Palmer, 1999: Signature of recent climate change in frequencies of natural atmospheric circulation regimes. *Nature,* **398**, 799-802.

Cubasch, U., J. Waszkewitz, G. Hegerl and J. Perlwitz, 1995: Regional climate changes as simulated in time-slice experiments. *Clim. Change,* **31**, 273-304.

Cuijpers, J.W.M. and A.A.M. Holtslag, 1998: Impact of skewness and nonlocal effects on scalar and buoyancy fluxes in convective boundary layers. *J. Atm. Sci.,* **55**, 151-162.

Curry, J., C.A. Clayson, W.B. Rossow, R. Reeder, Y.-C. Zhang, P.J. Webster, G. Liu and R.-S. Sheu, 1999: High-resolution satellite-derived dataset of the surface fluxes of heat, freshwater, and momentum for the TOGA COARE IOP. *Bull. Am. Met. Soc.,* **80**, 2059-2080.

Curry, J.A. and P.J. Webster, 1999: *Thermodynamics of Atmospheres and Oceans.* Academic Press, 465.

da Silva, A.M., C.C. Young and S. Levitus, 1994: Atlas of Surface Marine Data 1994 Volume 1: Algorithms and Procedures. In: *NOAA Atlas NESDIS (6)*. U.S. Department of Commerce, Washington D. C., 83.

Dai, A., F. Giorgi and K.E. Trenberth, 1999: Observed and model-simulated diurnal cycles of precipitation over the contiguous United States. *J. Geophys. Res.,* **104**, 6377-6402.

Dai, A.G. and I.Y. Fung, 1993: Can climate variability contribute to the "missing" CO_2 sink? *Global Biogeochemical Cycles,* **7**, 543-567.

Danabasoglu, G. and J.C. McWilliams, 1995: Sensitivity of the global ocean circulation to parameterizations of mesoscale tracer transports. *J. Clim.,* **8**, 2967-2987.

de Ruijter, W.P.M., A. Biastoch, S.S. Drijfhout, J.R.E. Lutjeharms, R.P. Matano, T. Pichevin, P.J. van Leeuwen and W. Weijer, 1999: Indian-Atlantic interocean exchange: dynamics, estimation and transport. *J. Geophys. Res.,* **104**, 20885-20910.

DeCosmo, J., K.B. Katsaros, S.D. Smith, R.J. Anderson, W. Oost, K. Bumke and H. Chadwick, 1996: Air-sea exchange of water vapor and sensible heat: The humidity exchange over the sea (HEXOS) results. *J. Geophys. Res.,* **101**, 12001-12016.

Del Genio, A.D., A.A. Lacis and R.A. Ruedy, 1991: Simulations of the effect of a warmer climate on atmospheric humidity. *Nature,* **251**, 382-385.

Del Genio, A.D., W. Kovari and M.-S. Yao, 1994: Climatic implications of the seasonal variation of upper tropospheric water vapor. *Geophys. Res. Lett.,* **21**, 2701-2704.

Del Genio, A.D., M.-S. Yao, W. Kovari and K.K.W. Lo, 1996: A prognostic cloud water parameterization for global climate models. *J. Clim.,* **9**, 270-304.

Delire, C. and J.A. Foley, 1999: Evaluating the performance of a land surface/ecosystem model with biophysical measurements from contrasting environments. *J. Geophys. Res.,* **104**, 16895-16909.

Delworth, T.L. and M.E. Mann, 2000: Observed and simulated multidecadal variability in the Northern Hemisphere. *Clim. Dyn.,* **16**, 661-676.

Denning, A.S., G.J. Collatz, C. Zhang, D.A. Randall, J.A. Berry, P.J. Sellers, G.D. Colello and D.A. Dazlich, 1996a: Simulations of terrestrial carbon metabolism and atmospheric CO_2 in a general circulation model. Part I: Surface carbon fluxes. *Tellus,* **48B**, 521-542.

Denning, A.S., D.A. Randall, G.J. Collatz and P.J. Sellers, 1996b: Simulations of terrestrial carbon metabolism and atmospheric CO_2 in a general circulation model. Part II: simulated CO_2 concentrations. *Tellus,* **48B**, 543-567.

Deser, C. and M.L. Blackmon, 1993: Surface climate variations over the North Atlantic Ocean during winter: 1900-1993. *J. Clim.,* **6**, 1743-1753.

Deser, C. and M.S. Timlin, 1997: Atmosphere-ocean interaction on weekly time scales in the North Atlantic and Pacific. *J. Clim.,* **10**, 393-408.

Deser, C., J.E. Walsh and M.S. Timlin, 2000: Arctic sea ice variability in the context of recent wintertime atmospheric circulation trends. *J. Clim.,* **13**, 617-633.

Desjardins, J., R.J. Hart, J.I. MacPherson, P.H. Schuepp and S.B. Verma, 1992: Aircraft- and tower-based fluxes of carbon dioxide, latent, and sensible heat. *J. Geophys. Res.,* **97**, 18477-18485.

Dessler, A.E. and S.C. Sherwood, 2000: Simulations of tropical upper tropospheric humidity. *J. Geophys. Res.,* **105**, 20155-20163.

Dickinson, R.E., M. Shaikh, R. Bryant and L. Graumlich, 1998: Interactive canopies for a climate model. *J. Clim.,* **11**, 2823-2836.

Dickson, R.R., J. Lazier, J. Meincke, P. Rhines and J. Swift, 1996: Long-term coordinated changes in the convective activity of the North Atlantic. *Prog. Oceanogr.,* **38**, 241-295.

Dickson, R.R., J. Meincke, S.-A. Malmberg and A.J. Lee, 1988: The "Great Salinity Anomaly" in the northern North Atlantic 1968-1982. *Prog. Oceanogr.,* **20**, 103-151.

Dickson, R.R., T.J. Osborn, J.W. Hurrell, J. Meincke, J. Blindheim, B. Adlandsvik, T. Vinje, G. Alekseev and W. Maslowski, 2000: The Arctic Ocean response to the North Atlantic Oscillation. *J. Clim.,* **13**, 2671-2696.

Dixon, K.W., T.L. Delworth, M.J. Spelman and R.J. Stouffer, 1999: The influence of transient surface fluxes on North Atlantic overturning in a coupled GCM climate change experiment. *Geophys. Res. Lett.,* **26**, 2749-2752.

Doney, S.C., W.G. Large and F.O. Bryan, 1998: Surface ocean fluxes and water-mass transformation rates in the coupled NCAR Climate System Model. *J. Clim.,* **11**, 1420-1441.

Döscher, R., C.W. Boening and P. Herrmann, 1994: Response of circulation and heat transport in the North Atlantic to changes in thermohaline forcing in northern latitudes: A model study. *J. Phys. Oceanogr.,* **24**, 2303-2320.

Douville, H., J.F. Royer and J.F. Mahfouf, 1995: A new snow parameterization for the Meteo-France climate model. 1. Validation in stand-alone experiments. *Clim. Dyn.,* **12**, 21-35.

Dowdeswell, J.A. and M.J. Siegert, 1999: The dimensions and topographic setting of Antarctic subglacial lakes and implications for large-scale water storage beneath continental ice sheets. *Geology,* **111**, 254-263.

Ducharne, A., K. Laval and J. Polcher, 1996: Sensitivity of the hydrological cycle to the parameterization of soil hydrology in a GCM. *Clim. Dyn.,* **14**, 307-327.

Duffy, P.B. and K. Caldeira, 1997: Sensitivity of simulated salinity in a three-dimensional ocean model to upper-ocean transport of salt from sea-ice formation. *Geophys. Res. Lett.,* **24**, 1323-1326.

Duffy, P.B., M. Eby and A.J. Weaver, 1999: Effects of sinking of salt rejected during formation of sea ice on results of an ocean-atmosphere-sea ice climate model. *Geophys. Res. Lett.,* **26**, 1739-1742.

Dümenil, L., S. Hagemann and K. Arpe (eds.), 1997: *Validation of the hydrological cycle in the Arctic using river discharge data*, Workshop on Polar Processes in Global Climate, Cancun, Mexico.

Dunkerton, T.J., 1997: The role of gravity waves in the quasi-biennial oscillation. *J. Geophys. Res.,* **102**, 26053-26076.

Duvel, J.-P., S. Bony and H. Le Treut, 1997: Clear-sky greenhouse effect sensitivity to sea surface temperature changes: an evaluation of AMIP simulations. *Clim. Dyn.,* **13**, 259-273.

Duynkerke, P.G., P.J. Jonker, A. Chlond, M.C. van Zanten, J. Cuxart, P. Clark, E. Sanchez, G. Martin, G. Lenderink and J. Teixeira, 1999: Intercomparison of three- and one-dimensional model simulations and aircraft observations of stratocumulus. *Bound.-Lay. Meteorol.,* **92**, 453-488.

Eby, M. and G. Holloway, 1994: Sensitivity of a large-scale ocean model to a parameterization of topographic stress. *J. Phys. Oceanogr.,* **24**, 2577-2588.

Eluszkiewicz, J.E., R. Zurek, L. Elson, E. Fishbein, L. Froidevaux, J. Waters, R. Grainger, A. Lambert, R. Harwood and G. Peckham, 1996: Residual circulation in the stratosphere and lower mesosphere as diagnosed from Microwave Limb Sounder data. *J. Atm. Sci.,* **53**, 217-240.

Emanuel, K., 1991: A scheme for representing cumulus convection in large scale models. *J. Atm. Sci.,* **48**, 2313-2333.

Emanuel, K.A. and M. Zivkovic-Rothman, 1999: Development and evaluation of a convection scheme for use in climate models. *J. Atm. Sci.,* **56**, 1766-1782.

Engelhardt, H. and B. Kamb, 1998: Basal sliding of Ice Stream B, West Antarctica. *J. Glaciol.,* **44**, 223-230.

Fairall, C.W., E.F. Bradley, D.P. Rogers, J.B. Edson and G.S. Young, 1996: Bulk parametrization of air-sea fluxes for TOGA COARE. *J. Geophys. Res.,* **101**, 1295-1308.

Farquhar, G.D., S. von Caemmerer and J.A. Berry, 1980: A biochemical model of photosynthetic CO_2 fixation in leaves of C3 species. *Planta,* **149**, 78-90.

Fastook, J.L. and M. Prentice, 1994: A finite-element model of Antarctica: sensitivity test for meteorological mass-balance relationship. *J. Glaciol.,* **40**, 167-175.

Fetterer, F. and N. Untersteiner, 1998: Observations of melt ponds on Arctic sea ice. *J. Geophys. Res.,* **103**, 24821-24835.

Field, C.B. and I.Y. Fung, 1999: The not-so-big US carbon sink. *Science,* **285**, 544-545.

Field, C.B., J.T. Randerson and C.M. Malmstrong, 1995: Global net primary production: combining ecology and remote sensing. *Rem. Sens. Environ.,* **51**, 74-88.

Findell, K.L. and E.A.B. Eltahir, 1997: An analysis of the soil moisture-rainfall feedback, based on direct observations from Illinois. *Water Resour. Res.,* **33**, 725-735.

Foley, J.A., I.C. Prentice, N. Ramankutty, S. Levis, D. Pollard, S. Sitch and A. Haxeltine, 1996: An integrated biosphere model of land surface processes, terrestrial carbon balance and vegetation dynamics. *Glob. Biogeochem. Cyc.,* **10**, 603-628.

Foley, J.A., S. Levis, I.C. Prentice, D. Pollard and S.L. Thompson, 1998: Coupling dynamic models of climate and vegetation. *Glob. Change Biol.,* **4**, 561-579.

Forster, P., R.S. Freckleton and K.P. Shine, 1997: On aspects of the concept of radiative forcing. *Clim. Dyn.,* **13**, 547-560.

Fowler, A.C. and E. Schiavi, 1998: A theory of ice-sheet surges. *J. Glaciol.,* **44**, 104-118.

Fowler, A.M. and K.J. Hennessy, 1995: Potential impacts of global warming on the frequency and magnitude of heavy precipitation. *Natural Hazards,* **11**, 283-304.

Fowler, L.D., D.A. Randall and S.A. Rutledge, 1996: Liquid and ice cloud microphysics in the CSU general circulation model. Part I: Model description and simulated microphysical processes. *J. Clim.,* **9**, 489-529.

Francey, R.J., P.P. Tans, C.E. Allison, I.G. Enting, J.W.C. White and M. Troller, 1995: Changes in oceanic and terrestrial carbon uptake since 1982. *Nature,* **373**, 326-330.

Frankignoul, C. and R.W. Reynolds, 1983: Testing a dynamical model for mid-latitude sea surface temperature anomalies. *J. Phys. Oceanogr.,* **13**, 1131-1145.

Frei, C., C. Schär, D. Lüthi and H.C. Davies, 1998: Heavy precipitation processes in a warmer climate. *Geophys. Res. Lett.,* **25**, 1431-1434.

Fung, I.Y., C.B. Field, J.A. Berry, M.V. Thompson, J.T. Randerson, C.M. Malmstrom, P.M. Vitousek, G.J. Collatz, P.J. Sellers, D.A. Randall, A.S. Denning, F. Badeck and J. John, 1997: Carbon-13 exchanges between the atmosphere and biosphere. *Glob. Biogeochem. Cyc.,* **11**, 507-533.

Gaffen, D.J., A. Robock and W.P. Elliott, 1992: Annual cycles of tropospheric water vapor. *J. Geophys. Res.,* **97**, 18185-18193.

Gamache, J.F. and R.A. Houze, 1983: Water budget of a meso-scale convective system in the tropics. *J. Atm. Sci.,* **40**, 1835-1850.

Gargett, A.E. and G. Holloway, 1992: Sensitivity of the GFDL ocean model to different diffusivities for heat and salt. *J. Phys. Oceanogr.,* **22**, 1158-1177.

Gash, J.H.C., C.A. Nobre, J.M. Robert and R.L. Victoria, 1996: *Amazonian Deforestation and Climate.* Wiley, Chichester, 595.

Gates, W.L., J.S. Boyle, C. Covey, C.G. Dease, C.M. Doutriaux, R.S. Drach, M. Fiorino, P.J. Gleckler, J.J. Hnilo, S.M. Marlais, T.J. Phillips, G.L. Potter, B.D. Santer, K.R. Sperber, K.E. Taylor and D.N. Williams, 1999: An overview of the results of the Atmospheric Model Intercomparison Project (AMIP I). *Bull. Am. Met. Soc.,* **80**, 29-55.

Gent, P.R., J. Willebrand, T.J. McDougall and J.C. McWilliams, 1995: Parameterizing eddy-induced transports in ocean circulation models. *J. Phys. Oceanogr.,* **25**, 463-474.

Giorgi, F., L.O. Mearns, C. Shields and L. Mayer, 1996: A regional model study of the importance of local versus remote controls of the 1988 drought and the 1993 flood over the Central United States. *J. Clim.,* **9**, 1150-1162.

Giorgi, F., L.O. Mearns, C. Shields and L. McDaniel, 1998: Regional nested model simulations of present day and 2 x CO_2 climate over the central plains of the US. *Clim. Change,* **40**, 457-493.

Gleckler, P.J. and B.C. Weare, 1997: Uncertainties in global ocean surface heat flux climatologies derived from ship observations. *J. Clim.,* **10**, 2764-2781.

Glen, J.W., 1955: The creep of polycrystalline ice. *Proc. Roy. Soc. Lond. A,* **228**, 519-538.

Godfrey, J.S., 1996: The effect of the Indonesian throughflow on ocean circulation and heat exchange with the atmosphere: a review. *J. Geophys. Res.,* **101**, 12217-12238.

Godfrey, J.S., R.A. Houze, R.H. Johnson, R. Lukas, J.-L. Redelsperger, A. Sumi and R. Weller, 1998: Coupled Ocean-Atmosphere Response Experiment (COARE): An interim report. *J. Geophys. Res.,* **103**,

14395-14450.

Goosse, H. and T. Fichefet, 1999: Importance of ice-ocean interactions for the global ocean circulation: a model study. *J. Geophys. Res.,* **104**, 23337-23355.

Goosse, H., J.M. Campin, T. Fichefet and E. Deleersnijder, 1997: The impact of sea-ice formation on the properties of Antarctic Bottom Water. *Ann. Glaciol.,* **25**, 276-281.

Goosse, H., E. Deleersnijder, T. Fichefet and M. England, 1999: Sensitivity of a global coupled ocean-sea ice model to the parameterization of vertical mixing. *J. Geophys. Res.,* **104**, 13681-13695.

Gordon, C., C. Cooper, C.A. Senior, H. Banks, J.M. Gregory, T.C. Johns, J.F.B. Mitchell and R.A. Wood, 2000: The simulation of SST, sea ice extents and ocean heat transports in a version of the Hadley Centre coupled model without flux adjustments. *Clim. Dyn.,* **16**, 147-168.

Goulden, M., J. Munger, S.-M. Fan, B. Daube and S. Wofsy, 1996: Exchange of carbon dioxide by a deciduous forest: response to interannual climate variability. *Science,* **271**, 1576-1578.

Goulden, M., S. Wofsy, J. Harden, S. Trumbore, P. Crill, S. Gower, T. Fries, B. Daube, S. Fan, D. Sutton, A. Bazzaz and J. Munger, 1998: Sensitivity of boreal forest carbon balance to soil thaw. *Science,* **279**, 214-217.

Goutorbe, J.-P., 1994: HAPEX-Sahel: A large-scale study of land-atmosphere interactions in the semi-arid tropics. *Ann. Geophys.,* **12**, 53-64.

Graham, N.E., 1994: Decadal-scale climate variability in the tropical and North Pacific during the 1970s and 1980s: Observations and model results. *Clim. Dyn.,* **10**, 135-162.

Greenwald, T.J., G.L. Stephens, S.A. Christopher and T.H. Vonder Haar, 1995: Observations of the global characteristics and regional radiative effects of marine cloud liquid water. *J. Clim.,* **8**, 2928-2946.

Gregg, M.C., 1989: Scaling turbulent dissipation in the thermocline. *J. Geophys. Res.,* **94**, 9686-9698.

Gregory, J.M. and J.F.B. Mitchell, 1995: Simulation of daily variability of surface temperature and precipitation over Europe in the current and 2xCO$_2$ climates of the UKMO climate model. *Quart. J. Roy. Met. Soc.,* **121**, 1451-1476.

Gregory, J.M. and J.F.B. Mitchell, 1997: The climate response to CO$_2$ of the Hadley Centre coupled AOGCM with and without flux adjustment. *Geophys. Res. Lett.,* **24**, 1943-1946.

Grenier, H. and C.S. Bretherton, 2001: A moist PBL parameterization for large-scale models and its application to subtropical cloud-topped marine boundary layers. *Mon. Wea. Rev.,* **129**, 357-377.

Griffies, S.M., A. Gnanadesikan, R.C. Pacanowski, V.D. Larichev, J.K. Dukowicz and R.D. Smith, 1998: Isoneutral diffusion in a z-coordinate ocean model. *J. Phys. Oceanogr.,* **28**, 805-830.

Groetzner, A., M. Latif and T.P. Barnett, 1998: A decadal climate cycle in the North Atlantic Ocean as simulated by the ECHO coupled GCM. *J. Clim.,* **11**, 831-847.

Gwarkiewicz, G. and D.C. Chapman, 1995: A numerical study of dense water formation and transport on a shallow, sloping continental shelf. *J. Geophys. Res.,* **100**, 4489-4507.

Hack, J.J., 1998: Analysis of the improvement in implied meridional ocean energy transport as simulated by the NCAR CCM3. *J. Clim.,* **11**, 1237-1244.

Hahmann, A.N. and R. Dickinson, 1997: RCCM2-BATS model over tropical South America: Application to tropical deforestation. *J. Clim.,* **10**, 1944-1964.

Haigh, J.D., 1996: The impact of solar variability on climate. *Science,* **272**, 981-983.

Hakkinen, S., 1993: An Arctic source for the Great Salinity Anomaly: A simulation of the Arctic ice-ocean system for 1955-1975. *J. Geophys. Res.,* **98**, 16397-16410.

Hall, A. and S. Manabe, 1997: Can local linear stochastic theory explain sea surface temperature and salinity variability? *Clim. Dyn.,* **13**, 167-180.

Hall, A. and S. Manabe, 1999: The role of water vapor feedback in unperturbed climate variability and global warming. *J. Clim.,* **12**, 2327-2346.

Hallberg, R., 2000: Time integration of diapycnal diffusion and Richardson number-dependent mixing in isopycnal coordinate ocean models. *Mon. Wea. Rev.,* **128**, 1402-1419.

Hansen, J.E., M. Sato and R. Ruedy, 1997: Radiative forcing and climate response. *J. Geophys. Res.,* **102**, 6831-6864.

Harder, M., P. Lemke and M. Hilmer, 1998: Simulation of sea ice transport through Fram Strait: Natural variability and sensitivity to forcing. *J. Geophys. Res.,* **103**, 5595-5606.

Harvey, L.D.D., 2000: An assessment of the potential impact of a downward shift of tropospheric water vapor on climate sensitivity. *Clim. Dyn.,* **16**, 491-500.

Hasselmann, K., 1976: Stochastic climate models. Part I: Theory. *Tellus,* **28**, 473-485.

Hasumi, H. and N. Suginohara, 1999: Effects of locally enhanced vertical diffusivity over rough bathymetry on the world ocean circulation. *J. Geophys. Res.,* **104**, 23367-23374.

Haynes, P.H., C.J. Marks, M.E. McIntyre, T.G. Shepherd and K.P. Shine, 1991: On the downward control of extratropical diabatic circulations by eddy-induced mean forces. *J. Atm. Sci.,* **48**, 651-678.

Hazeleger, W. and S.S. Drijfhout, 2000: Eddy subduction in a model of the subtropical gyre. *J. Phys. Oceanogr.,* **30**, 677-695.

Held, I.M. and B.J. Soden, 2000: Water vapor feedback and global warming. *Ann. Rev. Energy Env.,* **25**, 441-475.

Henderson-Sellers, A., H. Zhang and W. Howe, 1996: Human and physical aspects of tropical deforestation. In: *Climate Change: Developing Southern Hemisphere Perspectives* [Giambelluca, T. W. and A. Henderson-Sellers (eds.)]. John Wiley & Sons, Chichester, 259-292.

Hennessy, K.J., J.M. Gregory and J.F.B. Mitchell, 1997: Changes in daily precipitation under enhanced greenhouse conditions. *Clim. Dyn.,* **13**, 667-680.

Hense, A., P. Krahe and H. Flohn, 1988: Recent fluctuations of tropospheric temperature and water vapour content in the tropics. *Meteorology and Atmospheric Physics,* **38**, 215-227.

Hibler, W.D., 1979: A dynamic thermodynamic sea ice model. *J. Phys. Oceanogr.,* **9**, 815-846.

Hibler, W.D., 1984: The role of sea ice dynamics in modeling CO$_2$ increases. In: *Climate Processes and Climate Sensitivity* [Hansen, J. E. and T. Takahashi (eds.)]. American Geophysical Union, Washington DC, 238-253.

Hilmer, M., M. Harder and P. Lemke, 1998: Sea ice transport: a highly variable link between Arctic and North Atlantic. *Geophys. Res. Lett.,* **25**, 3359-3362.

Hindmarsh, R.C.A., 1993: Qualitative dynamics of marine ice sheets. In: *NATO ASI, I 12: Ice in the Climate System* [Peltier, W. R. (ed.)]., 67-99.

Hindmarsh, R.C.A., 1998: The stability of a viscous till sheet coupled with ice flow, considered at wavelengths less than the ice thickness. *J. Glaciol.,* **44**, 285-292.

Holland, E.A., B.H. Braswell, J.-F. Lamarque, A. Townsend, J. Sulzman, J.-F. Muller, F. Dentener, G. Brasseur, H. Levy, J.E. Penner and G.-U. Roelofs, 1997a: Variations in the predicted spatial distribution of atmospheric nitrogen deposition and their impact on carbon uptake by terrestrial ecosystems. *J. Geophys. Res.,* **102**, 15849-15866.

Holland, M.M. and J.A. Curry, 1999: The role of different physical processes in determining the interdecadal variability of Central Arctic sea ice. *J. Clim.,* **12**, 3319-3330.

Holland, M.M., J.A. Curry and J.L. Schramm, 1997b: Modeling the thermodynamics of a sea ice thickness distribution. 2. Sea ice/ocean interactions. *J. Geophys. Res.,* **102**, 23093-23107.

Holtslag, A.A.M. and P.G. Duynkerke, 1998: *Clear and cloudy boundary layers.* Royal Netherlands Academy of Arts and Sciences, 372 pp.

Horinouchi, T. and S. Yoden, 1998: Wave-mean flow interaction associated with a QBO like oscillation in a simplified GCM. *J. Atm. Sci.,* **55**, 502-526.

Houghton, R.A. and J.L. Hackler, 1999: Emissions of carbon from forestry and land-use change in tropical Asia. *Glob. Change Biol.,* **5**, 481-492.

Houze, R.A., 1993: *Cloud Dynamics.* Academic Press, San Diego, 570.

Hu, H. and W.T. Liu, 1998: The impact of upper tropospheric humidity from microwave limb sounder on the midlatitude greenhouse effect. *Geophys. Res. Lett.,* **25**, 3151-3154.

Hunke, E.C. and J.K. Dukowicz, 1997: An elastic-viscous-plastic model for sea ice dynamics. *J. Phys. Oceanogr.,* **27**, 1849-1867.

Hurrell, J.W., 1995: Decadal trends in the North Atlantic Oscillation regional temperatures and precipitation. *Science,* **269**, 676-679.

Hurrell, J.W., 1996: Influence of variations in extratropical wintertime teleconnections on Northern Hemisphere temperatures. *Geophys. Res. Lett.,* **23**, 665-668.

Hurrell, J.W. and K.E. Trenberth, 1996: Satellite versus surface estimates of air temperature since 1979. *J. Clim.,* **9**, 2222-2232.

Huybrechts, P. and J. Oerlemans, 1990: Response of the Antarctic Ice Sheet to future greenhouse warming. *Clim. Dyn.,* **5**, 93-102.

Huybrechts, P., A.J. Payne and EISMINT Intercomparison Group, 1996: The EISMINT benchmarks for testing ice-sheet models. *Ann. Glaciol.,* **23**, 1-12.

Iken, A., K. Echelmeyer, W. Harrison and M. Funk, 1993: Mechanism of fast flow in Jakobshavns Isbrae, West Greenland: Part I. Measurements of temperature and water level in deep boreholes. *J. Glaciol.,* **39**, 15-25.

Imre, D.G., E.H. Abramson and P.H. Daum, 1996: Quantifying cloud-induced shortwave absorption: An examination of uncertainties and of recent arguments for large excess absorption. *J. Appl. Met.,* **35**, 1991-2010.

Inamdar, A.K. and V. Ramanathan, 1998: Tropical and global scale interactions among water vapor, atmospheric greenhouse effect, and surface temperature. *J. Geophys. Res.,* **103**, 32177-32194.

IPCC, 1990: *Climate Change – The IPCC Scientific Assessment* [Houghton, J.T., G.J. Jenkins and J.J. Ephraums (eds.)]. Cambridge University Press, 365 pp.

IPCC, 1996: *Climate Change 1995: The Science of Climate Change. Contribution of Working Group I to the Second Assessment Report of the Intergovernmental Panel on Climate Change* [Houghton, J. T., L. G. Meira Filho, B. A. Callander, N. Harris, A. Kattenberg and K. Maskell (eds.)]. Cambridge University Press, 572 pp.

Iwashima, T. and R. Yamamoto, 1993: A statistical analysis of the extreme events: Long-term trend of heavy daily precipitation. *J. Met. Soc. Japan,* **71**, 637-640.

Jacob, C. and S.A. Klein, 1999: The role of vertically varying cloud fraction in the parameterization of microphysical processes in the ECMWF model. *Quart. J. Roy. Met. Soc.,* **125**, 941-965.

Jacobson, H.P. and C.F. Raymond, 1998: Thermal effects on the location of ice stream margins. *J. Geophys. Res.,* **103**, 12111-12122.

Jones, R.G., J.M. Murphy and M. Noguer, 1995: Simulation of climate change over Europe using a nested regional climate model. Part I: Assessment of control climate including sensitivity to location of lateral boundaries. *Quart. J. Roy. Met. Soc.,* **121**, 1413-1449.

Jones, R.G., J.M. Murphy, M. Noguer and A.B. Keen, 1997: Simulation of climate change over Europe using a nested regional climate model. Part II: Comparison of driving and regional model responses to a doubling of carbon dioxide. *Quart. J. Roy. Met. Soc.,* **123**, 265-292.

Joos, F., G.-K. Plattner, T.F. Stocker, O. Marchal and A. Schmittner, 1999: Global warming and marine carbon cycle feedbacks on future atmospheric CO_2. *Science,* **284**, 464-467.

Josey, S.A., E.C. Kent and P.K. Taylor, 1999: New insights into the ocean heat budget closure problem from analysis of the SOC air-sea flux climatology. *J. Clim.,* **12**, 2685-2718.

Kamb, B., C.F. Raymond, W.D. Harrison, H. Engelhardt, K.A. Echelmeyer, N. Humphrey, M.M. Brugman and T. Pfeffer, 1985: Glacier surge mechanism: 1982-1983 surge of Variegated Glacier, Alaska. *Science,* **227**, 469-479.

Karl, T.R. and R.W. Knight, 1998: Secular trends of precipitation amount, frequency and intensity in the USA. *Bull. Am. Met. Soc.,* **79**, 231-242.

Karl, T.R., R.W. Knight and N. Plummer, 1995: Trends in high-frequency climate variability in the twentieth century. *Nature,* **377**, 217-220.

Kato, S., T.P. Ackerman, E.E. Clothiaux and J.H. Mather, 1997: Uncertainties in modeled and measured clear-sky surface shortwave irradiances. *J. Geophys. Res.,* **102**, 25881-25898.

Keeling, C.D., T.P. Whorf, M. Wahlen and M. van der Plicht, 1995: Interannual extremes in the rate of rise of atmospheric carbon dioxide since 1980. *Nature,* **375**, 666-670.

Keith, D.A., 1995: Meridional energy transport: Uncertainty in zonal means. *Tellus,* **47A**, 30-44.

Kelly, P.M., P. Jia and P.D. Jones, 1996: The spatial response of the climate system to explosive volcanic eruptions. *Int. J. Clim.,* **16**, 537-550.

Kicklighter, D.W., M. Bruno, S. Donges, G. Esser, M. Heimann, J. Helfrich, F. Ift, F. Joos, J. Kaduk, G.H. Kohlmaier, A.D. McGuire, J.M. Melillo, R. Meyer, B. Moore, A. Nadler, I.C. Prentice, W. Sauf, A.L. Schloss, S. Sitch, U. Wittenberg and G. Wurth, 1998: A first-order analysis of the potential role of CO_2 fertilization to affect the global carbon budget: a comparison of four terrestrial biosphere models. *Tellus,* **51B**, 343-366.

Kiehl, J.T. and K.E. Trenberth, 1997: Earth's annual global mean energy budget. *Bull. Am. Met. Soc.,* **78**, 197-208.

Kiehl, J.T., J.J. Hack, M.H. Zhang and R.D. Cess, 1995: Sensitivity of a GCM climate to enhanced shortwave absorption. *J. Atm. Sci.,* **8**, 2200-2212.

Kiehl, J.T., J.J. Hack and J.W. Hurrell, 1998: The energy budget of the NCAR Community Climate Model CCM3. *J. Clim.,* **11**, 1151-1178.

Killworth, P.D., 1994: On reduced-gravity flow through sills. *Geophys. Astrophys. Fluid Dyn.,* **75**, 91-106.

Killworth, P.D., 1997: On the parametrization of eddy transfer. Part I: Theory. *J. Mar. Res.,* **55**, 1171-1197.

Killworth, P.D. and N.R. Edwards, 1999: A turbulent bottom boundary layer code for use in numerical ocean models. *J. Phys. Oceanogr.,* **29**, 1221-1238.

Kim, Y.J., 1996: Representation of subgrid-scale orographic effects in a general circulation model, 1: Impact on the dynamics of simulated January climate. *J. Clim.,* **9**, 2698-2717.

Kirk-Davidoff, D.B. and R.S. Lindzen, 2000: An energy balance model based on potential vorticity homogenization. *J. Clim.,* **13**, 431-448.

Kitoh, A., T. Motoi and H. Koide, 1999: SST variability and its mechanism in a coupled atmosphere-mixed layer ocean model. *J. Clim.,* **12**, 1221-1239.

Klein, B., R.L. Molinari, T.J. Muller and G. Siedler, 1995: A transatlantic section at 14.5N: Meridional volume and heat fluxes. *J. Mar. Res.,* **53**, 929-957.

Kley, D., H.G.J. Smit, H. Vömel, H. Grassl, V. Ramanathan, P.J. Crutzen, S. Williams, J. Meywerk and S.J. Oltmans, 1997: Tropospheric water-vapour and ozone cross-sections in a zonal plane over the central equatorial Pacific Ocean. *Quart. J. Roy. Met. Soc.,* **123**, 2009-2040.

Klinger, B., J. Marshall and U. Send, 1996: Representation of convective plumes by vertical adjustment. *J. Geophys. Res.,* **101**, 18175-18182.

Knutson, T.R. and S. Manabe, 1998: Model assessment of decadal variability and trends in the Tropical Pacific Ocean. *J. Clim.,* **11**, 2273-2296.

Knutti, R. and T.F. Stocker, 2000: Influence of the thermohaline circulation on projected sea level rise. *J. Clim.,* **13**, 1997-2001.

Kodera, K., 1994: Influence of volcanic eruptions on the troposphere through stratospheric dynamical processes in the Northern Hemisphere winter. *J. Geophys. Res.,* **99**, 1273-1282.

Koltermann, K.P., A.V. Sokov, V.P. Tereschenkov, S.A. Dobroliubov, K. Lorbacher and A. Sy, 1999: Decadal changes in the thermohaline circulation of the North Atlantic. *Deep-Sea Res. II,* **46**, 109-138.

Kondratyev, K.Y., V.I. Bieneko and I.N. Melnikova, 1998: Absorption of solar radiation by clouds and aerosols in the visible wavelength region. *Meteorology and Atmospheric Physics,* **65**, 1-10.

Koshlyakov, M.N. and T.G. Sazhina, 1996: Meridional volume and heat transport by large-scale geostrophic currents in the Pacific sector of the Antarctic. *Oceanology,* **35**, 767-777.

Koster, R. and P.C.D. Milly, 1997: The interplay between transpiration and runoff formulations in land surface schemes used with atmospheric models. *J. Clim.,* **10**, 1578-1591.

Kreyscher, M., M. Harder and P. Lemke, 1997: First results of the Sea-Ice Model Intercomparison Project (SIMIP). *Ann. Glaciol.,* **25**, 8-11.

Labitzke, K. and H. van Loon, 1997: The signal of the 11-year sunspot cycle in the upper troposphere-lower stratosphere. *Space Sciences Reviews,* **80**, 393-410.

LabSea Group, 1998: The Labrador Sea deep convection experiment. *Bull. Am. Met. Soc.,* **79**, 2033-2058.

Lacis, A.A. and J.E. Hansen, 1974: A parameterization for the absorption of solar radiation in the earth's atmosphere. *J. Atm. Sci.,* **31**, 118-133.

Lander, M., 1994: An exploratory analysis of the relationship between tropical storm formation in the Western North Pacific and ENSO. *Mon. Wea. Rev.,* **122**, 636-651.

Large, W.G. and P.R. Gent, 1999: Validation of vertical mixing in an equatorial ocean model using large eddy simulations and observations. *J. Phys. Oceanogr.,* **29**, 449-464.

Large, W.G., G. Danabasoglu, S.C. Doney and J.C. McWilliams, 1997: Sensitivity to surface forcing and boundary layer mixing in a global ocean model: Annual-mean climatology. *J. Phys. Oceanogr.,* **27**, 2418-2447.

Larson, K., D.L. Hartmann and S.A. Klein, 1999: The role of clouds, water vapor, circulation, and boundary layer structure in the sensitivity of the tropical climate. *J. Clim.,* **12**, 2359-2374.

Latif, M. and T.P. Barnett, 1996: Decadal climate variability over the North Pacific and North America: Dynamics and predictability. *J. Clim.,* **9**, 2407-2423.

Latif, M., R. Kleeman and C. Eckert, 1997: Greenhouse warming, decadal variability or El Niño: An attempt to understand the anomalous 1990s. *J. Clim.,* **10**, 2221-2239.

Latif, M., E. Roeckner, U. Mikolajewicz and R. Voss, 2000: Tropical stabilization of the thermohaline circulation in a greenhouse warming simulation. *J. Clim.,* **13**, 1809-1813.

Lau, N.-C. and M.J. Nath, 1999: Observed and GCM-simulated westward-propagating, planetary-scale fluctuation with approximately three-week periods. *Mon. Wea. Rev.,* **127**, 2324-2345.

Lavin, A., H.L. Bryden and G. Parrilla, 1998: Meridional transport and heat flux variations in the subtropical North Atlantic. *Glob. Atm. Oc. Sys.,* **6**, 269-293.

Le Treut, H. and Z.X. Li, 1991: The sensitivity of an atmospheric general circulation model to prescribed SST changes: Feedback effects associated with the simulation of cloud optical properties. *Clim. Dyn.,* **5**, 175-187.

Le Treut, H., Z.X. Li and M. Forichon, 1994: Sensitivity of the LMD general circulation model to greenhouse forcing associated with 2 different cloud-water parameterizations. *J. Clim.,* **7**, 1827-1841.

Le Treut, H. and B. McAvaney, 2000: Equilibrium climate change in response to a CO_2 doubling: an intercomparison of AGCM simulations coupled to slab oceans. *Technical Report, Institut Pierre Simon Laplace,* **18**, 20 pp.

Lean, J., C.B. Bunton, C.A. Nobre and P.R. Rowntree, 1996: The simulated impacts of Amazonian deforestation on climate using measured ABRACOS vegetation characteristics. In: *Amazonian Deforestation and Climate* [Gash, J. H. C., C. A. Nobre, J. M. Robert and R. L. Victoria (eds.)]. Wiley, Chichester, 549-576.

Lean, J. and P. Rowntree, 1997: Understanding the sensitivity of a GCM simulation of Amazonian deforestation to the specification of vegetation and soil characteristics. *J. Clim.,* **10**, 1216-1235.

Ledwell, J.R., E.T. Montogmery, K.L. Polzin, L.C. St. Laurent, R.W. Schmitt and J.M. Toole, 2000: Evidence for enhanced mixing over rough topography in the abyssal ocean. *Nature,* **403**, 179-181.

Ledwell, J.R., A.J. Watson and C.S. Law, 1993: Evidence for slow mixing across the pycnocline from an open-ocean tracer-release experiment. *Nature,* **364**, 701-703.

Lee, T.N., W. Johns, R. Zantopp and E. Fillenbaum, 1996: Moored observations of western boundary current variability and thermohaline circulation at 26.5°N in the subtropical North Atlantic. *J. Phys. Oceanogr.,* **26**, 962-983.

Lee, W.-H., S.F. Iacobellis and R.C.J. Somerville, 1997: Cloud radiation forcings and feedbacks: general circulation model test and observational validation. *J. Clim.,* **10**, 2479-2496.

Legg, S., J. McWilliams and G. Jianbo, 1998: Localization of deep ocean convection by a mesoscale eddy. *J. Phys. Oceanogr.,* **28**, 944-970.

Legutke, S., E. Maier-Reimer, A. Stössel and A. Hellbach, 1997: Ocean-sea-ice coupling in a global ocean general circulation model. *Ann. Glaciol.,* **25**, 116-120.

Lemke, P., W.D. Hibler, G. Flato, M. Harder and M. Kreyscher, 1997: On the improvement of sea-ice models for climate simulations: the Sea-Ice Model Intercomparison Project. *Ann. Glaciol.,* **25**, 183-187.

Lenderink, G. and A.A.M. Holtslag, 2000: Evaluation of the kinetic energy approach for modelling fluxes in stratocumulus. *Mon. Wea. Rev.,* **128**, 244-258.

Levis, S., J.A. Foley and D. Pollard, 1999: Potential high-latitude vegetation feedbacks on CO_2-induced climate change. *Geophys. Res. Lett.,* **26**, 747-750.

Lewis, E.L., E.P. Jones, P. Lemke, T.D. Prowse, P. Wadhams (eds.), 2000: *The Freshwater Budget of the Arctic Ocean.* NATO Science Series 2-70. Kluwer Academic Publishers, 625.

Li, Z., 1998: Influence of absorbing aerosols on the inference of solar surface radiation budget and cloud absorption. *J. Clim.,* **11**, 5-17.

Li, Z. and L. Moreau, 1996: Alteration of atmospheric solar absorption by clouds: simulation and observation. *J. Appl. Met.,* **35**, 653-670.

Li, Z., H.W. Barker and L. Moreau, 1995: The variable effect of clouds on atmospheric absorption of solar radiation. *Nature,* **376**, 486-490.

Li, Z., L. Moreau and A. Arking, 1997: On solar energy disposition: A perspective from observation and modeling. *Bull. Am. Met. Soc.,* **78**, 53-70.

Li, Z., A. Trishchenko, H.W. Barker, G.L. Stephens and P.T. Partain, 1999: Analysis of Atmospheric Radiation Measurement (ARM) programs's Enhanced Shortwave Experiment (ARESE) multiple data sets for studying cloud absorption. *J. Geophys. Res.,* **104**, 19127-19134.

Lindzen, R.S., M.-D. Chou and A. Hou, 2001: Does the earth have an adaptive iris? *Bull. Am. Met. Soc.,* **82**, 417-432.

Lohmann, U. and E. Roeckner, 1996: Design and performance of a new cloud microphysics scheme developed for the ECHAM general circulation model. *Clim. Dyn.,* **12**, 557-572.

Lohmann, G. and R. Gerdes, 1998: Sea ice effects on the sensitivity of the thermohaline circulation. *J. Clim.,* **11**, 2789-2803.

Lorenz, E.N., 1993: *The Essence of Chaos.* University of Washington Press, Seattle, USA, 227.

Loth, B., H.-F. Graf and J.M. Oberhuber, 1993: Snow cover model for global climate simulations. *J. Geophys. Res.,* **98**, 10451-10464.

Lott, F. and M.J. Miller, 1997: A new subgrid-scale orographic drag parametrization: Its formulation and testing. *Quart. J. Roy. Met. Soc.,* **123**, 101-127.

Lüthi, D., A. Cress, H.C. Davies, C. Frei and C. Schär, 1996: Interannual

variability and regional climate simulations. *Theor. Appl. Clim.,* **53**, 185-209.

Lynch-Stieglitz, M., 1994: The development and validation of a simple snow model for the GISS GCM. *J. Clim.,* **7**, 1842-1855.

MacAyeal, D.R., 1992: Irregular oscillations of the West Antarctic Ice Sheet. *Nature,* **359**, 29-32.

MacAyeal, D.R., R.A. Bindschadler and T.A. Scambos, 1995: Basal friction of Ice Stream E, West Antarctica. *J. Glaciol.,* **41**, 247-262.

MacAyeal, D.R., V. Rommelaere, C.L. Hulbe, J. Determann and C. Ritz, 1996: An ice-shelf model test based on the Ross Ice Shelf, Antarctica. *Ann. Glaciol.,* **23**, 46-51.

Macdonald, A.M., 1998: The global ocean circulation: a hydrographic estimate and regional analysis. *Prog. Oceanogr.,* **41**, 281-382.

Macdonald, A.M. and C. Wunsch, 1996: An estimate of global ocean circulation and heat fluxes. *Nature,* **382**, 436-439.

Manabe, S. and R.J. Stouffer, 1988: Two stable equilibria of a coupled ocean atmosphere model. *J. Clim.,* **1**, 841-866.

Manabe, S. and R.J. Stouffer, 1993: Century-scale effects of increased atmospheric CO_2 on the ocean-atmosphere system. *Nature,* **364**, 215-218.

Manabe, S. and R.T. Wetherald, 1987: Large-scale changes of soil wetness induced by an increase in atmospheric carbon dioxide. *J. Atm. Sci.,* **44**, 1211-1235.

Manzini, E. and L. Bengtsson, 1996: Stratospheric climate and variability from a general circulation model and observations. *Clim. Dyn.,* **12**, 615-639.

Marotzke, J., 1991: Influence of convective adjustment on the stability of the thermohaline circulation. *J. Phys. Oceanogr.,* **21**, 903-907.

Marotzke, J. and J. Willebrand, 1991: Multiple equilibria of the global thermohaline circulation. *J. Phys. Oceanogr.,* **21**, 1372-1385.

Marshall, J. and F. Schott, 1999: Open-ocean convection: observations, theory and models. *Rev. Geophys.,* **37**, 1-64.

Marshall, S.J. and G.K.C. Clarke, 1997: A continuum mixture model of ice stream thermodynamics in the Laurentide Ice Sheet 1. Theory. *J. Geophys. Res.,* **102**, 20599-20613.

Marshunova, M.S. and A.A. Mishin, 1994: Handbook on the Radiation Regime of the Arctic Basin: Results from the Drift Stations. In: *Arctic Ocean Snow and Meteorological Observations from Drifting Stations: University of Washington, Applied Physics Laboratory, Tech. Rep. APL-URW TR 9413* [Radionov, V. F. and R. Colony (eds.)]., 52. (Available on: Arctic Ocean Snow and Meteorological Observations from Drifting Stations, CD ROM, NSIDC, University of Colorado, 1996).

Mauritzen, C., 1996: Production of dense overflow waters feeding the North Atlantic across the Greenland-Scotland Ridge: Evidence for a revised circulation scheme. *Deep-Sea Res.,* **43**, 769-806.

Maxworthy, T., 1997: Convection into domains with open boundaries. *Ann. Rev. Fluid Mech.,* **29**, 327-371.

McCartney, M.S., R.G. Curry and H.F. Bezdek, 1996: North Atlantic's transformation pipeline chills and redistributed subtropical water. *Oceanus,* **39**, 19-23.

McGuffie, K., A. Henderson-Sellers, N. Holbrook, Z. Kothavala, O. Balachova and J. Hoekstra, 1999: Assessing simulations of daily temperature and precipitation variability with global climate models for present and enhanced greenhouse climates. *Int. J. Clim.,* **19**, 1-26.

McWilliams, J.C., P.P. Sullivan and C.-H. Moeng, 1997: Langmuir turbulence in the ocean. *J. Fluid Mech.,* **334**, 1-30.

Mearns, L.O., F. Giorgi, L. McDaniel and C. Shields, 1995: Analysis of daily variability of precipitation in a nested regional climate model: comparison with observations and doubled CO_2 results. *Glob. Planet. Change,* **10**, 55-78.

Meehl, G.A., 1997: The south Asian monsoon and the tropospheric biennial oscillation. *J. Clim.,* **10**, 1921-1943.

Meehl, G.A., W.D. Collins, B.A. Boville, J.T. Kiehl, T.M.L. Wigley and J.M. Arblaster, 2000: Response of the NCAR Climate System Model to increased CO_2 and the role of physical processes. *J. Clim.,* **13**, 1879-1898.

Mehta, V.M., M.J. Suarez, J.V. Manganello and T.L. Delworth, 2000: Oceanic influence of the North Atlantic Oscillation and associated Northern Hemisphere climate variations: 1959-1993. *Geophys. Res. Lett.,* **27**, 121-124.

Meleshko, V.M., Kattsov, P.V. Sporyshev, S.V. Vavulin and V.A. Govorkova, 2000: Feedback processes in climate system: cloud radiation and water vapour feedbacks interaction. *Meteorologia i Gidrologia (Russian Meteorology and Hydrology),* **2**, 22-45.

Merryfield, W.J. and G. Holloway, 1997: Topographic stress parameterization in a quasi-geostrophic barotropic model. *J. Fluid Mech.,* **341**, 1-18.

Mikolajewicz, U. and E. Maier-Reimer, 1994: Mixed boundary conditions in ocean general circulation models and their influence on the stability of the model's conveyor belt. *J. Geophys. Res.,* **99**, 22633-22644.

Mikolajewicz, U. and R. Voss, 2000: The role of the individual air-sea flux components in CO_2-induced changes of the ocean's circulation and climate. *Clim. Dyn.,* **16**, 627-642.

Milly, P.C.D. and K.A. Dunne, 1994: Sensitivity of the global water cycle to the water-holding capacity of land. *J. Clim.,* **7**, 506-526.

Mitchell, J.F.B., C.A. Wilson and W.M. Cunnington, 1987: On CO_2 climate sensitivity and model dependence of results. *Quart. J. Roy. Met. Soc.,* **113**, 293-322.

Moeng, C.-H., D.H. Lenschow and D.A. Randall, 1995: Numerical investigations of the roles of radiative and evaporative feedbacks in stratocumulus entrainment and breakup. *J. Atm. Sci.,* **52**, 2869-2883.

Moeng, C.-H., W.R. Cotton, C.S. Bretherton, A. Chlond, M. Khairoutdinov, S. Krueger, W.S. Lewellen, M.K.M. Vean, J.R.M. Pasquier, H.A. Rand, A.P. Siebesma, R.I. Sykes and B. Stevens, 1996: Simulations of a stratocumulus-topped PBL: Intercomparison among different numerical codes. *Bull. Am. Met. Soc.,* **77**, 261-278.

Monahan, A.H., J.C. Fyfe and G.M. Flato, 2000: A regime view of northern hemisphere atmospheric variability and change under global warming. *Geophys. Res. Lett.,* **27**, 1139-1142.

Morassutti, M.P. and E.F. LeDrew, 1996: Albedo and depth of melt ponds on sea ice. *Int. J. Clim.,* **16**, 817-838.

Morcrette, J.-J. and C. Jakob, 2000: The response of the ECMWF model to changes in cloud overlap assumption. *Mon. Wea. Rev.,* **128**, 1707-1732.

Mote, T.L., M.R. Anderson, K.C. Kuivinen and C.M. Rowe, 1993: Passive microwave-derived spatial and temporal variations of summer melt on the Greenland ice sheet. *Ann. Glaciol.,* **17**, 233-238.

Munk, W., 1966: Abyssal recipes. *Deep-Sea Res.,* **13**, 707-730.

Munk, W. and C. Wunsch, 1998: Abyssal recipes II, energetics of tidal and wind mixing. *Deep-Sea Res.,* **45**, 1977-2010.

Murphy, J., 1999: An evaluation of statistical and dynamical techniques for downscaling local climate. *J. Clim.,* **12**, 2256-2284.

Muszynski, I. and G.E. Birchfield, 1987: A coupled marine ice-stream ice-shelf model. *J. Glaciol.,* **33**, 3-15.

Myneni, R.B., F.G. Hall, P.J. Sellers and A.L. Marshak, 1995: The interpretation of spectral vegetation indexes. *IEEE Trans. Geosci. Rem. Sens.,* **33**, 481-486.

Myneni, R.B., C.D. Keeling, C.J. Tucker, G. Asrar and R.R. Nemani, 1997: Increased plant growth in the northern high latitudes from 1981-1991. *Nature,* **386**, 698-701.

Neelin, J.D., D.S. Battisti, A.C. Hirst, F.-F. Jin, Y. Wakata, T. Yamagata and S.E. Zebiak, 1998: ENSO theory. *J. Geophys. Res.,* **103**, 14,261-14,290.

Nobre, C.A., P.J. Sellers and J. Shukla, 1991: Amazonian deforestation and regional climate change. *J. Clim.,* **4**, 957-988.

O'Hirok, W. and C. Gautier, 1998a: A three-dimensional radiative transfer model to investigate the solar radiation within a cloudy atmosphere. Part I: Spatial effects. *J. Atm. Sci.,* **55**, 2162-2179.

O'Hirok, W. and C. Gautier, 1998b: A three-dimensional radiative transfer model to investigate the solar radiation within a cloudy atmosphere. Part II: Spectral effects. *J. Atm. Sci.,* **55**, 3065-3076.

Oreopoulos, L. and H.W. Barker, 1999: Accounting for subgrid-scale cloud variability in a multi-layer 1D solar radiative transfer radiative algorithm. *Quart. J. Roy. Met. Soc.,* **125**, 301-330.

Orsi, A., G. Johnson and J. Bullister, 1999: Circulation, mixing and production of Antarctic Bottom Water. *Prog. Oceanogr.,* **43**, 55-109.

Osborn, T.J., K.R. Briffa, S.F.B. Tett, P.D. Jones and R.M. Trigo, 1999: Evaluation of the North Atlantic oscillation as simulated by a coupled climate model. *Clim. Dyn.,* **15**, 685-702.

Osborn, T.J. and M. Hulme, 1997: Development of a relationship between station and grid-box rainday frequencies for climate model evaluation. *J. Clim.,* **10**, 1885-1908.

Palmer, T.N., 1999: A nonlinear dynamical perspective on climate prediction. *J. Clim.,* **12**, 575-591.

Palmer, T.N., 2000: Predicting uncertainty in forecasts of weather and climate. *Rep. Prog. Phys.,* **63**, 71-116.

Palmer, T.N. and D.A. Mansfield, 1986: A study of the wintertime circulation anomalies during past El Niño events, using a high resolution general circulation model. I. Influence of model climatology. *Quart. J. Roy. Met. Soc.,* **112**, 613-638.

Palmer, T.N., G.J. Shutts and R. Swinbank, 1986: Alleviation of a systematic westerly bias in general circulation and numerical weather prediction models through an orographic gravity wave drag parametrization. *Quart. J. Roy. Met. Soc.,* **112**, 1001-1039.

Paluszkiewicz, T. and R.D. Romea, 1997: A one-dimensional model for the parameterization of deep convection in the ocean. *Dyn. Atm. Ocean,* **26**, 95-130.

Pan, L., S. Solomon, W. Randel, J.F. Lamarque, P. Hess, J. Gille, E.W. Chiou and M.P. McCormick, 1997: Hemispheric asymmetries and seasonal variations of the lowermost stratospheric water vapor and ozone derived from SAGE II data. *J. Geophys. Res.,* **102**, 28177-28184.

Parkinson, C.L., D.J. Cavalieri, P. Gloersen, H.J. Zwally and J.C. Comiso, 1999: Arctic sea ice extent, areas, and trends, 1978-1996. *J. Geophys. Res.,* **104**, 20837-20856.

Payne, A.J., P. Huybrechts, A. Abe-Ouchi, R. Calov, J.L. Fastook, R. Greve, S.J. Marshall, I. Marsiat, C. Ritz, L. Tarasov and M.P.A. Thomassen, 2000: Results from the EISMINT model intercomparison: the effects of thermomechanical coupling. *J. Glaciol.,* **46**, 227-238

Perlwitz, J. and H.-F. Graf, 1995: The statistical connection between tropospheric and stratospheric circulation of the Northern Hemisphere in winter. *J. Clim.,* **8**, 2281-2295.

Perovich, D.K., E.L. Andreas, J.A. Curry, H. Eiken, C.W. Fairall, T.C. Grenfell, P.S. Guest, J. Intrieri, D. Kadko, R.W. Lindsay, M.G. McPhee, J. Morison, R.E. Moritz, C.A. Paulson, W.S. Pegau, P.O.G. Persson, R. Pinkel, J.A. Richter-Menge, T. Stanton, H. Stern, M. Sturm, W.B. Tucker III and T. Uttal, 1999: Year on ice gives climate insights. *EOS; Trans. Am. Geophys. Un.,* **80**, 481-486.

Petroliagis, T., R. Buizza, A. Lanzinger and T.N. Palmer, 1996: Extreme rainfall prediction using the European centre for medium-range weather forecasts ensemble prediction system. *J. Geophys. Res.,* **101**, 26227-26236.

Pierrehumbert, R.T., 1995: Thermostats, radiator fins and the local runaway greenhouse. *J. Atm. Sci.,* **52**, 1784-1806.

Pierrehumbert, R.T., 1999: Subtropical water vapor as a mediator of rapid climate change. In: *Geophysical Monograph: Mechanisms of global climate change at millennial time scales (112)* [Clark, P. U., R. S. Webb and L. D. Keigwin (eds.)]. American Geophysical Union, Washington, 339-361.

Pierrehumbert, R.T. and R. Roca, 1998: Evidence for control of Atlantic subtropical humidity by large scale advection. *Geophys. Res. Lett.,* **25**, 4537-4540.

Pilewskie, P. and F.P.J. Valero, 1995: Direct observations of excess absorption by clouds. *Science,* **267**, 1626-1629.

Pinnock, S., M.D. Hurley, K.P. Shine, T.J. Wallington and T.J. Smyth, 1995: Radiative forcing by hydrochlorofluorocarbons and hydrofluorocarbons. *J. Geophys. Res.,* **100**, 23227-23238.

Polcher, J., 1995: Sensitivity of tropical convection to land surface processes. *J. Atm. Sci.,* **52**, 3143-3161.

Pollard, D. and S.L. Thompson, 1994: Sea-ice dynamics and CO_2 sensitivity in a global climate model. *Atm.-Oce.,* **32**, 449-467.

Polyakov, I.V., A.Y. Proshutinsky and M.A. Johnson, 1999: Seasonal cycles in two regimes of Arctic climate. *J. Geophys. Res.,* **104**, 25761-25788.

Polzin, K., J.M. Toole and R.W. Schmitt, 1995: Finescale parameterizations of turbulent dissipation. *J. Phys. Oceanogr.,* **25**, 306-328.

Polzin, K.L. and E. Firing, 1997: Estimates of diapycnal mixing using LADCP and CTD data from 18S. *International WOCE Newsletter,* **29**, 39-42.

Polzin, K.L., J.M. Toole, J.R. Ledwell and R.W. Schmitt, 1997: Spatial variability of turbulent mixing in the abyssal ocean. *Science,* **276**, 93-96.

Pope, S.K. and F.P.J. Valero, 2000: Observations and models of irradiance profiles, column transmittance, and column reflectance during the Atmospheric Radiation Measurements Enhanced Shortwave Experiment. *J. Geophys. Res.,* **105**, 12521-12528.

Pratt, L.J. and M. Chechelnitsky, 1997: Principles for capturing the upstream effects of deep sills in low resolution ocean models. *Dyn. Atm. Ocean,* **26**, 1-25.

Proshutinsky, A.Y. and M.A. Johnson, 1997: Two circulation regimes of the wind-driven Arctic Ocean. *J. Geophys. Res.,* **102**, 12493-12514.

Ramanathan, V. and W. Collins, 1991: Thermodynamic regulation of ocean warming by cirrus clouds deduced from observations of the 1987 El Niño. *Nature,* **351**, 27-32.

Ramanathan, V., B. Subasilar, G. Zhang, W. Conant, R.D. Cess, J.T. Kiehl, H. Grassl and L. Shi, 1995: Warm Pool heat budget and shortwave cloud forcing - A missing physics. *Science,* **267**, 499-503.

Ramankutty, N. and J.A. Foley, 1998: Characterizing patterns of global land use: an analysis of global croplands data. *Glob. Biogeochem. Cyc.,* **12**, 667-685.

Ramaswamy, V., M.D. Schwarzkopf and W. Randel, 1996: Fingerprint of ozone depletion in the spatial and temporal pattern of recent lower-stratospheric cooling. *Nature,* **382**, 616-618.

Randall, D., J. Curry, D. Battisti, G. Flato, R. Grumbine, S. Hakkinen, D. Martinson, R. Preller, J. Walsh and J. Weatherly, 1998: Status and outlook for large-scale modelling of atmosphere-ice-ocean interactions in the Arctic. *Bull. Am. Met. Soc.,* **79**, 197-219.

Randall, D.A., 1995: Parameterizing fractional cloudiness produced by cumulus detrainment. In: *Technical Document: Workshop on Cloud Microphysics Parameterizations in Global Atmospheric General Circulation Models (713)* . World Meteorological Organization, 1-16.

Randall, D.A., P.J. Sellers, J.A. Berry, D.A. Dazlich, C. Zhang, C.J. Collatz, A.S. Denning, S.O. Los, C.B. Field, I. Fung, C.O. Justice and C.J. Tucker, 1996: A revised land surface parameterization (SiB2) for atmospheric GCMs. Part 3: The greening of the CSU GCM. *J. Clim.,* **9**, 738-763.

Randel, W.J. and F. Wu, 1999: Cooling of the Arctic and Antarctic polar stratosphere due to ozone depletion. *J. Clim.,* **12**, 1467-1479.

Randerson, J.T. and M.V. Thompson, 1999: Linking C-13 based estimates of land and ocean sinks with predictions of carbon storage from CO_2 fertilization of plant growth. *Tellus,* **51B**, 668-678.

Randerson, J.T., M.V. Thompson, T.J. Conway, I. Fung and C.B. Field, 1997: The contribution of terrestrial sources and sinks to trends in the seasonal cycle of atmospheric carbon dioxide. *Glob. Biogeochem. Cyc.,* **11**, 535-560.

Randerson, J.T., C.B. Field, I.Y. Fung and P.P. Tans, 1999: Increases in early season ecosystem uptake explain recent changes in the seasonal

cycle of atmospheric CO_2 at high northern latitudes. *Geophys. Res. Lett.,* **26**, 2765-2768.

Raval, A. and V. Ramanathan, 1989: Observational determination of the greenhouse effect. *Nature,* **342**, 758-761.

Rayner, P. and R. Law, 1999: The interannual variability of the global carbon cycle. *Tellus,* **51B**, 210-212.

Ricard, J.-L. and J.-F. Royer, 1993: A statistical cloud scheme for use in an AGCM. *Ann. Geophys.,* **11**, 1095-1115.

Roads, J.O., S. Marshall, R. Oglesby and S.-C. Chen, 1996: Sensitivity of the CCM1 hydrological cycle to CO_2. *J. Geophys. Res.,* **101**, 7321-7339.

Robbins, P.E. and J.M. Toole, 1997: The dissolved silica budget as a constraint on the meridional overturning circulation of the Indian Ocean. *Deep-Sea Res. I,* **44**, 879-906.

Roberts, M. and D. Marshall, 1998: Do we require adiabatic dissipation schemes in eddy-resolving ocean models? *J. Phys. Oceanogr.,* **28**, 2050-2063.

Roberts, M.J. and R.A. Wood, 1997: Topography sensitivity studies with a Bryan-Cox type ocean model. *J. Phys. Oceanogr.,* **27**, 823-836.

Robertson, A.W., M. Ghil and M. Latif, 2000a: Interdecadal changes in atmospheric low-frequency variability with and without boundary forcing. *J. Atm. Sci.,* **57**, 1132-1140.

Robertson, A.W., C.R. Mechoso and Y.-J. Kim, 2000b: The influence of Atlantic sea surface temperature anomalies on the North Atlantic Oscillation. *J. Clim.,* **13**, 122-138.

Rodbell, D., G.O. Seltzer, D.M. Anderson, D.B. Enfield, M.B. Abbott and J.H. Newman, 1999: A high-resolution 15,000 year record of El Niño driven alluviation in southwestern Ecuador. *Science,* **283**, 516-520.

Rodwell, M.J., D.P. Rowell and C.K. Folland, 1999: Oceanic forcing of the wintertime North Atlantic oscillation and European climate. *Nature,* **398**, 320-323.

Roeckner, E., M. Rieland and E. Keup, 1991: Modeling of cloud and radiation in the ECHAM model. In: *Procs. ECMWF/WCRP Workshop on "Clouds, radiative transfer and the hydrological cycle" 12-15 November 1990* . ECMWF, Reading, UK, 199-222.

Roeckner, E., K. Arpe, L. Bengtsson, M. Christoph, M. Claussen, L. Dümenil, M. Esch, M. Giorgetta, U. Schlese and U. Schulzweida, 1996: The atmospheric general circulation model ECHAM-4: Model description and simulation of present-day climate. Report **218**, *Max-Planck Institut für Meteorologie,* Hamburg, 90 pp.

Roemmich, D. and T. McCallister, 1989: Large scale circulation of the North Pacific Ocean. *Prog. Oceanogr.,* **22**, 171-204.

Rosenlof, K.H., 1995: Seasonal cycle of the residual mean meridional circulation in the stratosphere. *J. Geophys. Res.,* **100**, 5173-5191.

Ross, R.J. and W.P. Elliot, 1996: Tropospheric water vapor climatology and trends over North America: 1973-93. *J. Clim.,* **9**, 3561-3574.

Rotstayn, L.D., 1997: A physically based scheme for the treatment of clouds and precipitation in large-scale models. I: Description and evaluation of the microphysical processes. *Quart. J. Roy. Met. Soc.,* **123**, 1227-1282.

Royer, J.-F., F. Chauvain, P. Timbal, P. Araspin and D. Grimal, 1998: A GCM study of the impact of greenhouse gas increase on the frequency of occurrence of tropical cyclones. *Clim. Change,* **38**, 307-343.

Saji, N.H., B.N. Goswami, P.N. Vinayachandran and T. Yamagata, 1999: A dipole mode in the tropical Indian Ocean. *Nature,* **401**, 360-363.

Salathe, E.P. and D.L. Hartmann, 1997: A trajectory analysis of tropical upper-tropospheric moisture and convection. *J. Clim.,* **10**, 2533-2547.

Sandweiss, D.H., J.B. Richardson, E.J. Reitz, H.B. Rollins and K.A. Maasch, 1996: Geoarchaeological evidence from Peru for a 5,000 BP onset of El Niño. *Science,* **273**, 1531-1533.

SAR, see IPCC, 1996.

Saravanan, R., 1998: Atmospheric low frequency variability and its relationship to midlatitude SST variability: studies using the NCAR Climate System Model. *J. Clim.,* **11**, 1386-1404.

Saravanan, R. and J.C. McWilliams, 1998: Advective ocean-atmosphere interaction: An analytical stochastic model with implications for decadal variability. *J. Clim.,* **11**, 165-188.

Saunders, P.M. and B.A. King, 1995: Oceanic fluxes on the WOCE A11 section. *J. Phys. Oceanogr.,* **25**, 1942-1958.

Schär, C., D. Lüthi, U. Beyerle and E. Heise, 1999: The soil-precipitation feedback: a process study with a regional climate model. *J. Clim.,* **12**, 722-741.

Schiller, A., U. Mikolajewicz and R. Voss, 1997: The stability of the North Atlantic thermohaline circulation in a coupled ocean-atmosphere general circulation model. *Clim. Dyn.,* **13**, 325-347.

Schlosser, C.A., A.G. Slater, A.J. Pitman, A. Robock, K.Y. Vinnikov, A. Henderson-Sellers, N.A. Speranskaya, K. Mitchell, A. Boone, H. Braden, F. Chen, P. Cox, P. de Rosnay, C.E. Desborough, R.E. Dickinson, Y.-J. Dai, Q. Duan, J. Entin, P. Etchevers, N. Gedney, Y.M. Gusev, F. Habets, J. Kim, V. Koren, E. Kowalczyk, O.N. Nasonova, J. Noilhan, J. Schaake, A.B. Shmakin, T.G. Smirnova, D. Verseghy, P. Wetzel, Y. Xue and Z.-L. Yang, 2000: Simulations of a boreal grassland hydrology at Valdai, Russia: PILPS Phase 2(d). *Mon. Wea. Rev.,* **128**, 301-321.

Schmittner, A., C. Appenzeller and T.F. Stocker, 2000: Enhanced Atlantic freshwater export during El Niño. *Geophys. Res. Lett.,* **27**, 1163-1166.

Schmittner, A. and T.F. Stocker, 1999: The stability of the thermohaline circulation in global warming experiments. *J. Clim.,* **12**, 1117-1133.

Schneider, E.K., B.P. Kirtman and R.S. Lindzen, 1999: Tropospheric water vapor and climate sensitivity. *J. Atm. Sci.,* **36**, 1649-1658.

Schott, F., M. Visbeck and J. Fischer, 1993: Observations of vertical currents and convection in the central Greenland Sea during winter 1988/89. *J. Geophys. Res.,* **98**, 14401-14421.

Schott, F., M. Visbeck, U. Send, J. Fischer, L. Stramma and Y. Desaubies, 1996: Observations of deep convection in the Gulf of Lions, northern Mediterranean, during the winter of 1991/92. *J. Phys. Oceanogr.,* **26**, 505-524.

Schramm, J.L., M.M. Holland, J.A. Curry and E.E. Ebert, 1997: Modeling the thermodynamics of a sea ice thickness distribution. 1. Sensitivity to ice thickness resolution. *J. Geophys. Res.,* **102**, 23079-23091.

Schulz, J. and V. Jost (eds.), 1998: *HOAPS: A Satellite-Derived Water Balance Climatology*, WOCE Conference, May, Halifax.

Sellers, P.J., J.A. Berry, G.J. Collatz, C.B. Field and F.G. Hall, 1992a: Canopy reflectance, photosynthesis and transpiration. Part III: A reanalysis using enzyme kinetics-electron transport models of leaf physiology. *Rem. Sens. Environ.,* **42**, 187-216.

Sellers, P.J., F.G. Hall, G. Asrar, D.E. Strebel and R.E. Murphy, 1992b: An overview of the First International Satellite Land Surface Climatology Project (ISLSCP) Field Experiment (FIFE). *J. Geophys. Res.,* **97**, 18345-18731.

Sellers, P.J., M.D. Heiser and F.G. Hall, 1992c: Relationship between surface conductance and spectral vegetation indices at intermediate ($100 m^2$-15 km^2) length scales. *J. Geophys. Res.,* **97**, 19033-19060.

Sellers, P.J., F.G. Hall, H. Margolis, B. Kelly, D. Baldocchi, J. denHartog, J. Cihlar, M. Ryan, B. Goodison, P. Crill, J. Ranson, D. Lettenmaier and D.E. Wickland, 1995: The Boreal Ecosystem-Atmosphere Study (BOREAS): an overview and early results from the 1994 field year. *Bull. Am. Met. Soc.,* **76**, 1549-1577.

Sellers, P.J., L. Bounoua, G.J. Collatz, D.A. Randall, D.A. Dazlich, S.O. Los, J.A. Berry, I. Fung, C.J. Tucker, C.B. Field and T.G. Jensen, 1996a: Comparison of radiative and physiological effects of doubled atmospheric CO_2 on climate. *Science,* **271**, 1402-1406.

Sellers, P.J., B.W. Meeson, J. Closs, F. Corprew, D. Dazlich, F.G. Hall, Y. Kerr, R. Koster, S. Los, K. Mitchell, J. McManus, D. Myers, K.-J. Sun and P. Try, 1996b: The ISLSCP Initiative I Global Data Sets: Surface boundary conditions and atmospheric forcings for land-atmosphere studies. *Bull. Am. Met. Soc.,* **77**, 1987-2005.

Sellers, P.J., D.A. Randall, G.J. Collatz, J.A. Berry, C.B. Field, D.A. Dazlich, C. Zhang, G.D. Collelo and L. Bounoua, 1996c: A revised land surface parameterization (SiB2) for atmospheric GCMs. Part I: Model formulation. *J. Clim.,* **9**, 676-705.

Sellers, P.J., R.E. Dickinson, D.A. Randall, A.K. Betts, F.G. Hall, J.A. Berry, G.J. Collatz, A.S. Denning, H.A. Mooney, C.A. Nobre, N. Sato, C.B. Field and A. Henderson-Sellers, 1997: Modeling the exchange of energy, water and carbon between continents and the atmosphere. *Science,* **275**, 502-509.

Senior, C.A. and J.F.B. Mitchell, 1993: Carbon dioxide and climate: the impact of cloud parameterization. *J. Clim.,* **6**, 393-418.

Shao, Y. and A. Henderson-Sellers, 1996: Validation of soil moisture simulation in land surface parameterization schemes with HAPEX data. *Glob. Planet. Change,* **13**, 11-46.

Shaw, J., B. Rains, R. Eyton and L. Weissling, 1996: Laurentide subglacial outburst floods: landform evidence from digital elevation models. *Can. J. Earth Sci.,* **33**, 1154-1168.

Shepherd, T.G., K. Semeniuk and J.N. Koshyk, 1996: Sponge layer feedbacks in middle atmosphere models. *J. Geophys. Res.,* **101**, 23447-23464.

Sherwood, S.C., 1996: Maintenance of the free-troposphere tropical water vapor distribution. Part II: Simulation by large-scale advection. *J. Clim.,* **9**, 2919-2934.

Shindell, D., D. Rind, N. Balachandran, J. Lean and P. Lonergan, 1999a: Solar cycle variability, ozone, and climate. *Science,* **284**, 305-308.

Shindell, D.T., R.L. Miller, G.A. Schmidt and L. Pandolfo, 1999b: Simulation of recent northern winter climate trends by greenhouse-gas forcing. *Nature,* **399**, 452-455.

Shine, K.P., 1993: The greenhouse effect and stratosheric change. In: *NATO ASI I8: The role of the stratosphere in global change* [Chanin, M.-L. (ed.)]. Springer-Verlag, Berlin, 285-300.

Shine, K.P. and P.M.F. Forster, 1999: The effect of human activity on radiative forcing of climate change: a review of recent developments. *Glob. Planet. Change,* **20**, 205-225.

Shine, K.P., B. Briegleb, A. Grossman, D. Hauglustaine, H. Mao, V. Ramaswamy, D. Schwarzkopf, R.V. Dorland and W.-C. Wang, 1995: Radiative forcing due to changes in ozone: A comparison of different codes. In: *NATO ASI I32: Atmospheric Ozone as a Climate Gas* [Wang, W.-C. and I. Isaksen (eds.)]., 373-396.

Slater, A.G., A.J. Pitman and C.E. Desborough, 1998a: The simulation of freeze-thaw cycles in a GCM land surface scheme. *J. Geophys. Res.,* **103**, 11303-11312.

Slater, A.G., A.J. Pitman and C.E. Desborough, 1998b: The validation of a snow parameterization designed for use in General Circulation Models. *Int. J. Clim.,* **18**, 595-617.

Slingo, J.M., K.R. Sperber, J.S. Boyle, J.P. Ceron, M. Dix, B. Dugas, W. Ebisuzaki, J. Fyfe, D. Gregory, J.F. Gueremy, J. Hack, A. Harzallah, P. Inness, A. Kitoh, W.K.M. Lau, B. McAvaney, R. Madden, A. Matthews, T.N. Palmer and C.K. Park, 1996: Intraseasonal oscillations in 15 atmospheric general circulation models: results from an AMIP diagnostic subproject. *Clim. Dyn.,* **12**, 325-357.

Smith, R.D., M.E. Maltrud, F.O. Bryan and M.W. Hecht, 2000: Numerical simulation of the North Atlantic at 1/10°. *J. Phys. Oceanogr.,* **30**, 1532-1561.

Smith, R.N.B., 1990: A scheme for predicting layer clouds and their water content in a general circulation model. *Quart. J. Roy. Met. Soc.,* **116**, 435-460.

Soden, B.J., 1997: Variations in the tropical greenhouse effect during El Niño. *J. Clim.,* **10**, 1050-1055.

Soden, B.J., 1998: Tracking upper tropospheric water vapor radiances: A satellite perspective. *J. Geophys. Res.,* **103**, 17069-17081.

Soden, B.J., 2000: The sensitivity of the tropical hydrological cycle to ENSO. *J. Clim.,* **13**, 538-549.

Soden, B.J. and R. Fu, 1995: A satellite analysis of deep convection, upper-tropospheric humidity, and the greenhouse effect. *J. Clim.,* **8**, 2333-2351.

Solomon, S., R.W. Portmann, R.R. Garcia, L.W. Thomason, L.R. Poole and M.P. McCormick, 1996: The role of aerosol variations in anthropogenic ozone depletion at northern midlatitudes. *J. Geophys. Res.,* **101**, 6713-6727.

Spall, M.A. and J.F. Price, 1998: Mesoscale variability in Denmark Strait: the PV outflow hypothesis. *J. Phys. Oceanogr.,* **28**, 1598-1623.

Spall, M.A., R.A. Weller and P. Furey, 2000: Modelling the three-dimensional upper ocean heat budget and subduction rate during the Subduction Experiment. *J. Geophys. Res.,* **105**, 26151-26166.

Speer, K.G., J. Holfort, T. Reynard and G. Siedler**,** 1996: South Atlantic heat transport at 11°S. In: *The South Atlantic: Present and Past Circulation* [Wefer, G., W. H. Berger, G. Siedler and D. J. Webb (eds.)]. Springer, 105-120.

Spencer, R.W. and W.D. Braswell, 1997: How dry is the tropical free troposphere? Implications for global warming theory. *Bull. Am. Met. Soc.,* **78**, 1097-1106.

St. Laurent, L. and R.W. Schmitt, 1999: The contribution of salt fingers to vertical mixing in the North Atlantic Tracer Release Experiment. *J. Phys. Oceanogr.,* **29**, 1404-1424.

Stephens, G.L., 1996: How much solar radiation do clouds absorb? *Science,* **271**, 1131-1133.

Stocker, T.F., 2000: Past and future reorganization in the climate system. *Quat. Sci. Rev.,* **19**, 301-319.

Stocker, T.F. and D.G. Wright, 1991: Rapid transitions of the ocean's deep circulation induced by changes in surface water fluxes. *Nature,* **351**, 729-732.

Stocker, T.F. and A. Schmittner, 1997: Influence of CO_2 emission rates on the stability of the thermohaline circulation. *Nature,* **388**, 862-865.

Stocker, T.F. and O. Marchal, 2000: Abrupt climate change in the computer: is it real? *PNAS,* **97**, 1362-1365.

Stommel, H., 1961: Thermohaline convection with two stable regimes of flow. *Tellus,* **13**, 224-230.

Stössel, A., S.-J. Kim and S.S. Drijfhout, 1998: The impact of Southern Ocean sea ice in a global ocean model. *J. Phys. Oceanogr.,* **28**, 1999-2018.

Stouffer, R.J. and S. Manabe, 1999: Response of a coupled ocean-atmosphere model to increasing atmospheric carbon dioxide: sensitivity to the rate of increase. *J. Clim.,* **12**, 2224-2237.

Stroeve, J., A.W. Nolin and K. Steffen, 1997: Comparison of AVHRR-derived and in situ surface albedo over the Greenland ice sheet. *Rem. Sens. Environ.,* **62**, 262-276.

Sud, Y.C. and G.K. Walker, 1999: Microphysics of clouds with the relaxed Arakawa-Schubert scheme (McRAS). Part I: design and evaluation with GATE phase III data. *J. Atm. Sci.,* **56**, 3196-3220.

Sud, Y.C., G.K. Walker, J.-H. Kim, G.E. Liston, P.J. Sellers and W.K.-M. Lau, 1996: Biogeophysical consequences of a tropical deforestation scenario: a GCM simulation study. *J. Clim.,* **9**, 3225-3247.

Sun, D.-Z. and K.E. Trenberth, 1998: Coordinated heat removal from the tropical Pacific during the 1986-87 El Niño. *Geophys. Res. Lett.,* **25**, 2659-2662.

Suppiah, R. and K.J. Hennessy, 1998: Trends in the intensity and frequency of heavy rainfall in tropical Australia and links with the Southern Oscillation. *Austr. Meteorol. Mag.,* **45**, 1-17.

Sutton, R.T. and M.R. Allen, 1997: Decadal predictability of North Atlantic sea surface temperature and climate. *Nature,* **388**, 563-567.

Takahashi, M., 1996: Simulation of the stratospheric quasi-biennial oscillation using a general circulation model. *Geophys. Res. Lett.,* **23**, 661-664.

Takle, E.S., J. Gutowski, W. J., R.W. Arritt, Z. Pan, C.J. Anderson, R.R. da Silva, D. Caya, S.-C. Chen, F. Giorgi, J.H. Christensen, S.-Y. Hong, H.-M.H. Juang, J. Katzfey, W.M. Lapenta, R. Laprise, G.E. Liston, P. Lopez, J. McGregor, R.A. Pielke Sr. and J.O. Roads, 1999: GEWEX Continental-scale International Project (GCIP), Part 2: Project to intercompare regional climate simulations (PIRCS):

Description and initial results. *J. Geophys. Res.,* **104**, 19443-19462.

Tans, P.P., I.Y. Fung and T. Takahashi, 1990: Observational constraints on the global atmospheric CO_2 budget. *Science,* **247**, 1431-1438.

Tett, S.F.B., J.F.B. Mitchell, D.E. Parker and M.R. Allen, 1996: Human influence on the atmospheric vertical temperature structure: detection and observations. *Science,* **274**, 1170-1173.

Thomas, G. and P.R. Rowntree, 1992: The boreal forest and climate. *Quart. J. Roy. Met. Soc.,* **118**, 469-497.

Thomas, R.H. and C.R. Bentley, 1978: A model for Holocene retreat of the West Antarctic Ice Sheet. *Quat. Res.,* **10**, 150-170.

Thompson, D.W.J. and J.M. Wallace, 1998: The Arctic Oscillation signature in the wintertime geopotential height and temperature fields. *Geophys. Res. Lett.,* **25**, 1297-1300.

Thompson, D.W.J. and J.M. Wallace, 2000: Annular modes in the extra-tropical circulation Part I: month-to-month variability. *J. Clim.,* **13**, 1000-1016.

Thompson, S.L. and D. Pollard, 1995: A global climate model (GENESIS) with a land-surface transfer scheme (LSX). Part II CO_2 sensitivity. *J. Clim.,* **8**, 1104-1121.

Thompson, S.L. and D. Pollard, 1997: Greenland and Antarctic mass balances for present and doubled atmospheric CO_2 from the GENESIS version-2 global climate model. *J. Clim.,* **10**, 871-900.

Tian, H., J.M. Melillo, D.W. Kicklighter, A.D. McGuire and J. Helfrich, 1999: The sensitivity of terrestrial carbon storage to historical climate variability and atmospheric CO_2 in the United States. *Tellus,* **51B**, 414-452.

Tiedtke, M., 1993: Representation of clouds in large-scale models. *Mon. Wea. Rev.,* **121**, 3040-3061.

Timmermann, A., M. Latif, R. Voss and R.A. Grotzner, 1998: Northern hemispheric interdecadal variability: a coupled air-sea mode. *J. Clim.,* **11**, 1906-1931.

Timmermann, A., J.M. Oberhuber, A. Bacher, M. Esch, M. Latif and E. Roeckner, 1999: Increased El Niño frequency in a climate model forced by future greenhouse warming. *Nature,* **398**, 694-696.

Toggweiler, J.R. and B. Samuels, 1995: Effect of Drake Passage on the global thermohaline circulation. *Deep-Sea Res. I,* **42**, 477-500.

Tompkins, A.M. and K.A. Emanuel, 2000: The vertical resolution sensitivity of simulated equilibrium temerature and water vapour profiles. *Quart. J. Roy. Met. Soc.,* **126**, 1219-1238.

Trenberth, K.E., 1998: Atmospheric moisture residence times and cycling: Implications for rainfall rates and climate change. *Clim. Change,* **39**, 667-694.

Trenberth, K.E., 1999: Conceptual framework for changes of extremes of the hydrological cycle with climate change. *Clim. Change,* **42**, 327-339.

Trenberth, K.E. and J.W. Hurrell, 1994: Decadal atmosphere-ocean variations in the Pacific. *Clim. Dyn.,* **9**, 303-319.

Trenberth, K.E. and A. Solomon, 1994: The global heat balance: heat transports in the atmosphere and ocean. *Clim. Dyn.,* **10**, 107-134.

Trenberth, K.E. and T.J. Hoar, 1997: El Niño and climate change. *Geophys. Res. Lett.,* **24**, 3057-3060.

Trenberth, K.E. and C.J. Guillemot, 1998: Evaluation of the atmospheric moisture and hydrological cycle in the NCEP/NCAR reanalyses. *Clim. Dyn.,* **14**, 213-231.

Trenberth, K.E. and J.W. Hurrell, 1999: Comments on "The interpreta-tion of short climate records with comments on the North Atlantic and Southern Oscillations". *Bull. Am. Met. Soc.,* **80**, 2721-2722.

Trenberth, K.E., G.W. Branstator, D. Karoly, A. Kumar, N.-C. Lau and C. Ropelewski, 1998: Progress during TOGA in understanding and modeling global teleconnections associated with tropical sea surface temperatures. *J. Geophys. Res.,* **103**, 14291-14324.

Trenberth, K.E., J.M. Caron and D.P. Stepaniak, 2001: The atmospheric energy budget and implications for surface fluxes and ocean heat transports. *Clim. Dyn.,* **17**, 259-276.

Tselioudis, G. and W.B. Rossow, 1994: Global, multiyear variations of

optical thickness with temperature in low and cirrus clouds. *Geophys. Res. Lett.,* **21**, 2211-2214.

Tselioudis, G., W. Rossow and D. Rind, 1992: Global patterns of cloud optical thickness variation with temperature. *J. Clim.,* **5**, 1484-1495.

Tselioudis, G., A.D. Del Genio, W. Kowari Jr. and M.-S. Yao, 1998: Temperature dependence of low cloud optical thickness in the GISS GCM: Contributing mechanisms and climate implication. *J. Clim.,* **11**, 3268-3281.

Tselioudis, G., Y. Zhang and W.B. Rossow, 2000: Cloud and radiation variations associated with northern midlatitude low and high sea level pressure regimes. *J. Clim.,* **13**, 312-327.

Tsimplis, M.N., S. Bacon and H.L. Bryden, 1998: The circulation of the sub-tropical South Pacific derived from hydrographic data. *J. Geophys. Res.,* **103**, 21443-21468.

Tucker, C.J.B., I.Y. Fung, C.D. Keeling and R.H. Gammon, 1986: Relationship between atmospheric CO_2 variation and a satellite-derived vegetation index. *Nature,* **319**, 195-199.

Tulaczyk, S., B. Kamb, R.P. Scherer and H. Engelhardt, 1998: Sedimentary processes at the base of a West Antarctic ice stream: Constraints from textural and compositional properties of subglacial debris. *J. Sed. Res.,* **68**, 487-496.

Twomey, S.A., 1974: Pollution and the planetary albedo. *Atmos. Env.,* **8**, 1251-1256.

Tziperman, E., 2000: Proximity of the present-day thermohaline circula-tion to an instability threshold. *J. Phys. Oceanogr.,* **30**, 90-104.

Udelhofen, P.M. and D.L. Hartmann, 1995: Influence of tropical cloud systems on the relative humidity in the upper troposphere. *J. Geophys. Res.,* **100**, 7423-7440.

Valero, F.P.J., R.D. Cess, M. Zhang, S.K. Pope, A. Bucholtz, B. Bush and J. Vitko Jr., 1997: Absorption of solar radiation by clouds. *J. Geophys. Res.,* **102**, 29917-29927.

Valero, F.P.J., P. Minnis, S.K. Pope, A. Bucholtz, D.R. Doelling, W.L. Smith and X.Q. Dong, 2000: Absorption of solar radiation by the atmosphere as determined using satellite, aircraft, and surface data during the Atmospheric Radiation Measurement Enhanced Shortwave Experiment (ARESE). *J. Geophys. Res.,* **105**, 4743-4758.

van der Veen, C.J. and I.M. Whillans, 1996: Model experiments on the evolution and stability of ice streams. *Ann. Glaciol.,* **23**, 129-137.

Verseghy, D.L., N.A. McFarlane and M. Lazare, 1993: CLASS - A Canadian land surface scheme for GCMs. II: Vegetation model and coupled runs. *Int. J. Clim.,* **13**, 347-370.

Vinje, T., N. Nordlund and A. Kvambekk, 1998: Monitoring ice thickness in Fram Strait. *J. Geophys. Res.,* **103**, 10437-10449.

Vinnikov, K.Y., A. Robock, R.J. Stouffer, J.E. Walsh, C.L. Parkinson, D.J. Cavalieri, J.F.B. Mitchell, D. Garrett and V.F. Zakharov, 1999: Global warming and Northern Hemisphere sea ice extent. *Science,* **286**, 1934-1937.

Visbeck, M., J. Fischer and F. Schott, 1995: Preconditioning the Greenland Sea for deep convection: Ice formation and ice drift. *J. Geophys. Res.,* **100**, 18489-18502.

Visbeck, M., J. Marshall, T. Haine and M. Spall, 1997: Specification of eddy transfer coefficients in coarse-resolution ocean circulation models. *J. Phys. Oceanogr.,* **27**, 381-402.

Viterbo, P., A.C.M. Beljaars, J.-F. Mahfouf and J. Teixeira, 1999: The representation of soil moisture and freezing and its impact on the stable boundary layer. *Quart. J. Roy. Met. Soc.,* **125**, 2401-2426.

Wallace, J.M., Y. Zhang and J.A. Renwick, 1995: Dynamic contribution to hemispheric mean temperature trends. *Science,* **270**, 780-783.

Wang, W.-C., M.P. Dudek, X.-Z. Liang and J.T. Kiehl, 1991: Inadequacy of effective CO_2 as a proxy in simulating the greenhouse effect of other radiatively active gases. *Nature,* **350**, 573-577.

Watanabe, M. and T. Nitta, 1999: Decadal changes in the atmospheric circulation and associated surface climate variations in the Northern Hemisphere winter. *J. Clim.,* **12**, 494-510.

Watterson, I.G., M.R. Dix and R.A. Colman, 1999: A comparison of

present and doubled CO_2 climates and feedbacks simulated by three general circulation models. *J. Geophys. Res.,* **104**, 1943-1956.

Waugh, D.W., T.M. Hall, W.J. Randel, K.A. Boering, S.C. Wofsy, B.C. Daube, J.W. Elkins, D.W. Fahey, G.S. Dutton, C.M. Volk and P. Vohralik, 1997: Three-dimensional simulations of long-lived tracers using winds from MACCM2. *J. Geophys. Res.,* **102**, 21493-21513.

Weare, B.C., 2000a: Insights into the importance of cloud vertical structure in climate. *Geophys. Res. Lett.,* **27**, 907-910.

Weare, B.C., 2000b: Near-global observations of low clouds. *J. Clim.,* **13**, 1255-1268.

Weare, B.C. and I.I. Mokhov, 1995: Evaluation of total cloudiness and its variability in the Atmospheric Model Intercomparison Project. *J. Clim.,* **8**, 2224-2238.

Weaver, A.J. and T.M.C. Hughes, 1994: Rapid interglacial climate fluctuations driven by North Atlantic ocean circulation. *Nature,* **367**, 447-450.

Webster, P.J., V.O. Magaña, T.N. Palmer, J. Shukla, R.A. Tomas, M. Yanai and T. Yasunari, 1998: Monsoons: Processes, predictability and the prospects for prediction. *J. Geophys. Res.,* **103**, 14451-14510.

Webster, P.J., A.M. Moore, J.P. Loschnigg and R.R. Leben, 1999: Coupled ocean-atmosphere dynamics in the Indian Ocean during 1997-98. *Nature,* **401**, 356-360.

Weller, R.A. and S.P. Anderson, 1996: Surface Meteorology and air-sea fluxes in the western equatorial Pacific warm pool during the TOGA Coupled Ocean-Atmosphere Experiment. *J. Clim.,* **9**, 1959-1990.

Weller, R.A. and J.F. Price, 1988: Langmuir circulation within the oceanic mixed layer. *Deep-Sea Res.,* **35**, 711-747.

Weng, W.J. and J.D. Neelin, 1998: On the role of ocean-atmosphere interaction in midlatitude interdecadal variability. *Geophys. Res. Lett.,* **25**, 167-170.

Wentz, F.J. and M. Schabel, 2000: Precise climate monitoring using complementary satellite data sets. *Nature,* **403**, 414-416.

Wetherald, R.T. and S. Manabe, 1999: Detectability of summer dryness caused by greenhouse warming. *Clim. Change,* **43**, 495-511.

Whetton, P.H., A.M. Fowler and M.R. Haylock, 1993: Implications of climate change due to the enhanced greenhouse effect on floods and draughts in Australia. *Clim. Change,* **25**, 289-317.

Whillans, I.M. and C.J. van der Veen, 1993: New and improved determinations of velocity of Ice Streams B and C, West Antarctica. *J. Glaciol.,* **39**, 483-490.

Wijffels, S.E., R.W. Schmitt, H.L. Bryden and A. Stigebrandt, 1992: Transport of freshwater by the oceans. *J. Phys. Oceanogr.,* **22**, 155-162.

Wijffels, S.E., J.M. Toole, H.L. Bryden, R.A. Fine, W.J. Jenkins and J.L. Bullister, 1996: The water masses and circulation at 10N in the Pacific. *Deep-Sea Res.,* **43**, 501-544.

Wild, M., A. Ohmura, H. Gilgen, E. Roeckner, M. Giorgetta and J.-J. Morcrette, 1998: The disposition of radiative energy in the global climate system: GCM-calculated versus observational estimates. *Clim. Dyn.,* **14**, 853-869.

Willebrand, J., B. Barnier, C. Böning, C. Dieterich, P. Killworth, C. LeProvost, Y. Jia, J.-M. Molines and A.L. New, 2001: Circulation characteristics in three eddy-permitting models of the North Atlantic. *Prog. Oceanogr.,* **in press**,

Williamson, D.L. and P.J. Rasch, 1994: Water-vapor transport in the NCAR-CCM2. *Tellus,* **46A**, 34-51.

Winton, M., 1995: Why is the deep sinking narrow? *J. Phys. Oceanogr.,* **25**, 997-1005.

WMO, 1999: Scientific Assessment of Ozone Depletion: 1998, Global Ozone Research and Monitoring Project. Report *World Meteorological Organization,* Geneva, Chapter 5

Wood, E.F., D.P. Lettenmaier, X. Liang, D. Lohmann, A. Boone, S. Chang, F. Chen, Y. Dai, R.E. Dickinson, Q. Duan, M. Ek, Y.M. Gusev, F. Habets, P. Irannejad, R. Koster, K.E. Mitchel, O.N. Nasonova, J. Noilhan, J. Schaake, A. Schlosser, Y. Shao, A.B. Shmakin, D.

Verseghy, K. Warrach, P. Wetzel, Y. Xue, Z.-L. Yang and Q.-C. Zeng, 1998: The Project for Intercomparison of Land-surface Parameterization Schemes (PILPS) Phase 2(c) Red-Arkansas River basin experiment: 1. Experiment description and summary intercomparisons. *Glob. Planet. Change,* **19**, 115-135.

Woodwell, G.M., F.T. Mackenzie, R.A. Houghton, M. Apps, E. Gorham and E. Davidson, 1998: Biotic feedbacks in the warming of the Earth. *Clim. Change,* **40**, 495-518.

Wu, X. and M.W. Moncrieff, 1999: Effects of sea surface temperature and large-scale dynamics on the thermodynamic equilibrium state and convection over the tropical western Pacific. *J. Geophys. Res.,* **104**, 6093-6100.

Wunsch, C., 1999: The interpretation of short climate records, with comments on the North Atlantic and Southern Oscillations. *Bull. Am. Met. Soc.,* **80**, 245-256.

Xiao, X., J.M. Melillo, D.W. Kicklighter, A.D. McGuire, R.G. Prinn, C. Wang, P.H. Stone and A. Sokolov, 1998: Transient climate change and net ecosystem production of the terrestrial biosphere. *Glob. Biogeochem. Cyc.,* **12**, 345-360.

Xie, P.P. and P.A. Arkin, 1997: Global precipitation: A 17-year monthly analysis based on gauge observations, satellite estimates, and numerical model outputs. *Bull. Am. Met. Soc.,* **78**, 2539-2558.

Xu, K.M. and K.A. Emanuel, 1989: Is the tropical atmosphere conditionally unstable? *Mon. Wea. Rev.,* **117**, 1471-1479.

Xue, Y., 1997: Biosphere feedback on regional climate in tropical north Africa. *Quart. J. Roy. Met. Soc.,* **123**, 1483-1515.

Xue, Y. and J. Shukla, 1996: The influence of land surface properties on Sahel climate. Part II: Afforestation. *J. Clim.,* **9**, 3260-3275.

Yang, G. and J. Slingo, 1998: The seasonal mean and diurnal cycle of tropical convection as inferred from CLAUS data and the Unified Model. *UGAMP Tech. Rep.,* **47**,(unpublished)

Yang, H. and R.T. Pierrehumbert, 1994: Production of dry air by isentropic mixing. *J. Atm. Sci.,* **51**, 3437-3454.

Yang, Z.-L., R.E. Dickinson, A. Robock and K.Y. Vinnikov, 1997: Validation of the snow sub-model of the biosphere-atmosphere transfer scheme with Russian snow cover and meteorological observational data. *J. Clim.,* **10**, 353-373.

Yao, M.-S. and A.D. Del Genio, 1999: Effect of cloud parameterization on the simulation of climate changes in the GISS GCM. *J. Clim.,* **12**, 761-779.

Yoshimura, J., M. Sugi and A. Noda (eds.), 1999: *Influence of greenhouse warming on tropical cyclone frequency simulated by a high-resolution AGCM.*, 23rd Conference on Hurricanes and Tropical Cyclones, Dallas, TX, 10-15.

Zebiak, S.E. and M.A. Cane, 1991: Natural climate variability in a coupled model. In: *Greenhouse Gas-Induced Climatic Change: Critical Appraisal of Simulations and Observations* [Schlesinger, M. E. (ed.)]. Elsevier, 457-470.

Zender, C.S., B. Bush, S.K. Pope, A. Bucholtz, W.D. Collins, J.T. Kiehl, F.P.J. Valero and J. Vitko Jr., 1997: Atmospheric absorption during the Atmospheric Radiation Measurement (ARM) Enhanced Shortwave Experiment (ARESE). *J. Geophys. Res.,* **102**, 29901-29915.

Zeng, N., J.D. Neelin, W.K.-M. Lau and C.J. Tucker, 1999: Enhancement of interdecadal climate variability in the Sahel by vegetation interaction. *Science,* **286**, 1537-1539.

Zhai, P. and R.E. Eskridge, 1997: Atmospheric water vapor over China. *J. Clim.,* **10**, 2643-2652.

Zhang, G.J. and N.A. McFarlane, 1995: Sensitivity of climate simulations to the parameterization of cumulus convection in the Canadian Climate Centre general circulation model. *Atm.-Oce.,* **33**, 407-446.

Zhang, H., A. Henderson-Sellers, B. McAvaney and A. Pitman, 1997a: Uncertainties in GCM evaluations of tropical deforestation: A comparison of two model simulations. In: *Assessing Climate Change: Results from the Model Evaluation Consortium for Climate Assessment* [Howe, W. and A. Henderson-Sellers (eds.)]. Gordon and

Breach Science Publisher, Sydney, 418.

Zhang, H., A. Henderson-Sellers and K. McGuffie, 1996a: Impacts of tropical deforestation I: Process analysis of local climate change. *J. Clim.,* **9**, 1497-1517.

Zhang, H., K. McGuffie and A. Henderson-Sellers, 1996b: Impacts of tropical deforestation II: The role of large-scale dynamics. *J. Clim.,* **9**, 2498-2521.

Zhang, J. and W.D. Hibler, 1997: On an efficient numerical method for modeling sea ice dynamics. *J. Geophys. Res.,* **102**, 8691-8702.

Zhang, J., R.W. Schmitt and R.X. Huang, 1998: Sensitivity of the GFDL Modular Ocean Model to the parameterization of double-diffusive processes. *J. Phys. Oceanogr.,* **28**, 589-605.

Zhang, J., R.W. Schmitt and R.X. Huang, 1999a: The relative influence of diapycnal mixing and hydrologic forcing on the stability of the thermohaline circulation. *J. Phys. Oceanogr.,* **29**, 1096-1108.

Zhang, M.H., J.J. Hack, J.T. Kiehl and R.D. Cess, 1994: Diagnostic study of climate feedback processes in atmospheric general circulation models. *J. Geophys. Res.,* **99**, 5525-5537.

Zhang, S., R.J. Greatbatch and C.A. Lin, 1993: A reexamination of the polar halocline catastrophe and implications for coupled ocean-atmosphere modelling. *J. Phys. Oceanogr.,* **23**, 287-299.

Zhang, T., R.G. Barry, K. Knowles, J.A. Heginbottom and J. Brown, 1999b: Statistics and characteristics of permafrost and ground ice distribution in the Northern Hemisphere. *Polar Geogr.,* **23**, 147-169.

Zhang, Y., J.M. Wallace and D.S. Battisti, 1997b: ENSO-like interdecadal variability: 1900-93. *J. Clim.,* **10**, 1004-1020.

Zhou, J.Y., Y.C. Sud and K.M. Lau, 1996: Impact of orographically induced gravity-wave drag in the GLA GCM. *Quart. J. Roy. Met. Soc.,* **122**, 903-927.

Zwiers, F.W. and V.V. Kharin, 1998: Changes in the extremes of the climate simulated by CCC GCM2 under CO_2 doubling. *J. Clim.,* **11**, 2200-2222.